

10-28-2019

Comprehensive Second-Order Adjoint Sensitivity Analysis Methodology (2nd-ASAM) Applied to a Subcritical Experimental Reactor Physics Benchmark: II. Effects of Imprecisely Known Microscopic Scattering Cross Sections

Daniel Gabriel Cacuci
cacuci@cec.sc.edu

Ruixian Fang
fangr@cec.sc.edu

Follow this and additional works at: https://scholarcommons.sc.edu/emec_facpub



Part of the [Mechanical Engineering Commons](#)

Publication Info

Published in *Energies*, Volume 12, Issue 21, 2019, pages 4114-.

© 2019 by the authors. Licensee MDPI, Basel, Switzerland. This article is an open access article distributed under the terms and conditions of the Creative Commons Attribution (CC BY) license (<http://creativecommons.org/licenses/by/4.0/>).

This Article is brought to you by the Mechanical Engineering, Department of at Scholar Commons. It has been accepted for inclusion in Faculty Publications by an authorized administrator of Scholar Commons. For more information, please contact digres@mailbox.sc.edu.

Article

Comprehensive Second-Order Adjoint Sensitivity Analysis Methodology (2nd-ASAM) Applied to a Subcritical Experimental Reactor Physics Benchmark: II. Effects of Imprecisely Known Microscopic Scattering Cross Sections

Ruixian Fang  and Dan Gabriel Cacuci * 

Center for Nuclear Science and Energy, Department of Mechanical Engineering, University of South Carolina, Columbia, SC 29208, USA; FANGR@cec.sc.edu

* Correspondence: cacuci@cec.sc.edu

Received: 27 August 2019; Accepted: 23 October 2019; Published: 28 October 2019



Abstract: This work continues the presentation commenced in Part I of the second-order sensitivity analysis of nuclear data of a polyethylene-reflected plutonium (PERP) benchmark using the Second-Order Adjoint Sensitivity Analysis Methodology (2nd-ASAM). This work reports the results of the computations of the first- and second-order sensitivities of this benchmark's computed leakage response with respect to the benchmark's 21,600 parameters underlying the computed group-averaged isotopic scattering cross sections. The numerical results obtained for the 21,600 first-order relative sensitivities indicate that the majority of these were small, the largest having relative values of $O(10^{-2})$. Furthermore, the vast majority of the $(21600)^2$ second-order sensitivities with respect to the scattering cross sections were much smaller than the corresponding first-order ones. Consequently, this work shows that the effects of variances in the scattering cross sections on the expected value, variance, and skewness of the response distribution were negligible in comparison to the corresponding effects stemming from uncertainties in the total cross sections, which were presented in Part I. On the other hand, it was found that 52 of the 21600×180 mixed second-order sensitivities of the leakage response with respect to the scattering and total microscopic cross sections had values that were significantly larger than the unmixed second-order sensitivities of the leakage response with respect to the group-averaged scattering microscopic cross sections. The first- and second-order mixed sensitivities of the PERP benchmark's leakage response with respect to the scattering cross sections and the other benchmark parameters (fission cross sections, average number of neutrons per fission, fission spectrum, isotopic atomic number densities, and source parameters) have also been computed and will be reported in subsequent works.

Keywords: polyethylene-reflected plutonium sphere; first- and second-order sensitivities; microscopic scattering and total cross sections; expected value; variance and skewness of leakage response

1. Introduction

In continuation of the results presented in Part I [1], this work presents the numerical results for the first- and second-order sensitivities of the leakage response of the polyethylene-reflected plutonium (PERP) benchmark described in [2] with respect to the benchmark's group-averaged isotopic scattering cross sections. This work also presents the results for the mixed second-order sensitivities to both the scattering and total cross sections. As has been described in Part I [1], the numerical model of the PERP benchmark includes 180 ($J_{\sigma t} = I \times G$) imprecisely-known parameters for the group-averaged total

microscopic cross sections and 21,600 ($J_{os} = (G \times G) \times I \times (ISCT + 1)$) imprecisely-known parameters for group-averaged scattering microscopic cross sections, where $I = 6$, $G = 30$ and $ISCT = 3$ are the number of isotopes, energy groups and Legendre expansion orders for the PERP benchmark, respectively. Therefore, there are 21,600 first-order sensitivities, 21600×21600 second-order sensitivities of the PERP benchmark's leakage response to the group-averaged microscopic scattering cross sections, and 21600×180 mixed second-order sensitivities to the scattering and total microscopic cross sections. These sensitivities will be computed by specializing the general expressions derived by Cacuci [3] to the PERP benchmark. Section 2 of this work presents computational results for the first- and second-order sensitivities of the PERP benchmark's leakage response with respect to the group-averaged microscopic scattering cross sections. Section 3 reports the numerical results for the matrix of mixed second-order leakage sensitivities to the group-averaged total and scattering microscopic cross sections. Section 4 presents the impact of the first- and second-order sensitivities on the uncertainties induced for the leakage response by the imprecisely-known group-averaged scattering microscopic cross section. Section 5 concludes this work. The computational results for the sensitivities of the PERP leakage response to the remaining imprecisely-known model parameters (fission cross sections and number of neutrons produced per fission, fission spectra, and isotopic number densities) will be reported in subsequent publications.

2. Computation of First- and Second-Order Sensitivities of the PERP Leakage Response to Scattering Cross Sections

The physical system considered in this work is the same polyethylene-reflected plutonium (acronym that will be used in this work: PERP) metal sphere benchmark [2] as described in Part I [1]. As in Part I [1], the neutron flux is computed by solving numerically the neutron transport equation using the PARTISN [4] multigroup discrete ordinates transport code. For the PERP benchmark under consideration, PARTISN [4] solves the following multi-group approximation of the neutron transport equation with a spontaneous fission source provided by the code SOURCES4C [5]:

$$B^g(\alpha)\varphi^g(r, \Omega) = Q^g(r), \quad g = 1, \dots, G, \quad (1)$$

$$\varphi^g(r_d, \Omega) = 0, r_d \in S_b, \Omega \cdot \mathbf{n} < 0, \quad g = 1, \dots, G, \quad (2)$$

where

$$B^g(\alpha)\varphi^g(r, \Omega) \triangleq \Omega \cdot \nabla \varphi^g(r, \Omega) + \Sigma_t^g(r) \varphi^g(r, \Omega) - \sum_{g'=14\pi}^G \int \Sigma_s^{g' \rightarrow g}(r, \Omega' \rightarrow \Omega) \varphi^{g'}(r, \Omega') d\Omega' - \chi^g(r) \sum_{g'=14\pi}^G \int (v\Sigma_f)^{g'}(r) \varphi^{g'}(r, \Omega') d\Omega'; \quad (3)$$

$$Q^g(r) \triangleq \sum_{k=1}^{N_f} \lambda_k N_{k,1} F_k^{SF} v_k^{SF} e^{-E^g/a_k} \sinh \sqrt{b_k E^g}, \quad g = 1, \dots, G, \quad (4)$$

and where α denotes the "vector of imprecisely-known model parameters", as defined in Part I [1].

The PARTISN [4] calculations used MENDF71X 618-group cross sections [6] collapsed to $G = 30$ energy groups, with group boundaries, E^g , as presented in Part I [1]. The MENDF71X library uses ENDF/B-VII.1 Nuclear Data [7]. As has been discussed in [1], the fundamental quantities (i.e., system responses) of interest for *subcritical* benchmarks (such as the PERP benchmark) are singles counting rate, doubles counting rate, the leakage multiplication, and the total leakage. The total leakage is physically more meaningful than count rates because it does not depend on the detector configuration. For this reason, many systems are characterized for practical applications by their total leakage rather than by the count rate that a particular detector would see at a particular distance. For this reason, this work considers the total leakage from the PERP benchmark to be the paradigm response of interest for sensitivity analysis; sensitivities analyses of counting rates and other responses can be performed in

an analogous manner, i.e., by following the general ideas that will be presented in this work (and in subsequent related works).

Mathematically, the total neutron leakage from the PERP sphere, denoted as $L(\alpha)$, will depend (indirectly, through the neutron flux) on all of the imprecisely-known model parameters and is defined as follows:

$$L(\alpha) \triangleq \int_{S_b} dS \sum_{g=1}^G \int_{\Omega \cdot \mathbf{n} > 0} d\Omega \Omega \cdot \mathbf{n} \varphi^g(r, \Omega). \tag{5}$$

Figure 1 shows the histogram plot of the leakage for each energy group for the PERP benchmark. The total leakage computed using Equation (5) for the PERP benchmark is 1.7648×10^6 neutrons/sec.

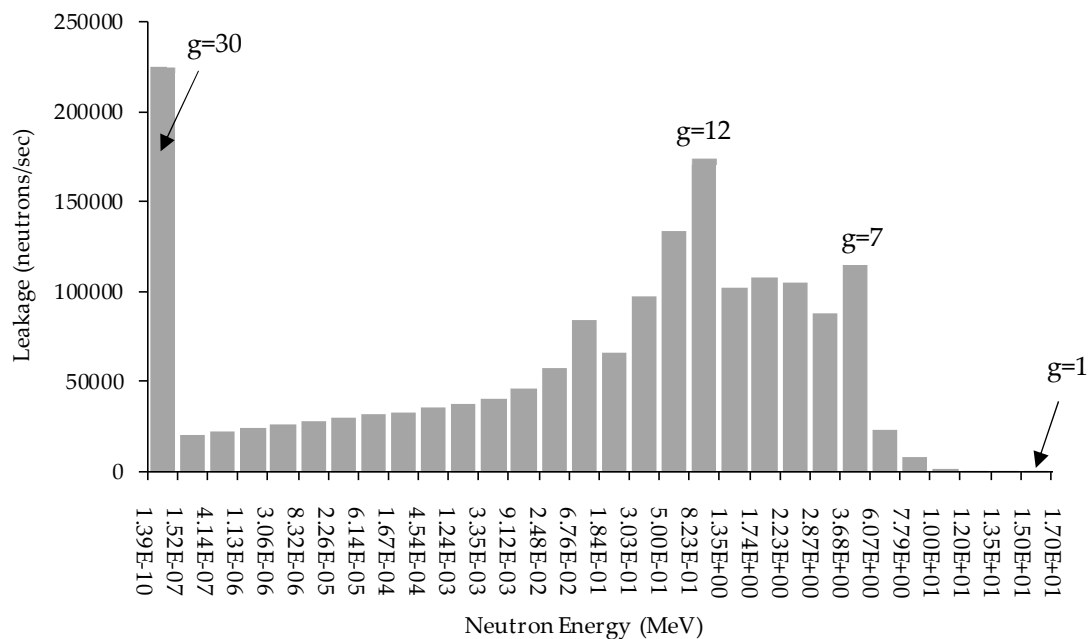


Figure 1. Histogram plot of the leakage for each energy group for the PERP benchmark.

The scattering transfer cross section $\Sigma_s^{g' \rightarrow g}(r, \Omega' \rightarrow \Omega)$ from energy group g' , $g' = 1, \dots, G$ into energy group g , $g = 1, \dots, G$, is computed in terms of the l -th order Legendre coefficient $\sigma_{s,l,i}^{g' \rightarrow g}$, of the Legendre-expanded microscopic scattering cross section from energy group g' into energy group g for isotope i . Since the cross-sections for every material are treated in the PARTISN [4] calculations as being space-independent within the respective material, the variable r will henceforth no longer appear in the arguments of the various cross sections. The coefficients $\sigma_{s,l,i}^{g' \rightarrow g}$ are tabulated parameters, and the finite-order Legendre-expansion of $\Sigma_s^{g' \rightarrow g}(\Omega' \rightarrow \Omega)$ has the following expression:

$$\begin{aligned} \Sigma_s^{g' \rightarrow g}(\Omega' \rightarrow \Omega) &= \sum_{m=1}^{M=2} \Sigma_{s,m}^{g' \rightarrow g}(\Omega' \rightarrow \Omega), \\ \Sigma_{s,m}^{g' \rightarrow g}(\Omega' \rightarrow \Omega) &\cong \sum_{i=1}^{I=6} N_{i,m} \sum_{l=0}^{ISCT=3} (2l+1) \sigma_{s,l,i}^{g' \rightarrow g} P_l(\Omega' \cdot \Omega), \quad m = 1, 2, \end{aligned} \tag{6}$$

where $ISCT = 3$ denotes the order of the respective finite expansion in Legendre polynomial.

The total cross section Σ_t^g for energy group g , $g = 1, \dots, G$, and material m is computed for the PERP benchmark using the following expression:

$$\Sigma_t^g = \sum_{m=1}^{M=2} \Sigma_{t,m}^g; \quad \Sigma_{t,m}^g = \sum_i^I N_{i,m} \sigma_{t,i}^g = \sum_i^I N_{i,m} \left[\sigma_{f,i}^g + \sigma_{c,i}^g + \sum_{g'=1}^G \sigma_{s,l=0,i}^{g \rightarrow g'} \right], \quad m = 1, 2, \tag{7}$$

where $\sigma_{f,i}^g$ and $\sigma_{c,i}^g$ denote, respectively, the tabulated group microscopic fission and neutron capture cross sections for group g , $g = 1, \dots, G$. Other nuclear reactions, including (n,2n) and (n,3n) reactions are not present in the PERP benchmark. The expressions in Equations (6) and (7) indicate that the zeroth order (i.e., $l = 0$) scattering cross sections must be considered separately from the higher order (i.e., $l \geq 1$) scattering cross sections, since the $l = 0$ scattering cross sections contribute to the total cross sections, while the $l \geq 1$ scattering cross sections do not contribute to the total cross sections.

As discussed in Part I [1], the total cross section $\Sigma_t^g \rightarrow \Sigma_t^g(\mathbf{t})$ will depend on the vector of parameter \mathbf{t} , which is defined as follows:

$$\mathbf{t} \triangleq [t_1, \dots, t_{J_t}]^\dagger \triangleq [t_1, \dots, t_{J_{ot}}; n_1, \dots, n_{J_n}]^\dagger \triangleq [\sigma_t; \mathbf{N}]^\dagger, \quad J_t = J_{ot} + J_n, \quad (8)$$

where

$$\mathbf{N} \triangleq [n_1, \dots, n_{J_n}]^\dagger \triangleq [N_{1,1}, N_{2,1}, N_{3,1}, N_{4,1}, N_{5,2}, N_{6,2}]^\dagger, \quad J_n = 6. \quad (9)$$

$$\sigma_t \triangleq [t_1, \dots, t_{J_{ot}}]^\dagger \triangleq [\sigma_{t,i=1}^1, \sigma_{t,i=1}^2, \dots, \sigma_{t,i=1}^G, \sigma_{t,i'}^g, \dots, \sigma_{t,i=I'}^1, \dots, \sigma_{t,i=I}^G]^\dagger, \quad (10)$$

$i = 1, \dots, I; \quad g = 1, \dots, G; \quad J_{ot} = I \times G.$

In Equations (8)–(10), the dagger denotes “transposition,” $\sigma_{t,i}^g$ denotes the microscopic total cross section for isotope i and energy group g , $N_{i,m}$ denotes the respective isotopic number density, and J_n denotes the total number of isotopic number densities in the model. Thus, the vector \mathbf{t} comprises a total of $J_t = J_{ot} + J_n = 30 \times 6 + 6 = 186$ imprecisely-known “model parameters” as its components.

In view of Equation (6), the scattering cross section $\Sigma_s^{g' \rightarrow g}(\Omega' \rightarrow \Omega) \rightarrow \Sigma_s^{g' \rightarrow g}(\mathbf{s}; \Omega' \rightarrow \Omega)$ depends on the vector of parameters \mathbf{s} , which is defined as follows:

$$\mathbf{s} \triangleq [s_1, \dots, s_{J_s}]^\dagger \triangleq [s_1, \dots, s_{J_{os}}; n_1, \dots, n_{J_n}]^\dagger \triangleq [\sigma_s; \mathbf{N}]^\dagger, \quad J_s = J_{os} + J_n, \quad (11)$$

$$\sigma_s \triangleq [s_1, \dots, s_{J_{os}}]^\dagger \triangleq [\sigma_{s,l=0,i=1}^{g'=1 \rightarrow g=1}, \sigma_{s,l=0,i=1}^{g'=2 \rightarrow g=1}, \dots, \sigma_{s,l=0,i=1}^{g'=G \rightarrow g=1}, \sigma_{s,l=0,i=1}^{g'=1 \rightarrow g=2}, \sigma_{s,l=0,i=1}^{g'=2 \rightarrow g=2}, \dots, \sigma_{s,l,i}^{g' \rightarrow g}, \dots, \sigma_{s,ISCT,i=1}^{G \rightarrow G}]^\dagger, \quad (12)$$

$l = 0, \dots, ISCT; \quad i = 1, \dots, I; \quad g, g' = 1, \dots, G; \quad J_{os} = (G \times G) \times I \times (ISCT + 1).$

As stated above, the zeroth order (i.e., $l = 0$) scattering cross sections need to be separately considered from the higher order (i.e., $l \geq 1$) ones. Therefore, in σ_s , the total number of zeroth order scattering cross section is denoted as $J_{os,l=0}$, where $J_{os,l=0} = G \times G \times I$; and the total number of higher order (i.e., $l \geq 1$) scattering cross sections is denoted as $J_{os,l \geq 1}$, where $J_{os,l \geq 1} = G \times G \times I \times ISCT$, with $J_{os,l=0} + J_{os,l \geq 1} = J_{os}$. The vector \mathbf{s} comprises a total of $J_{os} + J_n = 30 \times 30 \times 6 \times (3 + 1) + 6 = 21606$ imprecisely-known components (“model parameters”).

Recall from Part I [1] that the components of the vector of first-order sensitivities of the leakage response with respect to the model parameters are denoted as $\mathbf{S}^{(1)}(\alpha)$, which is defined as follows:

$$\mathbf{S}^{(1)}(\alpha) \triangleq \left[\frac{\partial L(\alpha)}{\partial \sigma_t}; \frac{\partial L(\alpha)}{\partial \sigma_s}; \frac{\partial L(\alpha)}{\partial \sigma_f}; \frac{\partial L(\alpha)}{\partial \mathbf{v}}; \frac{\partial L(\alpha)}{\partial \mathbf{p}}; \frac{\partial L(\alpha)}{\partial \mathbf{q}}; \frac{\partial L(\alpha)}{\partial \mathbf{N}} \right]^\dagger.$$

The symmetric matrix of second-order sensitivities of the leakage response with respect to the model parameters is denoted as $\mathbf{S}^{(2)}(\boldsymbol{\alpha})$, and is defined as follows:

$$\mathbf{S}^{(2)}(\boldsymbol{\alpha}) \triangleq \begin{bmatrix} \frac{\partial^2 L(\boldsymbol{\alpha})}{\partial \sigma_t \partial \sigma_t} & * & * & * & * & * & * \\ \frac{\partial^2 L(\boldsymbol{\alpha})}{\partial \sigma_s \partial \sigma_t} & \frac{\partial^2 L(\boldsymbol{\alpha})}{\partial \sigma_s \partial \sigma_s} & * & * & * & * & * \\ \frac{\partial^2 L(\boldsymbol{\alpha})}{\partial \sigma_f \partial \sigma_t} & \frac{\partial^2 L(\boldsymbol{\alpha})}{\partial \sigma_f \partial \sigma_s} & \frac{\partial^2 L(\boldsymbol{\alpha})}{\partial \sigma_f \partial \sigma_f} & * & * & * & * \\ \frac{\partial^2 L(\boldsymbol{\alpha})}{\partial \nu \partial \sigma_t} & \frac{\partial^2 L(\boldsymbol{\alpha})}{\partial \nu \partial \sigma_s} & \frac{\partial^2 L(\boldsymbol{\alpha})}{\partial \nu \partial \sigma_f} & \frac{\partial^2 L(\boldsymbol{\alpha})}{\partial \nu \partial \nu} & * & * & * \\ \frac{\partial^2 L(\boldsymbol{\alpha})}{\partial \mathbf{p} \partial \sigma_t} & \frac{\partial^2 L(\boldsymbol{\alpha})}{\partial \mathbf{p} \partial \sigma_s} & \frac{\partial^2 L(\boldsymbol{\alpha})}{\partial \mathbf{p} \partial \sigma_f} & \frac{\partial^2 L(\boldsymbol{\alpha})}{\partial \mathbf{p} \partial \nu} & \frac{\partial^2 L(\boldsymbol{\alpha})}{\partial \mathbf{p} \partial \mathbf{p}} & * & * \\ \frac{\partial^2 L(\boldsymbol{\alpha})}{\partial \mathbf{q} \partial \sigma_t} & \frac{\partial^2 L(\boldsymbol{\alpha})}{\partial \mathbf{q} \partial \sigma_s} & \frac{\partial^2 L(\boldsymbol{\alpha})}{\partial \mathbf{q} \partial \sigma_f} & \frac{\partial^2 L(\boldsymbol{\alpha})}{\partial \mathbf{q} \partial \nu} & \frac{\partial^2 L(\boldsymbol{\alpha})}{\partial \mathbf{q} \partial \mathbf{p}} & \frac{\partial^2 L(\boldsymbol{\alpha})}{\partial \mathbf{q} \partial \mathbf{q}} & * \\ \frac{\partial^2 L(\boldsymbol{\alpha})}{\partial \mathbf{N} \partial \sigma_t} & \frac{\partial^2 L(\boldsymbol{\alpha})}{\partial \mathbf{N} \partial \sigma_s} & \frac{\partial^2 L(\boldsymbol{\alpha})}{\partial \mathbf{N} \partial \sigma_f} & \frac{\partial^2 L(\boldsymbol{\alpha})}{\partial \mathbf{N} \partial \nu} & \frac{\partial^2 L(\boldsymbol{\alpha})}{\partial \mathbf{N} \partial \mathbf{p}} & \frac{\partial^2 L(\boldsymbol{\alpha})}{\partial \mathbf{N} \partial \mathbf{q}} & \frac{\partial^2 L(\boldsymbol{\alpha})}{\partial \mathbf{N} \partial \mathbf{N}} \end{bmatrix}.$$

The results as well as their impact on the uncertainties induced in the leakage response by the first- and second-order sensitivities $\partial L(\boldsymbol{\alpha})/\partial \sigma_t$ and, respectively, $\partial^2 L(\boldsymbol{\alpha})/\partial \sigma_t \partial \sigma_t$, were reported in Part I [1]. This work will report the computational results for the first-order sensitivities $\partial L(\boldsymbol{\alpha})/\partial \sigma_s$ and the second-order sensitivities $\partial^2 L(\boldsymbol{\alpha})/\partial \sigma_s \partial \sigma_s$ and $\partial^2 L(\boldsymbol{\alpha})/\partial \sigma_s \partial \sigma_t$, along with their effects on the uncertainties induced in the leakage response.

2.1. First-Order Sensitivities $\partial L(\boldsymbol{\alpha})/\partial \sigma_s$

The equations needed for deriving the expressions of the first-order sensitivities of $\partial L/\partial s_j, j = 1, \dots, J_{\sigma_s}$ will differ from each other depending on whether the parameters s_j correspond to the zeroth-order ($l = 0$) or to the higher order ($l \geq 1$) scattering cross sections. There are two distinct cases, as follows:

- (1) $\left(\frac{\partial L(\boldsymbol{\alpha})}{\partial s_j}\right)_{(s=\sigma_{s,l=0})}, j = 1, \dots, J_{\sigma_s, l=0}$, where the quantities s_j refer to the parameters underlying the zeroth-order scattering microscopic cross sections; and
- (2) $\left(\frac{\partial L(\boldsymbol{\alpha})}{\partial s_j}\right)_{(s=\sigma_{s,l \geq 1})}, j = 1, \dots, J_{\sigma_s, l \geq 1}$, where the quantities s_j refer to the parameters underlying the l^{th} -order ($l \geq 1$) scattering microscopic cross sections.

2.1.1. First-Order Sensitivities $\left(\frac{\partial L(\boldsymbol{\alpha})}{\partial s_j}\right)_{(s=\sigma_{s,l=0})}, j = 1, \dots, J_{\sigma_s, l=0}$

The first-order sensitivities of the leakage response with respect to zeroth-order scattering microscopic cross sections are computed by particularizing Equations (150) and (151) in [3], where Equation (151) provides the contributions arising directly from the scattering cross sections, while Equation (150) provides contributions arising indirectly through the total cross sections. The expression obtained by particularizing Equation (151) in [3] to the PERP benchmark yields:

$$\left(\frac{\partial L(\boldsymbol{\alpha})}{\partial s_j}\right)_{(s=\sigma_{s,l=0})}^{(1)} = \sum_{g=1}^G \int_V dV \int_{4\pi} d\boldsymbol{\Omega} \psi^{(1),g}(r, \boldsymbol{\Omega}) \sum_{g'=14\pi}^G \int d\boldsymbol{\Omega}' \frac{\partial \Sigma_s^{g' \rightarrow g}(\mathbf{s}; \boldsymbol{\Omega}' \rightarrow \boldsymbol{\Omega})}{\partial s_j} \varphi^{g'}(r, \boldsymbol{\Omega}'), \quad (13)$$

for $j = 1, \dots, J_{\sigma_s, l=0}$,

where the multigroup adjoint fluxes $\psi^{(1),g}(r, \boldsymbol{\Omega}), g = 1, \dots, G$ are the solutions of the following first-Level Adjoint Sensitivity System (1st-LASS) presented in Equations (156) and (157) in [3]:

$$A^{(1),g}(\boldsymbol{\alpha}) \psi^{(1),g}(r, \boldsymbol{\Omega}) = \boldsymbol{\Omega} \cdot \mathbf{n} \delta(r - r_d), \quad g = 1, \dots, G, \quad (14)$$

$$\psi^{(1),g}(r_d, \boldsymbol{\Omega}) = 0, \boldsymbol{\Omega} \cdot \mathbf{n} > 0, \quad g = 1, \dots, G, \quad (15)$$

where r_d is the radius of the PERP sphere, and where the adjoint operator $A^{(1),g}(\alpha)$ takes on the following particular form of Equation (149) in [3]:

$$\begin{aligned}
 & A^{(1),g}(\alpha)\psi^{(1),g}(r, \Omega) \\
 & \triangleq -\Omega \cdot \nabla \psi^{(1),g}(r, \Omega) + \Sigma_t^g(\mathbf{t}; r) \psi^{(1),g}(r, \Omega) - \sum_{g'=14\pi}^G \int d\Omega' \Sigma_s^{g \rightarrow g'}(\mathbf{s}; r, \Omega \rightarrow \Omega') \psi^{(1),g'}(r, \Omega') \\
 & - \nu \Sigma_f^g(\mathbf{f}; r) \sum_{g'=14\pi}^G \int d\Omega' \chi^{g'}(\mathbf{p}; r) \psi^{(1),g'}(r, \Omega'), \quad g = 1, \dots, G.
 \end{aligned} \tag{16}$$

The contributions stemming from the total cross sections are computed using Equation (150) in [3] in conjunction with the relations $\frac{\partial L}{\partial t_j} \frac{\partial t_j}{\partial s_j} = \frac{\partial L}{\partial s_j}$ and $\frac{\partial \Sigma_t^g(\mathbf{t})}{\partial t_j} \frac{\partial t_j}{\partial s_j} = \frac{\partial \Sigma_t^g(\mathbf{t})}{\partial s_j}$ to obtain:

$$\left(\frac{\partial L(\alpha)}{\partial s_j} \right)_{(s=\sigma_{s,l=0})}^{(2)} = - \sum_{g=1}^G \int_V dV \int_{4\pi} d\Omega \psi^{(1),g}(r, \Omega) \varphi^g(r, \Omega) \frac{\partial \Sigma_t^g(\mathbf{t})}{\partial s_j}, \quad j = 1, \dots, J_{\sigma s, l=0}. \tag{17}$$

Adding Equations (13) and (17) yields the following complete expression:

$$\begin{aligned}
 & \left(\frac{\partial L(\alpha)}{\partial s_j} \right)_{(s=\sigma_{s,l=0})} = \left(\frac{\partial L(\alpha)}{\partial s_j} \right)_{(s=\sigma_{s,l=0})}^{(1)} + \left(\frac{\partial L(\alpha)}{\partial s_j} \right)_{(s=\sigma_{s,l=0})}^{(2)} \\
 & = \sum_{g=1}^G \int_V dV \int_{4\pi} d\Omega \psi^{(1),g}(r, \Omega) \sum_{g'=14\pi}^G \int d\Omega' \frac{\partial \Sigma_s^{g' \rightarrow g}(\mathbf{s}; \Omega' \rightarrow \Omega)}{\partial s_j} \varphi^{g'}(r, \Omega') \\
 & - \sum_{g=1}^G \int_V dV \int_{4\pi} d\Omega \psi^{(1),g}(r, \Omega) \varphi^g(r, \Omega) \frac{\partial \Sigma_t^g(\mathbf{t})}{\partial s_j}, \quad \text{for } j = 1, \dots, J_{\sigma s, l=0}.
 \end{aligned} \tag{18}$$

For the PERP benchmark, when the parameters s_j correspond to the zeroth-order scattering microscopic cross sections, i.e., $s_j \equiv \sigma_{s,l_j=0,i_j}^{g' \rightarrow g_j}$, the following relations hold:

$$\begin{aligned}
 & \frac{\partial \Sigma_s^{g' \rightarrow g}(\mathbf{s}; \Omega' \rightarrow \Omega)}{\partial s_j} = \frac{\partial \Sigma_s^{g' \rightarrow g}(\mathbf{s}; \Omega' \rightarrow \Omega)}{\partial \sigma_{s,l_j,i_j}^{g' \rightarrow g_j}} = \frac{\partial \left[\sum_{m=1}^M \sum_{i=1}^I N_{i,m} \sigma_{s,i}^{g' \rightarrow g}(\mathbf{s}; \Omega' \rightarrow \Omega') \right]}{\partial \sigma_{s,l_j,i_j}^{g' \rightarrow g_j}} \\
 & = \frac{\partial \left[\sum_{m=1}^M \sum_{i=1}^I \sum_{l=0}^{ISCT} N_{i,m} (2l+1) \sigma_{s,l,i}^{g' \rightarrow g} P_l(\Omega' \cdot \Omega) \right]}{\partial \sigma_{s,l_j,i_j}^{g' \rightarrow g_j}} = \delta_{g_j g} \delta_{g' j} N_{i_j, m_j} (2l_j + 1) P_{l_j}(\Omega' \cdot \Omega),
 \end{aligned} \tag{19}$$

$$\begin{aligned}
 & \frac{\partial \Sigma_t^g(\mathbf{t})}{\partial s_j} = \frac{\partial \left[\sum_{m=1}^M \sum_{i=1}^I N_{i,m} \sigma_{t,i}^g(\mathbf{t}) \right]}{\partial \sigma_{s,l_j=0,i_j}^{g' \rightarrow g_j}} = \frac{\partial \left\{ \sum_{m=1}^M \sum_{i=1}^I N_{i,m} \left[\sigma_{f,i}^g(\mathbf{f}) + \sigma_{c,i}^g(\mathbf{c}) + \sum_{g'=1}^G \sigma_{s,l=0,i}^{g \rightarrow g'}(\mathbf{s}) \right] \right\}}{\partial \sigma_{s,l_j=0,i_j}^{g' \rightarrow g_j}} \\
 & = \frac{\partial \left[\sum_{m=1}^M \sum_{i=1}^I \sum_{g'=1}^G N_{i,m} \sigma_{s,l=0,i}^{g \rightarrow g'}(\mathbf{s}) \right]}{\partial \sigma_{s,l_j=0,i_j}^{g' \rightarrow g_j}} = \delta_{g' j} N_{i_j, m_j},
 \end{aligned} \tag{20}$$

where the subscripts i_j, l_j, g'_j, g_j and m_j refer to the isotope, order of Legendre expansion, energy groups, and material associated with the parameter s_j , respectively, and where $\delta_{g'_j, g}$ and $\delta_{g_j, g}$ denote the Kronecker-delta functionals (e.g., $\delta_{g'_j, g} = 1$ if $g'_j = g$; $\delta_{g'_j, g} = 0$ if $g'_j \neq g$). Inserting Equations (19) and (20) into Equation (18), using the addition theorem for spherical harmonics in one-dimensional geometry, performing the respective angular integrations, and finally setting $l_j = 0$ in the resulting expression yields the following expression:

$$\begin{aligned}
 & \left(\frac{\partial L(\alpha)}{\partial s_j} \right)_{(s=\sigma_{s,l=0})} = N_{i_j, m_j} \int_V dV \varphi_0^{g'_j}(r) \xi_0^{(1),g_j}(r) - N_{i_j, m_j} \int_V dV \int_{4\pi} d\Omega \psi^{(1),g'_j}(r, \Omega) \varphi^{g'_j}(r, \Omega), \\
 & \text{for } j = 1, \dots, J_{\sigma s, l=0},
 \end{aligned} \tag{21}$$

where the forward and adjoint flux moments $\varphi_0^{g'j}(r)$ and $\xi_0^{(1),gj}(r)$ are defined as follows:

$$\varphi_0^g(r) \triangleq \int_{4\pi} d\Omega \varphi^g(r, \Omega), \tag{22}$$

$$\xi_0^{(1),g}(r) \triangleq \int_{4\pi} d\Omega \psi^{(1),g}(r, \Omega). \tag{23}$$

2.1.2. First-Order Sensitivities $\left(\frac{\partial L(\alpha)}{\partial s_j}\right)_{(s=\sigma_{s,l \geq 1})}, j = 1, \dots, \sigma_{s,l \geq 1}$

The first-order sensitivities of the leakage response with respect to the l^{th} -order ($l \geq 1$) microscopic scattering cross sections are computed by particularizing Equation (151) in [3]:

$$\left(\frac{\partial L(\alpha)}{\partial s_j}\right)_{(s=\sigma_{s,l \geq 1})} = \sum_{g=1}^G \int_V dV \int_{4\pi} d\Omega \psi^{(1),g}(r, \Omega) \sum_{g'=1}^G \int_{4\pi} d\Omega' \frac{\partial \Sigma_s^{g' \rightarrow g}(\mathbf{s}; \Omega' \rightarrow \Omega)}{\partial s_j} \varphi^{g'}(r, \Omega'), \tag{24}$$

for $j = 1, \dots, \sigma_{s,l \geq 1}$.

Inserting Equation (19) into Equation (24), using the addition theorem for spherical harmonics in one-dimensional geometry and performing the respective angular integrations, yields the following expression:

$$\left(\frac{\partial L(\alpha)}{\partial s_j}\right)_{(s=\sigma_{s,l \geq 1})} = N_{i_j, m_j} (2l_j + 1) \int_V dV \varphi_{l_j}^{g'j}(r) \xi_{l_j}^{(1),gj}(r), \quad j = 1, \dots, J_{\sigma_s, l \geq 1}, \tag{25}$$

where the forward and adjoint flux moments $\varphi_{l_j}^{g'j}(r)$ and $\xi_{l_j}^{(1),gj}(r)$ are defined as follows:

$$\varphi_{l_j}^g(r) \triangleq \int_{4\pi} d\Omega P_{l_j}(\Omega) \varphi^g(r, \Omega), \tag{26}$$

$$\xi_{l_j}^{(1),g}(r) \triangleq \int_{4\pi} d\Omega P_{l_j}(\Omega) \psi^{(1),g}(r, \Omega). \tag{27}$$

The numerical values of the first-order relative sensitivities, $S^{(1)}(\sigma_{s,l=0,i}^{g \rightarrow g}) \triangleq \left(\frac{\partial L}{\partial \sigma_{s,l=0,i}^{g \rightarrow g}}\right) (\sigma_{s,l=0,i}^{g \rightarrow g} / L)$, $i = 1, \dots, 6; g = 1, \dots, 30$, of the leakage response with respect to the zeroth-order self-scattering microscopic cross sections for the six isotopes contained in the PERP benchmark will be presented in Section 2.3, in tables that will also include comparisons with the numerical values of the corresponding second-order unmixed relative sensitivities $S^{(2)}(\sigma_{s,l=0,i}^{g \rightarrow g}, \sigma_{s,l=0,i}^{g \rightarrow g}) \triangleq \left(\frac{\partial^2 L}{\partial \sigma_{s,l=0,i}^{g \rightarrow g} \partial \sigma_{s,l=0,i}^{g \rightarrow g}}\right) (\sigma_{s,l=0,i}^{g \rightarrow g} \sigma_{s,l=0,i}^{g \rightarrow g} / L)$, $i = 1, \dots, 6; g = 1, \dots, 30$.

2.2. Second-Order Sensitivities $\partial^2 L(\alpha) / \partial \sigma_s \partial \sigma_s$

As has already been mentioned, it is important to note that the equations needed for deriving the expressions of the second-order sensitivities of $\partial^2 L / \partial s_j \partial s_{m_2}$, $j = 1, \dots, J_{\sigma_s}; m_2 = 1, \dots, J_{\sigma_s}$ will differ from each other depending on whether the parameters s_j and s_{m_2} correspond to the zeroth-order ($l = 0$) or to the higher order ($l \geq 1$) scattering cross sections. There are four distinct cases, which will be presented in this Section's four sub-sections, as follows:

A. $\left(\frac{\partial^2 L}{\partial s_j \partial s_{m_2}}\right)_{(s=\sigma_{s,l=0}, s=\sigma_{s,l=0})}, j = 1, \dots, J_{\sigma_s, l=0}; m_2 = 1, \dots, J_{\sigma_s, l=0}$, where both parameters s_j and s_{m_2} correspond to the zeroth-order scattering cross sections;

B. $\left(\frac{\partial^2 L}{\partial s_j \partial s_{m_2}}\right)_{(s=\sigma_{s,l=0}, s=\sigma_{s,l \geq 1})}$, $j = 1, \dots, J_{\sigma s, l=0}; m_2 = 1, \dots, J_{\sigma s, l \geq 1}$, where parameters s_j correspond to the zeroth-order scattering cross sections, and s_{m_2} correspond to the l^{th} -order ($l \geq 1$) scattering cross sections;

C. $\left(\frac{\partial^2 L}{\partial s_j \partial s_{m_2}}\right)_{(s=\sigma_{s,l \geq 1}, s=\sigma_{s,l=0})}$, $j = 1, \dots, J_{\sigma s, l \geq 1}; m_2 = 1, \dots, J_{\sigma s, l=0}$, where parameters s_j correspond to the l^{th} -order ($l \geq 1$) scattering cross sections, and s_{m_2} correspond to the zeroth-order scattering cross sections;

D. $\left(\frac{\partial^2 L}{\partial s_j \partial s_{m_2}}\right)_{(s=\sigma_{s,l \geq 1}, s=\sigma_{s,l \geq 1})}$, $j = 1, \dots, J_{\sigma s, l \geq 1}; m_2 = 1, \dots, J_{\sigma s, l \geq 1}$, where both parameters s_j and s_{m_2} correspond to the l^{th} -order ($l \geq 1$) scattering cross sections.

2.2.1. Second-Order Sensitivities $\left(\frac{\partial^2 L}{\partial s_j \partial s_{m_2}}\right)_{(s=\sigma_{s,l=0}, s=\sigma_{s,l=0})}$, $j = 1, \dots, J_{\sigma s, l=0}; m_2 = 1, \dots, J_{\sigma s, l=0}$

For this case, both parameters s_j and s_{m_2} correspond to the zeroth-order scattering cross sections, and are therefore denoted as $s_j \equiv \sigma_{s, l_j=0, i_j}^{g' j \rightarrow g_j}$ and $s_{m_2} \equiv \sigma_{s, l_{m_2}=0, i_{m_2}}^{g' m_2 \rightarrow g_{m_2}}$, respectively. The subscripts i_{m_2} , l_{m_2} , g'_{m_2} and g_{m_2} refer to the isotope, order of Legendre expansion, and energy groups associated with the parameter s_{m_2} , respectively. When both parameters $s_j \equiv \sigma_{s, l_j=0, i_j}^{g' j \rightarrow g_j}$ and $s_{m_2} \equiv \sigma_{s, l_{m_2}=0, i_{m_2}}^{g' m_2 \rightarrow g_{m_2}}$ correspond to the zeroth-order scattering cross sections, the expression of $\left(\frac{\partial^2 L}{\partial s_j \partial s_{m_2}}\right)_{(s=\sigma_{s,l=0}, s=\sigma_{s,l=0})}$ must include the respective contributions stemming from the total cross sections, since the definition of the total cross sections comprises the zeroth-order scattering cross sections. The contributions from the total cross section due to the zeroth-order scattering cross section parameters s_j and s_{m_2} are computed using Equation (158) in [3] in conjunction with the relations $\frac{\partial^2 L}{\partial t_j \partial t_{m_2}} \frac{\partial t_j}{\partial s_j} \frac{\partial t_{m_2}}{\partial s_{m_2}} = \frac{\partial^2 L}{\partial s_j \partial s_{m_2}}, \frac{\partial \Sigma_t^g(\mathbf{t})}{\partial t_{m_2}} \frac{\partial t_{m_2}}{\partial s_{m_2}} = \frac{\partial \Sigma_t^g(\mathbf{t})}{\partial s_{m_2}}$, and $\frac{\partial^2 \Sigma_t^g(\mathbf{t})}{\partial t_j \partial t_{m_2}} \frac{\partial t_j}{\partial s_j} \frac{\partial t_{m_2}}{\partial s_{m_2}} = \frac{\partial^2 \Sigma_t^g(\mathbf{t})}{\partial s_j \partial s_{m_2}}$, which gives:

$$\begin{aligned} \left(\frac{\partial^2 L}{\partial s_j \partial s_{m_2}}\right)_{(s=\sigma_{s,l=0}, s=\sigma_{s,l=0})}^{(1)} &= - \sum_{g=1}^G \int_V dV \int_{4\pi} d\Omega \psi^{(1),g}(r, \Omega) \varphi^g(r, \Omega) \frac{\partial^2 \Sigma_t^g(\mathbf{t})}{\partial s_j \partial s_{m_2}} \\ &- \sum_{g=1}^G \int_V dV \int_{4\pi} d\Omega \left[\psi_{1,j}^{(2),g}(r, \Omega) \psi^{(1),g}(r, \Omega) + \psi_{2,j}^{(2),g}(r, \Omega) \varphi^g(r, \Omega) \right] \frac{\partial \Sigma_t^g(\mathbf{t})}{\partial s_{m_2}}, \end{aligned} \tag{28}$$

for $j = 1, \dots, J_{\sigma s, l=0}, m_2 = 1, \dots, J_{\sigma s, l=0}$,

where the second-level adjoint functions $\psi_{1,j}^{(2),g}, j = 1, \dots, J_{\sigma s, l=0}, g = 1, \dots, G$, and $\psi_{2,j}^{(2),g}, j = 1, \dots, J_{\sigma s, l=0}; g = 1, \dots, G$, are the solutions of the following particular form of the second-level adjoint sensitivity system (2nd-LASS) presented in Equations (164)–(166) of [3]:

$$B^g(\alpha^0) \psi_{1,j}^{(2),g}(r, \Omega) = -\varphi^g(r, \Omega) \frac{\partial \Sigma_t^g(\mathbf{t})}{\partial s_j}, j = 1, \dots, J_{\sigma s, l=0}; g = 1, \dots, G, \tag{29}$$

$$\psi_{1,j}^{(2),g}(r_d, \Omega) = 0, \Omega \cdot \mathbf{n} < 0; j = 1, \dots, J_{\sigma s, l=0}; g = 1, \dots, G, \tag{30}$$

$$A^{(1),g}(\alpha^0) \psi_{2,j}^{(2),g}(r, \Omega) = -\psi^{(1),g}(r, \Omega) \frac{\partial \Sigma_t^g(\mathbf{t})}{\partial s_j}, j = 1, \dots, J_{\sigma s, l=0}; g = 1, \dots, G, \tag{31}$$

$$\psi_{2,j}^{(2),g}(r_d, \Omega) = 0, \Omega \cdot \mathbf{n} > 0; j = 1, \dots, J_{\sigma s, l=0}; g = 1, \dots, G. \tag{32}$$

The expressions of the various derivatives appearing in Equations (28), (29), and (31) are obtained as follows:

$$\frac{\partial^2 \Sigma_t^g(\mathbf{t})}{\partial s_j \partial s_{m_2}} = \frac{\partial^2 \Sigma_t^g(\mathbf{t})}{\partial \sigma_{s, l_j, i_j}^{g' j \rightarrow g_j} \partial \sigma_{s, l_{m_2}, i_{m_2}}^{g' m_2 \rightarrow g_{m_2}}} = 0, \tag{33}$$

$$\frac{\partial \Sigma_t^g(\mathbf{t})}{\partial s_{m_2}} = \frac{\partial \left[\sum_{m=1}^M \sum_{i=1}^I N_{i,m} \sigma_{t,i}^g(\mathbf{t}) \right]}{\partial \sigma_{s,l_{m_2}=0,i_{m_2}}^{g'_{m_2} \rightarrow g_{m_2}}} = \frac{\partial \left[\sum_{m=1}^M \sum_{i=1}^I \sum_{g'=1}^G N_{i,m} \sigma_{s,l=0,i}^{g \rightarrow g'}(\mathbf{s}) \right]}{\partial \sigma_{s,l_{m_2}=0,i_{m_2}}^{g'_{m_2} \rightarrow g_{m_2}}} = \delta_{g'_{m_2} g} N_{i_{m_2}, m_{m_2}} \tag{34}$$

inserting Equations (33), (34) and (20) into Equations (28)–(31) yields the following simplified expression:

$$\left(\frac{\partial^2 L}{\partial s_j \partial s_{m_2}} \right)_{(s=\sigma_{s,l=0}, s=\sigma_{s,l=0})}^{(1)} = -N_{i_{m_2}, m_{m_2}} \int_V dV \int_{4\pi} d\Omega \left[\psi_{1,j}^{(2),g'_{m_2}}(r, \Omega) \psi_{1,j}^{(1),g'_{m_2}}(r, \Omega) + \psi_{2,j}^{(2),g'_{m_2}}(r, \Omega) \varphi_{s'_{m_2}}^{g'_{m_2}}(r, \Omega) \right], \tag{35}$$

where the second-level adjoint functions $\psi_{1,j}^{(2),g}, j = 1, \dots, J_{\sigma_{s,l=0}}, g = 1, \dots, G$, and $\psi_{2,j}^{(2),g}, j = 1, \dots, J_{\sigma_{s,l=0}}; g = 1, \dots, G$, are the solutions of the following simplified second-level adjoint sensitivity system (2nd-LASS):

$$B^g(\alpha^0) \psi_{1,j}^{(2),g}(r, \Omega) = -\delta_{g'_{jg}} N_{i_j, m_j} \varphi^g(r, \Omega), j = 1, \dots, J_{\sigma_{s,l=0}}; g = 1, \dots, G, \tag{36}$$

$$A^{(1),g}(\alpha^0) \psi_{2,j}^{(2),g}(r, \Omega) = -\delta_{g'_{jg}} N_{i_j, m_j} \psi_{1,j}^{(1),g}(r, \Omega), j = 1, \dots, J_{\sigma_{s,l=0}}; g = 1, \dots, G, \tag{37}$$

subject to the boundary conditions shown in Equations (30) and (32), respectively.

Additional contributions stem from Equation (159) in [3], in conjunction with the relation $\frac{\partial^2 L}{\partial t_j \partial s_{m_2}} \frac{\partial t_j}{\partial s_j} = \frac{\partial^2 L}{\partial s_j \partial s_{m_2}}$, which takes on the following particular form:

$$\begin{aligned} \left(\frac{\partial^2 L}{\partial s_j \partial s_{m_2}} \right)_{(s=\sigma_{s,l=0}, s=\sigma_{s,l=0})}^{(2)} &= \sum_{g=1}^G \int_V dV \int_{4\pi} d\Omega \psi_{1,j}^{(2),g}(r, \Omega) \sum_{g'=1}^G \int_{4\pi} d\Omega' \psi_{1,j}^{(1),g'}(r, \Omega') \frac{\partial \Sigma_s^{g \rightarrow g'}(\mathbf{s}; \Omega \rightarrow \Omega')}{\partial s_{m_2}} \\ &+ \sum_{g=1}^G \int_V dV \int_{4\pi} d\Omega \psi_{2,j}^{(2),g}(r, \Omega) \sum_{g'=1}^G \int_{4\pi} d\Omega' \varphi^{g'}(r, \Omega') \frac{\partial \Sigma_s^{g' \rightarrow g}(\mathbf{s}; \Omega' \rightarrow \Omega)}{\partial s_{m_2}}, \end{aligned} \tag{38}$$

for $j = 1, \dots, J_{\sigma_{s,l=0}}; m_2 = 1, \dots, J_{\sigma_{s,l=0}}$.

Noting that

$$\frac{\partial \Sigma_s^{g \rightarrow g'}(\mathbf{s}; \Omega \rightarrow \Omega')}{\partial s_{m_2}} = \frac{\partial \Sigma_s^{g \rightarrow g'}(\mathbf{s}; \Omega \rightarrow \Omega')}{\partial \sigma_{s,l_{m_2},i_{m_2}}^{g'_{m_2} \rightarrow g_{m_2}}} = \delta_{g'_{m_2} g} \delta_{g_{m_2} g'} N_{i_{m_2}, m_{m_2}} (2l_{m_2} + 1) P_{l_{m_2}}(\Omega' \cdot \Omega), \tag{39}$$

$$\frac{\partial \Sigma_s^{g' \rightarrow g}(\mathbf{s}; \Omega' \rightarrow \Omega)}{\partial s_{m_2}} = \frac{\partial \Sigma_s^{g' \rightarrow g}(\mathbf{s}; \Omega' \rightarrow \Omega)}{\partial \sigma_{s,l_{m_2},i_{m_2}}^{g'_{m_2} \rightarrow g_{m_2}}} = \delta_{g_{m_2} g} \delta_{g'_{m_2} g'} N_{i_{m_2}, m_{m_2}} (2l_{m_2} + 1) P_{l_{m_2}}(\Omega' \cdot \Omega), \tag{40}$$

inserting the results obtained in Equations (39) and (40) into Equation (38), using the addition theorem for spherical harmonics in one-dimensional geometry and performing the respective angular integrations, yields the following simplified expression for Equation (38):

$$\left(\frac{\partial^2 L}{\partial s_j \partial s_{m_2}} \right)_{(s=\sigma_{s,l=0}, s=\sigma_{s,l=0})}^{(2)} = N_{i_{m_2}, m_{m_2}} (2l_{m_2} + 1) \int_V dV \left[\xi_{l_{m_2}}^{(1),g_{m_2}}(r) \xi_{1,j;l_{m_2}}^{(2),g'_{m_2}}(r) + \varphi_{l_{m_2}}^{g'_{m_2}}(r) \xi_{2,j;l_{m_2}}^{(2),g_{m_2}}(r) \right], \tag{41}$$

where the flux moments $\xi_{1,j;l_{m_2}}^{(2),g'_{m_2}}(r)$ and $\xi_{2,j;l_{m_2}}^{(2),g_{m_2}}(r)$ are defined as follows:

$$\xi_{1,j;l}^{(2),g}(r) \triangleq \int_{4\pi} d\Omega P_l(\Omega) \psi_{1,j}^{(2),g}(r, \Omega), \tag{42}$$

$$\xi_{2,j;l}^{(2),g}(r) \triangleq \int_{4\pi} d\Omega P_l(\Omega) \psi_{2,j}^{(2),g}(r, \Omega). \tag{43}$$

Further contributions stem from Equation (167) in [3] in conjunction with the relations $\frac{\partial^2 L}{\partial s_j \partial s_{m_2}} \frac{\partial t_{m_2}}{\partial s_{m_2}} = \frac{\partial^2 L}{\partial s_j \partial s_{m_2}}$ and $\frac{\partial \Sigma_i^g(\mathbf{t})}{\partial t_{m_2}} = \frac{\partial \Sigma_i^g(\mathbf{t})}{\partial t_{m_2}} \frac{\partial t_{m_2}}{\partial s_{m_2}} = \frac{\partial \Sigma_i^g(\mathbf{t})}{\partial s_{m_2}}$, as follows:

$$\left(\frac{\partial^2 L}{\partial s_j \partial s_{m_2}}\right)_{(s=\sigma_{s,l}=0, s=\sigma_{s,l}=0)}^{(3)} = -\sum_{g=1}^G \int_V dV \int_{4\pi} d\Omega \left[\theta_{1,j}^{(2),g}(r, \Omega) \psi^{(1),g}(r, \Omega) + \theta_{2,j}^{(2),g}(r, \Omega) \varphi^g(r, \Omega) \right] \frac{\partial \Sigma_i^g(\mathbf{t})}{\partial s_{m_2}}, \quad (44)$$

for $j = 1, \dots, J_{\sigma s, l=0}; m_2 = 1, \dots, J_{\sigma s, l=0}$,

where the second-level adjoint functions, $\theta_{1,j}^{(2),g}, j = 1, \dots, J_{\sigma s}; g = 1, \dots, G$ and $\theta_{2,j}^{(2),g}, j = 1, \dots, J_{\sigma s}; g = 1, \dots, G$, in Equation (44) are the solutions of the following second-level adjoint sensitivity system (2nd-LASS):

$$B^g(\alpha^0) \theta_{1,j}^{(2),g}(r, \Omega) = \sum_{g'=1}^G \int_{4\pi} d\Omega' \frac{\partial \Sigma_s^{g' \rightarrow g}(\mathbf{s}; \Omega' \rightarrow \Omega)}{\partial s_j} \varphi^{g'}(r, \Omega'), j = 1, \dots, J_{\sigma s}; g = 1, \dots, G; \quad (45)$$

$$\theta_{1,j}^{(2),g}(r_d, \Omega) = 0, \Omega \cdot \mathbf{n} < 0; j = 1, \dots, J_{\sigma s}; g = 1, \dots, G, \quad (46)$$

$$A^{(1),g}(\alpha^0) \theta_{2,j}^{(2),g}(r, \Omega) = \sum_{g'=1}^G \int_{4\pi} d\Omega' \psi^{(1),g'}(r, \Omega') \frac{\partial \Sigma_s^{g \rightarrow g'}(\mathbf{s}; \Omega \rightarrow \Omega')}{\partial s_j}, j = 1, \dots, J_{\sigma s}; g = 1, \dots, G; \quad (47)$$

$$\theta_{2,j}^{(2),g}(r_d, \Omega) = 0, \Omega \cdot \mathbf{n} > 0; j = 1, \dots, J_{\sigma s}; g = 1, \dots, G. \quad (48)$$

Noting that

$$\frac{\partial \Sigma_s^{g \rightarrow g'}(\mathbf{s}; \Omega \rightarrow \Omega')}{\partial s_j} = \frac{\partial \Sigma_s^{g \rightarrow g'}(\mathbf{s}; \Omega \rightarrow \Omega')}{\partial \sigma_{s,l}^{g' j}} = \delta_{g' j, g} \delta_{g_j, g'} N_{i_j, m_j} (2l_j + 1) P_{l_j}(\Omega' \cdot \Omega), \quad (49)$$

and inserting the results obtained in Equations (49), (19), and (34), into Equations (45), (47), and (44) reduces the latter equation to the following expression:

$$\left(\frac{\partial^2 L}{\partial s_j \partial s_{m_2}}\right)_{(s=\sigma_{s,l}=0, s=\sigma_{s,l}=0)}^{(3)} = -N_{i_{m_2}, m_{m_2}} \int_V dV \int_{4\pi} d\Omega \left[\theta_{1,j}^{(2),g'}(r, \Omega) \psi^{(1),g'}(r, \Omega) + \theta_{2,j}^{(2),g'}(r, \Omega) \varphi^{g'}(r, \Omega) \right], \quad (50)$$

where the second-level adjoint functions, $\theta_{1,j}^{(2),g}, j = 1, \dots, J_{\sigma s}; g = 1, \dots, G$ and $\theta_{2,j}^{(2),g}, j = 1, \dots, J_{\sigma s}; g = 1, \dots, G$ are the solutions of the following simplified form of the second-level adjoint sensitivity system (2nd-LASS) shown in Equations (45)–(48):

$$B^g(\alpha^0) \theta_{1,j}^{(2),g}(r, \Omega) = \delta_{g, g} N_{i_j, m_j} (2l_j + 1) P_{l_j}(\Omega) \phi_l^{g' j}(r), j = 1, \dots, J_{\sigma s}; g = 1, \dots, G; l = 0, \dots, ISCT, \quad (51)$$

$$A^{(1),g}(\alpha^0) \theta_{2,j}^{(2),g}(r, \Omega) = \delta_{g', g} N_{i_j, m_j} (2l_j + 1) P_{l_j}(\Omega) \xi_{l_j}^{(1),g j}(r), j = 1, \dots, J_{\sigma s}; g = 1, \dots, G; l = 0, \dots, ISCT. \quad (52)$$

Finally, contributions to the expression of $\left(\frac{\partial^2 L}{\partial s_j \partial s_{m_2}}\right)_{(s=\sigma_{s,l}=0, s=\sigma_{s,l}=0)}$ also arise from Equation (168) of [3], namely:

$$\begin{aligned} \left(\frac{\partial^2 L}{\partial s_j \partial s_{m_2}}\right)_{(s=\sigma_{s,l}=0, s=\sigma_{s,l}=0)}^{(4)} &= \sum_{g=1}^G \int_V dV \int_{4\pi} d\Omega \psi^{(1),g}(r, \Omega) \sum_{g'=1}^G \int_{4\pi} d\Omega' \varphi^{g'}(r, \Omega') \frac{\partial \Sigma_s^{g' \rightarrow g}(\mathbf{s}; \Omega' \rightarrow \Omega)}{\partial s_j \partial s_{m_2}} \\ &+ \sum_{g=1}^G \int_V dV \int_{4\pi} d\Omega \theta_{1,j}^{(2),g}(r, \Omega) \sum_{g'=1}^G \int_{4\pi} d\Omega' \psi^{(1),g'}(r, \Omega') \frac{\partial \Sigma_s^{g \rightarrow g'}(\mathbf{s}; \Omega \rightarrow \Omega')}{\partial s_{m_2}} \\ &+ \sum_{g=1}^G \int_V dV \int_{4\pi} d\Omega \theta_{2,j}^{(2),g}(r, \Omega) \sum_{g'=1}^G \int_{4\pi} d\Omega' \varphi^{g'}(r, \Omega') \frac{\partial \Sigma_s^{g' \rightarrow g}(\mathbf{s}; \Omega' \rightarrow \Omega)}{\partial s_{m_2}}, \end{aligned} \quad (53)$$

for $j = 1, \dots, J_{\sigma s, l=0}; m_2 = 1, \dots, J_{\sigma s, l=0}$.

Noting that

$$\frac{\partial^2 \Sigma_s^{g' \rightarrow g}(\mathbf{s}; \mathbf{\Omega}' \rightarrow \mathbf{\Omega})}{\partial s_j \partial s_{m_2}} = \frac{\partial^2 \Sigma_s^{g' \rightarrow g}(\mathbf{s}; \mathbf{\Omega}' \rightarrow \mathbf{\Omega})}{\partial \sigma_{s,l_j,i_j}^{g' \rightarrow g_j} \partial \sigma_{s,l_{m_2},i_{m_2}}^{g_{m_2} \rightarrow g_{m_2}}} = 0, \tag{54}$$

inserting the above result together with the results obtained in Equations (39) and (40) into Equation (53), using the addition theorem for spherical harmonics in one-dimensional geometry, and performing the respective angular integrations, yields the following expression:

$$\left(\frac{\partial^2 L}{\partial s_j \partial s_{m_2}}\right)_{(s=\sigma_{s,l=0}, s=\sigma_{s,l=0})}^{(4)} = N_{i_{m_2}, m_{m_2}} (2l_{m_2} + 1) \int_V dV \left[\xi_{l_{m_2}}^{(1),g'_{m_2}}(r) \Theta_{1,j;l_{m_2}}^{(2),g'_{m_2}}(r) + \varphi_{l_{m_2}}^{g'_{m_2}}(r) \Theta_{2,j;l_{m_2}}^{(2),g_{m_2}}(r) \right], \tag{55}$$

where

$$\Theta_{1,j;l}^{(2),g}(r) \triangleq \int_{4\pi} d\Omega P_l(\Omega) \theta_{1,j}^{(2),g}(r, \Omega), \tag{56}$$

$$\Theta_{2,j;l}^{(2),g}(r) \triangleq \int_{4\pi} d\Omega P_l(\Omega) \theta_{2,j}^{(2),g}(r, \Omega). \tag{57}$$

Collecting the partial contributions obtained in Equations (35), (41), (50) and (55), and setting $l_{m_2} = 0$ yields the following result:

$$\begin{aligned} \left(\frac{\partial^2 L}{\partial s_j \partial s_{m_2}}\right)_{(s=\sigma_{s,l=0}, s=\sigma_{s,l=0})} &= \sum_{i=1}^4 \left(\frac{\partial^2 L}{\partial s_j \partial s_{m_2}}\right)_{(s=\sigma_{s,l=0}, s=\sigma_{s,l=0})}^{(i)} \\ &= N_{i_{m_2}, m_{m_2}} \left\{ \int_V dV \xi_0^{(1),g_{m_2}}(r) \left[\xi_{1,j;0}^{(2),g'_{m_2}}(r) + \Theta_{1,j;0}^{(2),g'_{m_2}}(r) \right] + \int_V dV \varphi_0^{g'_{m_2}}(r) \left[\xi_{2,j;0}^{(2),g_{m_2}}(r) + \Theta_{2,j;0}^{(2),g_{m_2}}(r) \right] \right. \\ &\quad - \int_V dV \int_{4\pi} d\Omega \left[\psi_{1,j}^{(2),g'_{m_2}}(r, \Omega) \psi^{(1),g'_{m_2}}(r, \Omega) + \psi_{2,j}^{(2),g'_{m_2}}(r, \Omega) \varphi^{g'_{m_2}}(r, \Omega) \right] \\ &\quad \left. - \int_V dV \int_{4\pi} d\Omega \left[\theta_{1,j}^{(2),g'_{m_2}}(r, \Omega) \psi^{(1),g'_{m_2}}(r, \Omega) + \theta_{2,j}^{(2),g'_{m_2}}(r, \Omega) \varphi^{g'_{m_2}}(r, \Omega) \right] \right\}, \tag{58} \end{aligned}$$

for $j = 1, \dots, J_{\sigma_s, l=0}; m_2 = 1, \dots, J_{\sigma_s, l=0}$,

where the zeroth-order moments of the forward and adjoint fluxes moments $\varphi_{l_{m_2}=0}^{g'_{m_2} m_2}(r)$, $\xi_{l_{m_2}=0}^{(1),g_{m_2}}(r)$, $\xi_{1,j;l_{m_2}=0}^{(2),g'_{m_2} m_2}(r)$, $\xi_{2,j;l_{m_2}=0}^{(2),g_{m_2}}(r)$, $\Theta_{1,j;l_{m_2}=0}^{(2),g'_{m_2} m_2}(r)$ and $\Theta_{2,j;l_{m_2}=0}^{(2),g_{m_2}}(r)$ are the special cases when $l = 0$ of the general definitions for $\varphi_l^g(r)$, $\xi_l^{(1),g}(r)$, $\xi_{1,j;l}^{(2),g}(r)$, $\xi_{2,j;l}^{(2),g}(r)$, $\Theta_{1,j;l}^{(2),g}(r)$, and $\Theta_{2,j;l}^{(2),g}(r)$ presented in Equations (26), (27), (42), (43), (56) and (57), respectively.

2.2.2. Second-Order Sensitivities $\left(\frac{\partial^2 L}{\partial s_j \partial s_{m_2}}\right)_{(s=\sigma_{s,l=0}, s=\sigma_{s,l \geq 1})}$, $j = 1, \dots, J_{\sigma_s, l=0}; m_2 = 1, \dots, J_{\sigma_s, l \geq 1}$

For computing the second-order sensitivities $\left(\frac{\partial^2 L}{\partial s_j \partial s_{m_2}}\right)_{(s=\sigma_{s,l=0}, s=\sigma_{s,l \geq 1})}$, the parameters $s_j \equiv \sigma_{s,l_j=0,i_j}^{g'_{j \rightarrow g_j}}$ correspond to the zeroth-order scattering cross sections, and the parameters $s_{m_2} \equiv \sigma_{s,l_{m_2},i_{m_2}}^{g'_{m_2} \rightarrow g_{m_2}}$ correspond to the l th-order ($l \geq 1$) scattering cross sections. Since the l th-order ($l \geq 1$) scattering cross sections do not contribute to the total cross sections, the final expression of $\left(\frac{\partial^2 L}{\partial s_j \partial s_{m_2}}\right)_{(s=\sigma_{s,l=0}, s=\sigma_{s,l \geq 1})}$ is obtained by particularizing Equations (159) and (168) in [3] to the PERP benchmark, and by performing the same sequence of operations as that leading to the expression shown in Equation (58). The final expression thus obtained is:

$$\begin{aligned} \left(\frac{\partial^2 L}{\partial s_j \partial s_{m_2}}\right)_{(s=\sigma_{s,l=0}, s=\sigma_{s,l \geq 1})} &= N_{i_{m_2}, m_{m_2}} (2l_{m_2} + 1) \left\{ \int_V dV \xi_{l_{m_2}}^{(1),g_{m_2}}(r) \left[\xi_{1,j;l_{m_2}}^{(2),g'_{m_2}}(r) + \Theta_{1,j;l_{m_2}}^{(2),g'_{m_2}}(r) \right] \right. \\ &\quad \left. + \int_V dV \varphi_{l_{m_2}}^{g'_{m_2}}(r) \left[\xi_{2,j;l_{m_2}}^{(2),g_{m_2}}(r) + \Theta_{2,j;l_{m_2}}^{(2),g_{m_2}}(r) \right] \right\}, \tag{59} \end{aligned}$$

for $j = 1, \dots, J_{\sigma_s, l=0}; m_2 = 1, \dots, J_{\sigma_s, l \geq 1}; l = 1, \dots, ISCT$.

2.2.3. Second-Order Sensitivities $\left(\frac{\partial^2 L}{\partial s_j \partial s_{m_2}}\right)_{(s=\sigma_{s,l \geq 1}, s=\sigma_{s,l=0})}$, $j = 1, \dots, J_{\sigma s, l \geq 1}$; $m_2 = 1, \dots, J_{\sigma s, l=0}$

For computing the second-order sensitivities $\left(\frac{\partial^2 L}{\partial s_j \partial s_{m_2}}\right)_{(s=\sigma_{s,l \geq 1}, s=\sigma_{s,l=0})}$, the parameters $s_j \equiv \sigma_{s,l,j}^{g' \rightarrow g_j}$ correspond to the l^{th} -order ($l \geq 1$) scattering cross sections and the parameters $s_{m_2} \equiv \sigma_{s,l,m_2=0,i,m_2}^{g' m_2 \rightarrow g_{m_2}}$ correspond to the zeroth-order scattering cross sections. Thus, the final expression of $\left(\frac{\partial^2 L}{\partial s_j \partial s_{m_2}}\right)_{(s=\sigma_{s,l \geq 1}, s=\sigma_{s,l=0})}$ is obtained by particularizing Equations (167) and (168) in [3] to the PERP benchmark. Performing the same sequence of operations as the sequence that produced the expression shown in Equation (58) yields the following result:

$$\begin{aligned} \left(\frac{\partial^2 L}{\partial s_j \partial s_{m_2}}\right)_{(s=\sigma_{s,l \geq 1}, s=\sigma_{s,l=0})} &= N_{i_{m_2}, m_{m_2}} \left\{ \int_V dV \left[\xi_{l_{m_2}=0}^{(1), g_{m_2}}(r) \Theta_{1, j; l_{m_2}=0}^{(2), g' m_2}(r) + \varphi_{l_{m_2}=0}^{g' m_2}(r) \Theta_{2, j; l_{m_2}=0}^{(2), g_{m_2}}(r) \right] \right. \\ &\quad \left. - \int_V dV \int_{4\pi} d\Omega \left[\theta_{1, j}^{(2), g' m_2}(r, \Omega) \psi^{(1), g' m_2}(r, \Omega) + \theta_{2, j}^{(2), g' m_2}(r, \Omega) \varphi^{g' m_2}(r, \Omega) \right] \right\}, \end{aligned} \tag{60}$$

for $j = 1, \dots, J_{\sigma s, l \geq 1}$; $m_2 = 1, \dots, J_{\sigma s, l=0}$.

In view of the symmetry of the mixed second-order sensitivities, the sensitivities $\left(\frac{\partial^2 L}{\partial s_j \partial s_{m_2}}\right)_{(s=\sigma_{s,l=0}, s=\sigma_{s,l \geq 1})}$ computed using Equation (59) must be equal to the sensitivities $\left(\frac{\partial^2 L}{\partial s_j \partial s_{m_2}}\right)_{(s=\sigma_{s,l \geq 1}, s=\sigma_{s,l=0})}$ computed using Equation (60). The second-level adjoint functions used in Equation (59) correspond to the zeroth-order scattering cross sections indexed by $j = 1, \dots, J_{\sigma s, l=0}$, whereas the second-level adjoint functions used in Equation (60) correspond to the l^{th} -order ($l \geq 1$) scattering cross sections indexed by $j = 1, \dots, J_{\sigma s, l \geq 1}$.

2.2.4. Second-Order Sensitivities $\left(\frac{\partial^2 L}{\partial s_j \partial s_{m_2}}\right)_{(s=\sigma_{s,l \geq 1}, s=\sigma_{s,l \geq 1})}$, $j = 1, \dots, J_{\sigma s, l \geq 1}$; $m_2 = 1, \dots, J_{\sigma s, l \geq 1}$

For computing the second-order sensitivities $\left(\frac{\partial^2 L}{\partial s_j \partial s_{m_2}}\right)_{(s=\sigma_{s,l \geq 1}, s=\sigma_{s,l \geq 1})}$, both parameters $s_j \equiv \sigma_{s,l,j}^{g' \rightarrow g_j}$ and $s_{m_2} \equiv \sigma_{s,l,m_2=0,i,m_2}^{g' m_2 \rightarrow g_{m_2}}$ correspond to the l^{th} -order ($l \geq 1$) scattering cross sections. Thus, the final expression for $\left(\frac{\partial^2 L}{\partial s_j \partial s_{m_2}}\right)_{(s=\sigma_{s,l \geq 1}, s=\sigma_{s,l \geq 1})}$ is obtained by particularizing Equation (168) in [3] only to the PERP benchmark. Performing the same sequence of operations as the sequence that produced the expression shown in Equation (58) yields the following result:

$$\begin{aligned} \left(\frac{\partial^2 L}{\partial s_j \partial s_{m_2}}\right)_{(s=\sigma_{s,l \geq 1}, s=\sigma_{s,l \geq 1})} &= N_{i_{m_2}, m_{m_2}} (2l_{m_2} + 1) \int_V dV \left[\xi_{l_{m_2}}^{(1), g_{m_2}}(r) \Theta_{1, j; l_{m_2}}^{(2), g' m_2}(r) \right. \\ &\quad \left. + \varphi_{l_{m_2}}^{g' m_2}(r) \Theta_{2, j; l_{m_2}}^{(2), g_{m_2}}(r) \right], \end{aligned} \tag{61}$$

$j = 1, \dots, J_{\sigma s, l \geq 1}$; $m_2 = 1, \dots, J_{\sigma s, l \geq 1}$; $l = 1, \dots, ISCT$.

2.3. Numerical Results for $\partial^2 L / \partial s_j \partial s_{m_2}$, $j = 1, \dots, J_s$; $m_2 = 1, \dots, J_s$

The dimensions of the sensitivity matrix $\partial^2 L / \partial s_j \partial s_{m_2}$, $j = 1, \dots, J_s$; $m_2 = 1, \dots, J_s$, of the leakage response with respect to the scattering cross sections of all isotopes for the PERP benchmark, are $J_{\sigma s} \times J_{\sigma s}$ ($= 21600 \times 21600$), where $J_{\sigma s} = (G \times G) \times I \times (ISCT + 1)$. The elements of $\partial^2 L / \partial s_j \partial s_{m_2}$, $j = 1, \dots, 21600$; $m_2 = 1, \dots, 21600$ were computed using Equations (58), (59), (60) and (61). The remainder of this section will present the numerical results for the relative second-order sensitivities, denoted as $\mathbf{S}^{(2)}\left(\sigma_{s,l,i}^{g' \rightarrow g}, \sigma_{s,l',k}^{h' \rightarrow h}\right)$, which correspond to the generic elements $\partial^2 L / \partial s_j \partial s_{m_2}$, and which are defined as follows:

$$\begin{aligned} \mathbf{S}^{(2)}\left(\sigma_{s,l,i}^{g' \rightarrow g}, \sigma_{s,l',k}^{h' \rightarrow h}\right) &\triangleq \left(\partial^2 L / \partial \sigma_{s,l,i}^{g' \rightarrow g} \partial \sigma_{s,l',k}^{h' \rightarrow h}\right) \left(\sigma_{s,l,i}^{g' \rightarrow g} \sigma_{s,l',k}^{h' \rightarrow h} / L\right), \\ &\text{for } l, l' = 0, \dots, 3; i, k = 1, \dots, 6; g, g', h, h' = 1, \dots, 30. \end{aligned} \tag{62}$$

While computing the sensitivities $\mathbf{S}^{(2)}\left(\sigma_{s,l,i}^{g' \rightarrow g}, \sigma_{s,l',k}^{h' \rightarrow h}\right)$, it has been verified, within the first five significant digits, that the numerical values obtained using Equation (59) are the same as the corresponding numerical values obtained using Equation (60). The numerical values of the second-order relative sensitivities of the leakage response with respect to the scattering cross sections are small by comparison to the corresponding leakage sensitivities to the total cross sections presented in Part I [1], the largest of them being of the order of 10^{-2} . The results for the second-order sensitivities of the leakage response with respect to the 0th-order scattering cross sections of isotope 1 (^{239}Pu) and to the second-order scattering cross sections of all of the other isotopes, i.e., $\mathbf{S}^{(2)}\left(\sigma_{s,l=0,i=1'}^{g' \rightarrow g}, \sigma_{s,l'=0,k}^{h' \rightarrow h}\right) = \left(\partial^2 L / \partial \sigma_{s,l=0,i=1}^{g' \rightarrow g} \partial \sigma_{s,l'=0,k}^{h' \rightarrow h}\right) \left(\sigma_{s,l=0,i=1}^{g' \rightarrow g} \sigma_{s,l'=0,k}^{h' \rightarrow h} / L\right)$ for $k = 1, \dots, 6; g, g', h, h' = 1, \dots, 30$, are summarized in Table 1. The dimensions of each of the submatrices presented in Table 1 are 900×900 . As shown in the table, these second-order relative sensitivities are all much smaller than 1.0.

Table 1. Overview of second-order relative sensitivities of the leakage response with respect to the zeroth-order ($l = 0$) scattering cross sections of isotope 1 (^{239}Pu) and to the zeroth-order ($l' = 0$) scattering cross sections of all isotopes, $\mathbf{S}^{(2)}\left(\sigma_{s,l=0,i=1'}^{g' \rightarrow g}, \sigma_{s,l'=0,k}^{h' \rightarrow h}\right)$, $k = 1, \dots, 6; g, g', h, h' = 1, \dots, 30$.

	$k = 1$ (^{239}Pu)	$k = 2$ (^{240}Pu)	$k = 3$ (^{69}Ga)	$k = 4$ (^{71}Ga)	$k = 5$ (C)	$k = 6$ (^1H)
$i = 1$ (^{239}Pu)	$\mathbf{S}^{(2)}\left(\sigma_{s,l=0,i=1'}^{g' \rightarrow g}, \sigma_{s,l'=0,k=1}^{h' \rightarrow h}\right)$ Max. value = 3.58×10^{-2}	$\mathbf{S}^{(2)}\left(\sigma_{s,l=0,i=1'}^{g' \rightarrow g}, \sigma_{s,l'=0,k=2}^{h' \rightarrow h}\right)$ Max. value = 2.56×10^{-3}	$\mathbf{S}^{(2)}\left(\sigma_{s,l=0,i=1'}^{g' \rightarrow g}, \sigma_{s,l'=0,k=3}^{h' \rightarrow h}\right)$ Max. value = 1.39×10^{-4}	$\mathbf{S}^{(2)}\left(\sigma_{s,l=0,i=1'}^{g' \rightarrow g}, \sigma_{s,l'=0,k=4}^{h' \rightarrow h}\right)$ Max. value = 1.03×10^{-4}	$\mathbf{S}^{(2)}\left(\sigma_{s,l=0,i=1'}^{g' \rightarrow g}, \sigma_{s,l'=0,k=5}^{h' \rightarrow h}\right)$ Max. value = 1.75×10^{-2}	$\mathbf{S}^{(2)}\left(\sigma_{s,l=0,i=1'}^{g' \rightarrow g}, \sigma_{s,l'=0,k=6}^{h' \rightarrow h}\right)$ Max. value = 3.45×10^{-2}

The largest of all of the sensitivities summarized in Table 1 are included among the elements of the submatrix $\mathbf{S}^{(2)}\left(\sigma_{s,l=0,i=1'}^{g' \rightarrow g}, \sigma_{s,l=0,k=1}^{h' \rightarrow h}\right)$, $g, g', h, h' = 1, \dots, 30$, which comprises the second-order relative sensitivities in submatrix of the leakage response with respect to the zeroth-order scattering cross sections of isotope 1 (^{239}Pu). Moreover, the largest 10 relative sensitivities comprised in $\mathbf{S}^{(2)}\left(\sigma_{s,l=0,i=1'}^{g' \rightarrow g}, \sigma_{s,l=0,k=1}^{h' \rightarrow h}\right)$, $g, g', h, h' = 1, \dots, 30$, are listed in Table 2. All of these sensitivities are with respect to the zeroth-order self-scattering cross sections, rather than the in-scattering or out-scattering cross sections. In particular, the largest second-order sensitivity is $S^{(2)}\left(\sigma_{s,l=0,i=1}^{12 \rightarrow 12}, \sigma_{s,l=0,k=1}^{13 \rightarrow 13}\right) = 3.579 \times 10^{-2}$, which corresponds to the second-order sensitivity of the leakage response with respect to the self-scattering cross section parameters of $\sigma_{s,l=0,i=1}^{12 \rightarrow 12}$ and $\sigma_{s,l=0,k=1}^{13 \rightarrow 13}$.

Table 2. Largest ten relative sensitivities comprised in $\mathbf{S}^{(2)}\left(\sigma_{s,l=0,i=1'}^{g' \rightarrow g}, \sigma_{s,l=0,k=1}^{h' \rightarrow h}\right)$; $g, g', h, h' = 1, \dots, 30$ (second-order sensitivities of the leakage with respect to the zeroth-order scattering cross sections of ^{239}Pu).

Rank	Relative Sensitivity	Rank	Relative Sensitivity
1	$S^{(2)}\left(\sigma_{s,l=0,i=1}^{12 \rightarrow 12}, \sigma_{s,l=0,k=1}^{13 \rightarrow 13}\right) = 3.579 \times 10^{-2}$	6	$S^{(2)}\left(\sigma_{s,l=0,i=1}^{12 \rightarrow 12}, \sigma_{s,l=0,k=1}^{12 \rightarrow 12}\right) = 2.602 \times 10^{-2}$
2	$S^{(2)}\left(\sigma_{s,l=0,i=1}^{7 \rightarrow 7}, \sigma_{s,l=0,k=1}^{12 \rightarrow 12}\right) = 3.131 \times 10^{-2}$	7	$S^{(2)}\left(\sigma_{s,l=0,i=1}^{8 \rightarrow 8}, \sigma_{s,l=0,k=1}^{12 \rightarrow 12}\right) = 2.487 \times 10^{-2}$
3	$S^{(2)}\left(\sigma_{s,l=0,i=1}^{7 \rightarrow 7}, \sigma_{s,l=0,k=1}^{13 \rightarrow 13}\right) = 2.712 \times 10^{-2}$	8	$S^{(2)}\left(\sigma_{s,l=0,i=1}^{10 \rightarrow 10}, \sigma_{s,l=0,k=1}^{12 \rightarrow 12}\right) = 2.476 \times 10^{-2}$
4	$S^{(2)}\left(\sigma_{s,l=0,i=1}^{12 \rightarrow 12}, \sigma_{s,l=0,k=1}^{14 \rightarrow 14}\right) = 2.653 \times 10^{-2}$	9	$S^{(2)}\left(\sigma_{s,l=0,i=1}^{13 \rightarrow 13}, \sigma_{s,l=0,k=1}^{14 \rightarrow 14}\right) = 2.323 \times 10^{-2}$
5	$S^{(2)}\left(\sigma_{s,l=0,i=1}^{9 \rightarrow 9}, \sigma_{s,l=0,k=1}^{12 \rightarrow 12}\right) = 2.604 \times 10^{-2}$	10	$S^{(2)}\left(\sigma_{s,l=0,i=1}^{9 \rightarrow 9}, \sigma_{s,l=0,k=1}^{13 \rightarrow 13}\right) = 2.257 \times 10^{-2}$

Tables 3–5 present an overview of the second-order relative sensitivities of the leakage response with respect to the zeroth-order scattering cross sections of isotope 1 (^{239}Pu) and to the l^{th} -order scattering cross sections of all isotopes, defined as $\mathbf{S}^{(2)}\left(\sigma_{s,l=0,i=1'}^{g' \rightarrow g}, \sigma_{s,l',k}^{h' \rightarrow h}\right) \triangleq \left(\partial^2 L / \partial \sigma_{s,l=0,i=1}^{g' \rightarrow g} \partial \sigma_{s,l',k}^{h' \rightarrow h}\right) \left(\sigma_{s,l=0,i=1}^{g' \rightarrow g} \sigma_{s,l',k}^{h' \rightarrow h} / L\right)$, $k = 1, \dots, 6; g, g', h, h' = 1, \dots, 30$, for $l' = 1, 2, 3$,

respectively. The results presented in these tables indicate that the higher the order of scattering cross sections, the smaller the mixed second-order sensitivities.

Table 3. Overview of the second-order mixed relative sensitivities of the leakage response with respect to the zeroth-order ($l = 0$) scattering cross sections of ^{239}Pu and to the first-order ($l' = 1$) scattering cross sections of all other isotopes: $\mathbf{S}^{(2)}(\sigma_{s,l=0,i=1}^{g' \rightarrow g} \sigma_{s,l'=1,k}^{h' \rightarrow h})$; $k = 1, \dots, 6$; $g, g', h, h' = 1, \dots, 30$.

	$k = 1$ (^{239}Pu)	$k = 2$ (^{240}Pu)	$k = 3$ (^{69}Ga)	$k = 4$ (^{71}Ga)	$k = 5$ (C)	$k = 6$ (^1H)
$i = 1$ (^{239}Pu)	$\mathbf{S}^{(2)}\left(\begin{matrix} \sigma_{s,l=0,i=1}^{g' \rightarrow g} \\ \sigma_{s,l'=1,k=1}^{h' \rightarrow h} \end{matrix}\right)$ Min. value = -2.70×10^{-2}	$\mathbf{S}^{(2)}\left(\begin{matrix} \sigma_{s,l=0,i=1}^{g' \rightarrow g} \\ \sigma_{s,l'=1,k=2}^{h' \rightarrow h} \end{matrix}\right)$ Min. value = -1.62×10^{-3}	$\mathbf{S}^{(2)}\left(\begin{matrix} \sigma_{s,l=0,i=1}^{g' \rightarrow g} \\ \sigma_{s,l'=1,k=3}^{h' \rightarrow h} \end{matrix}\right)$ Min. value = -5.45×10^{-5}	$\mathbf{S}^{(2)}\left(\begin{matrix} \sigma_{s,l=0,i=1}^{g' \rightarrow g} \\ \sigma_{s,l'=1,k=4}^{h' \rightarrow h} \end{matrix}\right)$ Min. value = -3.31×10^{-5}	$\mathbf{S}^{(2)}\left(\begin{matrix} \sigma_{s,l=0,i=1}^{g' \rightarrow g} \\ \sigma_{s,l'=1,k=5}^{h' \rightarrow h} \end{matrix}\right)$ Min. value = -6.60×10^{-3}	$\mathbf{S}^{(2)}\left(\begin{matrix} \sigma_{s,l=0,i=1}^{g' \rightarrow g} \\ \sigma_{s,l'=1,k=6}^{h' \rightarrow h} \end{matrix}\right)$ Min. value = -2.64×10^{-2}

Table 4. Overview of second-order mixed relative sensitivities of the leakage response with respect to the zeroth-order ($l = 0$) scattering cross sections of ^{239}Pu and to the second-order ($l' = 2$) scattering cross sections of all other isotopes: $\mathbf{S}^{(2)}(\sigma_{s,l=0,i=1}^{g' \rightarrow g} \sigma_{s,l'=2,k}^{h' \rightarrow h})$; $k = 1, \dots, 6$; $g, g', h, h' = 1, \dots, 30$.

	$k = 1$ (^{239}Pu)	$k = 2$ (^{240}Pu)	$k = 3$ (^{69}Ga)	$k = 4$ (^{71}Ga)	$k = 5$ (C)	$k = 6$ (^1H)
$i = 1$ (^{239}Pu)	$\mathbf{S}^{(2)}\left(\begin{matrix} \sigma_{s,l=0,i=1}^{g' \rightarrow g} \\ \sigma_{s,l'=2,k=1}^{h' \rightarrow h} \end{matrix}\right)$ Min. value = -2.32×10^{-3}	$\mathbf{S}^{(2)}\left(\begin{matrix} \sigma_{s,l=0,i=1}^{g' \rightarrow g} \\ \sigma_{s,l'=2,k=2}^{h' \rightarrow h} \end{matrix}\right)$ Min. value = -1.42×10^{-4}	$\mathbf{S}^{(2)}\left(\begin{matrix} \sigma_{s,l=0,i=1}^{g' \rightarrow g} \\ \sigma_{s,l'=2,k=3}^{h' \rightarrow h} \end{matrix}\right)$ Min. value = -4.25×10^{-6}	$\mathbf{S}^{(2)}\left(\begin{matrix} \sigma_{s,l=0,i=1}^{g' \rightarrow g} \\ \sigma_{s,l'=2,k=4}^{h' \rightarrow h} \end{matrix}\right)$ Min. value = -2.64×10^{-6}	$\mathbf{S}^{(2)}\left(\begin{matrix} \sigma_{s,l=0,i=1}^{g' \rightarrow g} \\ \sigma_{s,l'=2,k=5}^{h' \rightarrow h} \end{matrix}\right)$ Min. value = 2.13×10^{-3}	$\mathbf{S}^{(2)}\left(\begin{matrix} \sigma_{s,l=0,i=1}^{g' \rightarrow g} \\ \sigma_{s,l'=2,k=6}^{h' \rightarrow h} \end{matrix}\right)$ Min. value = 6.71×10^{-3}

Table 5. Overview of second-order mixed relative sensitivities of the leakage response with respect to the zeroth-order ($l = 0$) scattering cross sections of ^{239}Pu and to the third-order ($l' = 3$) scattering cross sections of all other isotopes: $\mathbf{S}^{(2)}(\sigma_{s,l=0,i=1}^{g' \rightarrow g} \sigma_{s,l'=3,k}^{h' \rightarrow h})$; $k = 1, \dots, 6$; $g, g', h, h' = 1, \dots, 30$.

	$k = 1$ (^{239}Pu)	$k = 2$ (^{240}Pu)	$k = 3$ (^{69}Ga)	$k = 4$ (^{71}Ga)	$k = 5$ (C)	$k = 6$ (^1H)
$i = 1$ (^{239}Pu)	$\mathbf{S}^{(2)}\left(\begin{matrix} \sigma_{s,l=0,i=1}^{g' \rightarrow g} \\ \sigma_{s,l'=3,k=1}^{h' \rightarrow h} \end{matrix}\right)$ Max. value = 3.44×10^{-5}	$\mathbf{S}^{(2)}\left(\begin{matrix} \sigma_{s,l=0,i=1}^{g' \rightarrow g} \\ \sigma_{s,l'=3,k=2}^{h' \rightarrow h} \end{matrix}\right)$ Max. value = 2.12×10^{-6}	$\mathbf{S}^{(2)}\left(\begin{matrix} \sigma_{s,l=0,i=1}^{g' \rightarrow g} \\ \sigma_{s,l'=3,k=3}^{h' \rightarrow h} \end{matrix}\right)$ Max. value = 6.02×10^{-8}	$\mathbf{S}^{(2)}\left(\begin{matrix} \sigma_{s,l=0,i=1}^{g' \rightarrow g} \\ \sigma_{s,l'=3,k=4}^{h' \rightarrow h} \end{matrix}\right)$ Max. value = 3.77×10^{-8}	$\mathbf{S}^{(2)}\left(\begin{matrix} \sigma_{s,l=0,i=1}^{g' \rightarrow g} \\ \sigma_{s,l'=3,k=5}^{h' \rightarrow h} \end{matrix}\right)$ Max. value = -5.47×10^{-4}	$\mathbf{S}^{(2)}\left(\begin{matrix} \sigma_{s,l=0,i=1}^{g' \rightarrow g} \\ \sigma_{s,l'=3,k=6}^{h' \rightarrow h} \end{matrix}\right)$ Max. value = -1.38×10^{-3}

The first-order sensitivities of the leakage response with respect to the zeroth-order self-scattering cross sections can be compared directly to the corresponding unmixed second-order sensitivities. These comparisons are presented in Tables 6–11 for all six of the isotopes contained in the PERP benchmark. The main conclusions that can be drawn from these comparisons are as follows:

- (i) both the first- and second-order unmixed sensitivities of the leakage response with respect to the zeroth-order self-scattering cross sections are very small; and
- (ii) the absolute values of the second-order unmixed relative sensitivities are much smaller, by at least an order of magnitude, than the corresponding first-order sensitivities (except for the second-order unmixed sensitivity of the leakage with respect to the self-scattering cross section of isotopes C and ^1H in their respective lowest-energy group).

Table 6. Comparison of first-order relative sensitivities $(\partial L / \partial \sigma_{s,l=0,i=1}^{g \rightarrow g})(\sigma_{s,l=0,i=1}^{g \rightarrow g} / L), g = 1, \dots, 30$ and second-order relative sensitivities $[\partial^2 L / (\partial \sigma_{s,l=0,i=1}^{g \rightarrow g})^2][(\sigma_{s,l=0,i=1}^{g \rightarrow g})^2 / L], g = 1, \dots, 30$ of the leakage response with respect to the zeroth-order self-scattering cross sections of isotope 1 (^{239}Pu).

g	1st Order	2nd Order	g	1st Order	2nd Order
1	4.586×10^{-5}	-3.230×10^{-6}	16	4.104×10^{-2}	-5.637×10^{-3}
2	9.107×10^{-5}	-6.176×10^{-6}	17	6.790×10^{-3}	-2.328×10^{-3}
3	2.603×10^{-4}	-1.726×10^{-5}	18	-2.449×10^{-3}	4.478×10^{-4}
4	1.205×10^{-3}	-7.814×10^{-5}	19	-5.053×10^{-3}	2.048×10^{-3}
5	6.195×10^{-3}	-3.836×10^{-4}	20	-6.677×10^{-3}	3.413×10^{-3}
6	1.866×10^{-2}	-9.125×10^{-4}	21	-7.081×10^{-3}	3.863×10^{-3}
7	1.026×10^{-1}	1.129×10^{-2}	22	-4.171×10^{-3}	1.791×10^{-3}
8	8.174×10^{-2}	4.572×10^{-3}	23	-2.227×10^{-3}	5.661×10^{-4}
9	8.556×10^{-2}	6.099×10^{-3}	24	-9.434×10^{-4}	2.124×10^{-4}
10	8.143×10^{-2}	5.782×10^{-3}	25	-5.436×10^{-4}	4.436×10^{-5}
11	7.336×10^{-2}	4.378×10^{-3}	26	-1.421×10^{-3}	2.785×10^{-4}
12	1.344×10^{-1}	2.602×10^{-2}	27	-4.065×10^{-4}	8.741×10^{-5}
13	1.156×10^{-1}	1.524×10^{-2}	28	2.812×10^{-5}	-3.808×10^{-7}
14	8.538×10^{-2}	3.317×10^{-3}	29	-1.201×10^{-5}	4.457×10^{-8}
15	5.069×10^{-2}	-3.971×10^{-3}	30	-3.721×10^{-4}	2.490×10^{-6}

Table 7. Comparison of first-order relative sensitivities $(\partial L / \partial \sigma_{s,l=0,i=2}^{g \rightarrow g})(\sigma_{s,l=0,i=2}^{g \rightarrow g} / L), g = 1, \dots, 30$ and second-order relative sensitivities $[\partial^2 L / (\partial \sigma_{s,l=0,i=2}^{g \rightarrow g})^2][(\sigma_{s,l=0,i=2}^{g \rightarrow g})^2 / L], g = 1, \dots, 30$ of the leakage response with respect to the zeroth-order self-scattering cross sections of isotope 2 (^{240}Pu).

g	1st Order	2nd Order	g	1st Order	2nd Order
1	2.663×10^{-6}	-1.089×10^{-8}	16	2.861×10^{-3}	-2.739×10^{-5}
2	5.126×10^{-6}	-1.956×10^{-8}	17	4.633×10^{-4}	-1.084×10^{-5}
3	1.459×10^{-5}	-5.419×10^{-8}	18	-1.664×10^{-4}	2.068×10^{-6}
4	6.664×10^{-5}	-2.389×10^{-7}	19	-3.487×10^{-4}	9.756×10^{-6}
5	3.452×10^{-4}	-1.191×10^{-6}	20	-5.301×10^{-4}	2.151×10^{-5}
6	1.064×10^{-3}	-2.971×10^{-6}	21	-5.338×10^{-4}	2.196×10^{-5}
7	5.996×10^{-3}	3.859×10^{-5}	22	-3.748×10^{-4}	1.446×10^{-5}
8	4.910×10^{-3}	1.650×10^{-5}	23	-5.268×10^{-4}	3.168×10^{-5}
9	5.255×10^{-3}	2.300×10^{-5}	24	-1.825×10^{-4}	7.949×10^{-6}
10	5.078×10^{-3}	2.249×10^{-5}	25	-2.841×10^{-5}	1.212×10^{-7}
11	4.775×10^{-3}	1.855×10^{-5}	26	-1.084×10^{-4}	1.619×10^{-6}
12	8.897×10^{-3}	1.141×10^{-4}	27	-1.745×10^{-4}	1.611×10^{-5}
13	8.253×10^{-3}	7.773×10^{-5}	28	9.535×10^{-5}	-4.379×10^{-6}
14	6.287×10^{-3}	1.799×10^{-5}	29	-1.568×10^{-8}	7.604×10^{-14}
15	3.561×10^{-3}	-1.960×10^{-5}	30	-2.615×10^{-6}	1.229×10^{-10}

Table 8. Comparison of first-order relative sensitivities $(\partial L / \partial \sigma_{s,l=0,i=3}^{g \rightarrow g})(\sigma_{s,l=0,i=3}^{g \rightarrow g} / L), g = 1, \dots, 30$ and second-order relative sensitivities $[\partial^2 L / (\partial \sigma_{s,l=0,i=3}^{g \rightarrow g})^2] [(\sigma_{s,l=0,i=3}^{g \rightarrow g})^2 / L], g = 1, \dots, 30$ of the leakage response with respect to the zeroth-order self-scattering cross sections of isotope 3 (^{69}Ga).

g	1st-Order	2nd-Order	g	1st-Order	2nd-Order
1	1.163×10^{-7}	-2.079×10^{-11}	16	1.546×10^{-4}	-7.993×10^{-8}
2	2.625×10^{-7}	-5.132×10^{-11}	17	2.689×10^{-5}	-3.652×10^{-8}
3	8.420×10^{-7}	-1.806×10^{-10}	18	-1.069×10^{-5}	8.538×10^{-9}
4	4.462×10^{-6}	-1.071×10^{-9}	19	-2.932×10^{-5}	6.897×10^{-8}
5	2.349×10^{-5}	-5.518×10^{-9}	20	-4.056×10^{-5}	1.259×10^{-7}
6	6.060×10^{-5}	-9.631×10^{-9}	21	-3.308×10^{-5}	8.430×10^{-8}
7	2.595×10^{-4}	7.230×10^{-8}	22	-1.335×10^{-5}	1.833×10^{-8}
8	1.755×10^{-4}	2.108×10^{-8}	23	-6.505×10^{-6}	4.831×10^{-9}
9	1.936×10^{-4}	3.123×10^{-8}	24	-3.084×10^{-6}	2.269×10^{-9}
10	2.151×10^{-4}	4.035×10^{-8}	25	-2.099×10^{-6}	6.614×10^{-10}
11	2.328×10^{-4}	4.409×10^{-8}	26	-7.099×10^{-6}	6.951×10^{-9}
12	5.141×10^{-4}	3.811×10^{-7}	27	-1.872×10^{-6}	1.854×10^{-9}
13	4.495×10^{-4}	2.306×10^{-7}	28	1.104×10^{-7}	-5.872×10^{-12}
14	3.241×10^{-4}	4.779×10^{-8}	29	-5.239×10^{-8}	8.486×10^{-13}
15	1.876×10^{-4}	-5.436×10^{-8}	30	-2.162×10^{-6}	8.410×10^{-11}

Table 9. Comparison of first-order relative sensitivities $(\partial L / \partial \sigma_{s,l=0,i=4}^{g \rightarrow g})(\sigma_{s,l=0,i=4}^{g \rightarrow g} / L), g = 1, \dots, 30$ and second-order relative sensitivities $[\partial^2 L / (\partial \sigma_{s,l=0,i=4}^{g \rightarrow g})^2] [(\sigma_{s,l=0,i=4}^{g \rightarrow g})^2 / L], g = 1, \dots, 30$ of the leakage response with respect to the zeroth-order self-scattering cross sections of isotope 4 (^{71}Ga).

g	1st-Order	2nd-Order	g	1st-Order	2nd-Order
1	7.828×10^{-8}	-9.413×10^{-12}	16	1.008×10^{-4}	-3.401×10^{-8}
2	1.789×10^{-7}	-2.383×10^{-11}	17	1.741×10^{-5}	-1.531×10^{-8}
3	5.712×10^{-7}	-8.311×10^{-11}	18	-6.772×10^{-6}	3.424×10^{-9}
4	3.004×10^{-6}	-4.855×10^{-10}	19	-1.725×10^{-5}	2.387×10^{-8}
5	1.586×10^{-5}	-2.514×10^{-9}	20	-2.506×10^{-5}	4.806×10^{-8}
6	4.095×10^{-5}	-4.398×10^{-9}	21	-2.106×10^{-5}	3.417×10^{-8}
7	1.626×10^{-4}	2.837×10^{-8}	22	-2.414×10^{-4}	5.999×10^{-6}
8	1.041×10^{-4}	7.408×10^{-9}	23	-6.918×10^{-6}	5.465×10^{-9}
9	1.177×10^{-4}	1.153×10^{-8}	24	-1.236×10^{-6}	3.644×10^{-10}
10	1.344×10^{-4}	1.576×10^{-8}	25	-8.839×10^{-7}	1.173×10^{-10}
11	1.491×10^{-4}	1.807×10^{-8}	26	-3.037×10^{-6}	1.272×10^{-9}
12	3.299×10^{-4}	1.569×10^{-7}	27	-8.052×10^{-7}	3.429×10^{-10}
13	2.943×10^{-4}	9.885×10^{-8}	28	4.757×10^{-8}	-1.090×10^{-12}
14	2.191×10^{-4}	2.184×10^{-8}	29	-2.259×10^{-8}	1.578×10^{-13}
15	1.272×10^{-4}	-2.502×10^{-8}	30	-9.317×10^{-7}	1.562×10^{-11}

Table 10. Comparison of first-order relative sensitivities $(\partial L / \partial \sigma_{s,l=0,i=5}^{g \rightarrow g})(\sigma_{s,l=0,i=5}^{g \rightarrow g} / L)$, $g = 1, \dots, 30$ and second-order relative sensitivities $[\partial^2 L / (\partial \sigma_{s,l=0,i=5}^{g \rightarrow g})^2] [(\sigma_{s,l=0,i=5}^{g \rightarrow g})^2 / L]$, $g = 1, \dots, 30$ of the leakage response with respect to the zeroth-order self-scattering cross sections of isotope 5 (C).

g	1st-Order	2nd-Order	g	1st-Order	2nd-Order
1	8.999×10^{-6}	-2.379×10^{-7}	16	4.322×10^{-2}	-4.681×10^{-3}
2	1.603×10^{-5}	-3.693×10^{-7}	17	2.231×10^{-2}	-3.523×10^{-3}
3	5.392×10^{-5}	-1.410×10^{-6}	18	1.355×10^{-2}	-2.419×10^{-3}
4	2.362×10^{-4}	-5.666×10^{-6}	19	9.436×10^{-3}	-1.810×10^{-3}
5	1.040×10^{-3}	-2.240×10^{-5}	20	6.954×10^{-3}	-1.444×10^{-3}
6	2.637×10^{-3}	-4.103×10^{-5}	21	5.184×10^{-3}	-1.174×10^{-3}
7	2.401×10^{-2}	3.824×10^{-4}	22	3.997×10^{-3}	-9.374×10^{-4}
8	1.644×10^{-2}	-2.327×10^{-5}	23	3.105×10^{-3}	-7.736×10^{-4}
9	1.407×10^{-2}	5.068×10^{-5}	24	2.858×10^{-3}	-6.495×10^{-4}
10	1.761×10^{-2}	8.554×10^{-5}	25	2.103×10^{-3}	-5.637×10^{-4}
11	1.939×10^{-2}	4.351×10^{-5}	26	1.859×10^{-3}	-4.938×10^{-4}
12	6.645×10^{-2}	4.252×10^{-3}	27	2.093×10^{-3}	-4.318×10^{-4}
13	6.257×10^{-2}	1.441×10^{-3}	28	2.042×10^{-3}	-3.829×10^{-4}
14	4.959×10^{-2}	-1.655×10^{-3}	29	9.596×10^{-4}	-2.858×10^{-4}
15	3.184×10^{-2}	-2.609×10^{-3}	30	2.301×10^{-3}	-3.293×10^{-3}

Table 11. Comparison of first-order relative sensitivities $(\partial L / \partial \sigma_{s,l=0,i=6}^{g \rightarrow g})(\sigma_{s,l=0,i=6}^{g \rightarrow g} / L)$, $g = 1, \dots, 30$ and second-order relative sensitivities $[\partial^2 L / (\partial \sigma_{s,l=0,i=6}^{g \rightarrow g})^2] [(\sigma_{s,l=0,i=6}^{g \rightarrow g})^2 / L]$, $g = 1, \dots, 30$ of the leakage response with respect to the zeroth-order self-scattering cross sections of isotope 6 (^1H).

g	1st-Order	2nd-Order	g	1st-Order	2nd-Order
1	8.168×10^{-7}	-1.961×10^{-9}	16	1.012×10^{-1}	-2.564×10^{-2}
2	1.627×10^{-6}	-3.805×10^{-9}	17	6.699×10^{-2}	-3.177×10^{-2}
3	8.710×10^{-6}	-3.681×10^{-8}	18	4.644×10^{-2}	-2.843×10^{-2}
4	6.054×10^{-5}	-3.722×10^{-7}	19	3.433×10^{-2}	-2.396×10^{-2}
5	3.873×10^{-4}	-3.106×10^{-6}	20	2.584×10^{-2}	-1.993×10^{-2}
6	1.272×10^{-3}	-9.542×10^{-6}	21	1.945×10^{-2}	-1.653×10^{-2}
7	1.362×10^{-2}	1.230×10^{-4}	22	1.504×10^{-2}	-1.327×10^{-2}
8	8.486×10^{-3}	-6.197×10^{-6}	23	1.170×10^{-2}	-1.099×10^{-2}
9	1.197×10^{-2}	3.672×10^{-5}	24	1.077×10^{-2}	-9.225×10^{-3}
10	1.535×10^{-2}	6.502×10^{-5}	25	7.931×10^{-3}	-8.013×10^{-3}
11	1.721×10^{-2}	3.427×10^{-5}	26	7.022×10^{-3}	-7.049×10^{-3}
12	6.573×10^{-2}	4.160×10^{-3}	27	7.917×10^{-3}	-6.180×10^{-3}
13	6.483×10^{-2}	1.547×10^{-3}	28	7.829×10^{-3}	-5.629×10^{-3}
14	5.767×10^{-2}	-2.238×10^{-3}	29	3.773×10^{-3}	-4.418×10^{-3}
15	4.284×10^{-2}	-4.722×10^{-3}	30	2.720×10^{-2}	-4.602×10^{-1}

The results presented in Tables 6–11 indicate that the largest values for both the first- and second-order relative sensitivities for the isotopes ^{239}Pu , ^{240}Pu , ^{69}Ga , and ^{71}Ga , are for the energy group 12. For the isotope C, the largest values for the first- and second-order relative sensitivities are for the 12th energy group and the 16th energy group, respectively. For the isotope ^1H , the largest values for the first- and second-order relative sensitivities are for the 12th energy group and the 30th energy group, respectively. It is noteworthy that all of the first-order relative sensitivities of the leakage response with respect to the zeroth-order scattering cross sections of isotopes C and ^1H are positive, signifying that an increase in the corresponding microscopic cross sections will cause an increase in the value of the response L (i.e., more neutrons will leak out of the sphere). These sensitivities indicate that an increase in low energy scattering moderates and reflects slow neutrons into the plutonium, which increases the induced fission rate in ^{239}Pu , thus increasing the neutron flux, which in turn increases the neutron leakage.

3. Mixed Second-Order Sensitivities of the PERP Total Leakage Response with respect to the Parameters Underlying the Benchmark’s Scattering and Total Cross Sections

This section presents the computation and analysis of the numerical results for the second-order mixed sensitivities of the leakage response with respect to the group-averaged scattering and total microscopic cross sections of all isotopes of the PERP benchmark. As has been shown by Cacuci [3], these mixed sensitivities can be computed using two distinct expressions, involving distinct second-level adjoint systems and the corresponding adjoint functions, by considering either the computation of $\partial^2 L / \partial s_j \partial t_{m_2}$, $j = 1, \dots, J_{\sigma s}$; $m_2 = 1, \dots, J_{\sigma t}$ or the computation of $\partial^2 L / \partial t_j \partial s_{m_2}$, $j = 1, \dots, J_{\sigma t}$; $m_2 = 1, \dots, J_{\sigma s}$. These two distinct paths for computing the 2nd-order sensitivities with respect to the group-averaged scattering and total microscopic cross sections will be presented in Sections 3.1 and 3.2, respectively. Of course, the end results produced by these two distinct paths must be identical, thus providing a mutual “solution verification” that the respective computations were performed correctly.

3.1. Second-Order Sensitivities $\partial^2 L / \partial s_j \partial t_{m_2}$, $j = 1, \dots, J_{\sigma s}$; $m_2 = 1, \dots, J_{\sigma t}$

The equations needed for deriving the expressions of the second-order sensitivities $\partial^2 L / \partial s_j \partial t_{m_2}$, $j = 1, \dots, J_{\sigma s, l=0}$; $m_2 = 1, \dots, J_{\sigma t}$ when the parameters s_j correspond to the zeroth-order ($l = 0$) scattering cross sections will differ from the equations needed for deriving the expressions of the second-order sensitivities $\partial^2 L / \partial s_j \partial t_{m_2}$, $j = 1, \dots, J_{\sigma s, l \geq 1}$; $m_2 = 1, \dots, J_{\sigma t}$ when the parameters s_j correspond to the higher-order ($l \geq 1$) scattering cross sections. There are two cases, as follows:

(1) $\left(\frac{\partial^2 L}{\partial s_j \partial t_{m_2}} \right)_{(s=\sigma_{s,l=0}, t=\sigma_t)}$, $j = 1, \dots, J_{\sigma s, l=0}$; $m_2 = 1, \dots, J_{\sigma t}$, where the quantities s_j enumerate the parameters underlying the zeroth-order scattering cross sections, and the quantities t_{m_2} enumerate the parameters underlying the total cross sections;

(2) $\left(\frac{\partial^2 L}{\partial s_j \partial t_{m_2}} \right)_{(s=\sigma_{s,l \geq 1}, t=\sigma_t)}$, $j = 1, \dots, J_{\sigma s, l \geq 1}$; $m_2 = 1, \dots, J_{\sigma t}$, where the quantities s_j enumerate the parameters underlying the l^{th} -order ($l \geq 1$) scattering cross sections, and the quantities t_{m_2} enumerate the parameters underlying the total cross sections.

3.1.1. Second-Order Sensitivities $\left(\frac{\partial^2 L}{\partial s_j \partial t_{m_2}} \right)_{(s=\sigma_{s,l=0}, t=\sigma_t)}$, $j = 1, \dots, J_{\sigma s, l=0}$; $m_2 = 1, \dots, J_{\sigma t}$

The direct expression for computing $\left(\frac{\partial^2 L}{\partial s_j \partial t_{m_2}} \right)_{(s=\sigma_{s,l=0}, t=\sigma_t)}$ is obtained by particularizing Equation (167) in [3] to the PERP benchmark, which yields:

$$\left(\frac{\partial^2 L}{\partial s_j \partial t_{m_2}} \right)_{(s=\sigma_{s,l=0}, t=\sigma_t)}^{(1)} = - \sum_{g=1}^G \int_V dV \int_{4\pi} d\Omega \left[\theta_{1,j}^{(2),g}(r, \Omega) \psi^{(1),g}(r, \Omega) + \theta_{2,j}^{(2),g}(r, \Omega) \varphi^g(r, \Omega) \right] \frac{\partial \Sigma_t^g(t)}{\partial t_{m_2}}, \tag{63}$$

for $j = 1, \dots, J_{\sigma s, l=0}$; $m_2 = 1, \dots, J_{\sigma t}$.

The expression of $\left(\frac{\partial^2 L}{\partial s_j \partial t_{m_2}} \right)_{(s=\sigma_{s,l=0}, t=\sigma_t)}$ must also include the contributions stemming from the total cross sections, since the total cross sections comprises the zeroth-order scattering cross sections. The contributions are computed by particularizing Equation (158) in [3] to the PERP benchmark and by noting that $\frac{\partial^2 L}{\partial t_j \partial t_{m_2}} \frac{\partial t_j}{\partial s_j} = \frac{\partial^2 L}{\partial s_j \partial t_{m_2}}$ and $\frac{\partial^2 \Sigma_t^g(t)}{\partial t_j \partial t_{m_2}} \frac{\partial t_j}{\partial s_j} = \frac{\partial^2 \Sigma_t^g(t)}{\partial s_j \partial t_{m_2}}$, to obtain:

$$\begin{aligned} \left(\frac{\partial^2 L}{\partial s_j \partial t_{m_2}} \right)_{(s=\sigma_{s,l=0}, t=\sigma_t)}^{(2)} &= - \sum_{g=1}^G \int_V dV \int_{4\pi} d\Omega \psi^{(1),g}(r, \Omega) \varphi^g(r, \Omega) \frac{\partial^2 \Sigma_t^g(t)}{\partial s_j \partial t_{m_2}} \\ &- \sum_{g=1}^G \int_V dV \int_{4\pi} d\Omega \left[\psi_{1,j}^{(2),g}(r, \Omega) \psi^{(1),g}(r, \Omega) + \psi_{2,j}^{(2),g}(r, \Omega) \varphi^g(r, \Omega) \right] \frac{\partial \Sigma_t^g(t)}{\partial t_{m_2}}, \end{aligned} \tag{64}$$

for $j = 1, \dots, J_{\sigma s, l=0}$; $m_2 = 1, \dots, J_{\sigma t}$.

Adding Equations (63) and (64) yields the following expression:

$$\begin{aligned} \left(\frac{\partial^2 L}{\partial s_j \partial t_{m_2}}\right)_{(s=\sigma_{s,l=0}, t=\sigma_t)} &= \left(\frac{\partial^2 L}{\partial s_j \partial t_{m_2}}\right)_{(s=\sigma_{s,l=0}, t=\sigma_t)}^{(1)} + \left(\frac{\partial^2 L}{\partial s_j \partial t_{m_2}}\right)_{(s=\sigma_{s,l=0}, t=\sigma_t)}^{(2)} \\ &= -\sum_{g=1}^G \int_V dV \int_{4\pi} d\Omega \left[\theta_{1,j}^{(2),g}(r, \Omega) \psi^{(1),g}(r, \Omega) + \theta_{2,j}^{(2),g}(r, \Omega) \varphi^g(r, \Omega) \right] \frac{\partial \Sigma_t^g(\mathbf{t})}{\partial t_{m_2}} \\ &\quad - \sum_{g=1}^G \int_V dV \int_{4\pi} d\Omega \psi^{(1),g}(r, \Omega) \varphi^g(r, \Omega) \frac{\partial^2 \Sigma_t^g(\mathbf{t})}{\partial s_j \partial t_{m_2}} \\ &\quad - \sum_{g=1}^G \int_V dV \int_{4\pi} d\Omega \left[\psi_{1,j}^{(2),g}(r, \Omega) \psi^{(1),g}(r, \Omega) + \psi_{2,j}^{(2),g}(r, \Omega) \varphi^g(r, \Omega) \right] \frac{\partial \Sigma_t^g(\mathbf{t})}{\partial t_{m_2}}, \end{aligned} \tag{65}$$

for $j = 1, \dots, J_{\sigma s, l=0}; m_2 = 1, \dots, J_{\sigma t}$.

In Equation (65), the parameters s_j correspond to the zeroth-order scattering cross sections, so that $s_j \equiv \sigma_{s,l=0,i_j}^{g' \rightarrow g_j}$ while the parameters t_{m_2} correspond to the total cross sections, so that $t_{m_2} \equiv \sigma_{t,i_{m_2}}^{g_{m_2}}$, where the subscripts i_{m_2} and g_{m_2} denote the isotope and energy group associated with t_{m_2} , respectively.

Noting that

$$\frac{\partial^2 \Sigma_t^g(\mathbf{t})}{\partial s_j \partial t_{m_2}} = \frac{\partial^2 \Sigma_t^g(\mathbf{t})}{\partial \sigma_{s,l,i_j}^{g' \rightarrow g_j} \partial \sigma_{t,i_{m_2}}^{g_{m_2}}} = 0, \tag{66}$$

$$\frac{\partial \Sigma_t^g(\mathbf{t})}{\partial t_{m_2}} = \frac{\partial \Sigma_t^g(\mathbf{t})}{\partial \sigma_{t,i_{m_2}}^{g_{m_2}}} = \frac{\partial \left(\sum_{m=1}^M \sum_{i=1}^I N_{i,m} \partial \sigma_{t,i}^g \right)}{\partial \sigma_{t,i_{m_2}}^{g_{m_2}}} = \delta_{g_{m_2} g} N_{i_{m_2}, m_{m_2}}, \tag{67}$$

and inserting the results obtained in Equations (66) and (67) into Equation (65), yields:

$$\begin{aligned} \left(\frac{\partial^2 L}{\partial s_j \partial t_{m_2}}\right)_{(s=\sigma_{s,l=0}, t=\sigma_t)} &= -N_{i_{m_2}, m_{m_2}} \int_V dV \int_{4\pi} d\Omega \left\{ \psi^{(1),g_{m_2}}(r, \Omega) \left[\psi_{1,j}^{(2),g_{m_2}}(r, \Omega) + \theta_{1,j}^{(2),g_{m_2}}(r, \Omega) \right] \right. \\ &\quad \left. + \varphi^{g_{m_2}}(r, \Omega) \left[\psi_{2,j}^{(2),g_{m_2}}(r, \Omega) + \theta_{2,j}^{(2),g_{m_2}}(r, \Omega) \right] \right\}, \quad j = 1, \dots, J_{\sigma s, l=0}; m_2 = 1, \dots, J_{\sigma t}. \end{aligned} \tag{68}$$

3.1.2. Second-Order Sensitivities $\left(\frac{\partial^2 L}{\partial s_j \partial t_{m_2}}\right)_{(s=\sigma_{s,l \geq 1}, t=\sigma_t)}$, $j = 1, \dots, J_{\sigma s, l \geq 1}; m_2 = 1, \dots, J_{\sigma t}$

When considering the higher-order scattering cross sections, $s_j \equiv \sigma_{s,l,i_j}^{g' \rightarrow g_j}$ enumerates the parameters underlying the l^{th} -order ($l \geq 1$) scattering cross sections, while the $t_{m_2} \equiv \sigma_{t,i_{m_2}}^{g_{m_2}}$ enumerates the parameters underlying the total cross sections. For this case, the contributions to $\left(\frac{\partial^2 L}{\partial s_j \partial t_{m_2}}\right)_{(s=\sigma_{s,l \geq 1}, t=\sigma_t)}$ stem just from the right side of the general expression shown in Equation (63), which gives:

$$\begin{aligned} \left(\frac{\partial^2 L}{\partial s_j \partial t_{m_2}}\right)_{(s=\sigma_{s,l \geq 1}, t=\sigma_t)} &= -\sum_{g=1}^G \int_V dV \int_{4\pi} d\Omega \left[\theta_{1,j}^{(2),g}(r, \Omega) \psi^{(1),g}(r, \Omega) \right. \\ &\quad \left. + \theta_{2,j}^{(2),g}(r, \Omega) \varphi^g(r, \Omega) \frac{\partial \Sigma_t^g(\mathbf{t})}{\partial t_{m_2}} \right], \quad \text{for } j = 1, \dots, J_{\sigma s, l \geq 1}; m_2 = 1, \dots, J_{\sigma t}. \end{aligned} \tag{69}$$

Using the result obtained in Equation (67) in Equation (69) transforms the latter into the following form:

$$\begin{aligned} \left(\frac{\partial^2 L}{\partial s_j \partial t_{m_2}}\right)_{(s=\sigma_{s,l \geq 1}, t=\sigma_t)} &= -N_{i_{m_2}, m_{m_2}} \int_V dV \int_{4\pi} d\Omega \left[\theta_{1,j}^{(2),g_{m_2}}(r, \Omega) \psi^{(1),g_{m_2}}(r, \Omega) \right. \\ &\quad \left. + \theta_{2,j}^{(2),g_{m_2}}(r, \Omega) \varphi^{g_{m_2}}(r, \Omega) \right], \quad j = 1, \dots, J_{\sigma s, l \geq 1}; m_2 = 1, \dots, J_{\sigma t}. \end{aligned} \tag{70}$$

3.2. Alternative Path: Computing the Second-Order Sensitivities $\partial^2 L / \partial t_j \partial s_{m_2}, j = 1, \dots, J_{\sigma t}; m_2 = 1, \dots, J_{\sigma s}$

The mixed second-order sensitivities $\partial^2 L / \partial s_j \partial t_{m_2}, j = 1, \dots, J_{\sigma s}; m_2 = 1, \dots, J_{\sigma t}$ can also be computed using the alternative expressions for $\partial^2 L / \partial t_j \partial s_{m_2}, j = 1, \dots, J_{\sigma t}; m_2 = 1, \dots, J_{\sigma s}$. The numerical results obtained from both expressions must be equal to each other, thus providing a mutual “solution verification” of the correctness of the numerical solution procedure employed for solving the respective second-level adjoint systems. As in Section 3.1, there will be two cases, as follows:

(1) $\left(\frac{\partial^2 L}{\partial t_j \partial s_{m_2}}\right)_{(t=\sigma_t, s=\sigma_{s,l}=0)}, j = 1, \dots, J_{\sigma t}; m_2 = 1, \dots, J_{\sigma s, l=0}$, where the quantities t_j enumerate the parameters underlying the total cross sections, and the quantities s_{m_2} denote the parameters underlying the zeroth-order scattering cross sections;

(2) $\left(\frac{\partial^2 L}{\partial t_j \partial s_{m_2}}\right)_{(t=\sigma_t, s=\sigma_{s,l} \geq 1)}, j = 1, \dots, J_{\sigma t}; m_2 = 1, \dots, J_{\sigma s, l \geq 1}$, where the quantities t_j enumerate the parameters underlying the total cross sections, and the quantities s_{m_2} denote the parameters underlying the l^{th} -order ($l \geq 1$) scattering cross sections.

3.2.1. Second-Order Sensitivities $\left(\frac{\partial^2 L}{\partial t_j \partial s_{m_2}}\right)_{(t=\sigma_t, s=\sigma_{s,l}=0)}, j = 1, \dots, J_{\sigma t}; m_2 = 1, \dots, J_{\sigma s, l=0}$

Contributions to the second-order sensitivities $\left(\frac{\partial^2 L}{\partial t_j \partial s_{m_2}}\right)_{(t=\sigma_t, s=\sigma_{s,l}=0)}$ stem from Equation (159) in [3], which takes the following form for the PERP benchmark:

$$\begin{aligned} \left(\frac{\partial^2 L}{\partial t_j \partial s_{m_2}}\right)_{(t=\sigma_t, s=\sigma_{s,l}=0)}^{(1)} &= \sum_{g=1}^G \int_V dV \int_{4\pi} d\Omega \psi_{1,j}^{(2),g}(r, \Omega) \sum_{g'=1}^G \int_{4\pi} d\Omega' \psi^{(1),g'}(r, \Omega') \frac{\partial \Sigma_s^{g \rightarrow g'}(s; \Omega \rightarrow \Omega')}{\partial s_{m_2}} \\ &+ \sum_{g=1}^G \int_V dV \int_{4\pi} d\Omega \psi_{2,j}^{(2),g}(r, \Omega) \sum_{g'=1}^G \int_{4\pi} d\Omega' \varphi^{g'}(r, \Omega') \frac{\partial \Sigma_s^{g' \rightarrow g}(s; \Omega' \rightarrow \Omega)}{\partial s_{m_2}}, \end{aligned} \tag{71}$$

for $j = 1, \dots, J_{\sigma t}; m_2 = 1, \dots, J_{\sigma s, l=0}$

Contributions to the second-order sensitivities $\left(\frac{\partial^2 L}{\partial t_j \partial s_{m_2}}\right)_{(t=\sigma_t, s=\sigma_{s,l}=0)}$, in addition to those shown in Equation (71), also arise from the zeroth-order scattering cross sections. These contributions are computed by particularizing Equation (158) in [3], and by noting that $\frac{\partial^2 L}{\partial t_j \partial t_{m_2}} \frac{\partial t_{m_2}}{\partial s_{m_2}} = \frac{\partial^2 L}{\partial t_j \partial s_{m_2}}, \frac{\partial^2 \Sigma_t^g(\mathbf{t})}{\partial t_j \partial t_{m_2}} \frac{\partial t_{m_2}}{\partial s_{m_2}} = \frac{\partial^2 \Sigma_t^g(\mathbf{t})}{\partial t_j \partial s_{m_2}}$ and $\frac{\partial^2 \Sigma_t^g(\mathbf{t})}{\partial t_{m_2}} \frac{\partial t_{m_2}}{\partial s_{m_2}} = \frac{\partial^2 \Sigma_t^g(\mathbf{t})}{\partial s_{m_2}}$, to obtain:

$$\begin{aligned} \left(\frac{\partial^2 L}{\partial t_j \partial s_{m_2}}\right)_{(t=\sigma_t, s=\sigma_{s,l}=0)}^{(2)} &= - \sum_{g=1}^G \int_V dV \int_{4\pi} d\Omega \psi^{(1),g}(r, \Omega) \varphi^g(r, \Omega) \frac{\partial^2 \Sigma_t^g(\mathbf{t})}{\partial t_j \partial s_{m_2}} \\ &- \sum_{g=1}^G \int_V dV \int_{4\pi} d\Omega \left[\psi_{1,j}^{(2),g}(r, \Omega) \psi^{(1),g}(r, \Omega) + \psi_{2,j}^{(2),g}(r, \Omega) \varphi^g(r, \Omega) \right] \frac{\partial \Sigma_t^g(\mathbf{t})}{\partial s_{m_2}}, \end{aligned} \tag{72}$$

for $j = 1, \dots, J_{\sigma t}; m_2 = 1, \dots, J_{\sigma s, l=0}$.

In Equations (71) and (72), the adjoint functions $\psi_{1,j}^{(2),g}, j = 1, \dots, J_{\sigma t}; g = 1, \dots, G$ and $\psi_{2,j}^{(2),g}, j = 1, \dots, J_{\sigma t}; g = 1, \dots, G$ are the solutions of the second-level adjoint sensitivity system (2nd-LASS) as presented in Equations (32), (24), (39) and (40) of Part I [1], which are reproduced below for convenient reference:

$$B^g(\alpha^0) \psi_{1,j}^{(2),g}(r, \Omega) = -\delta_{g,j} N_{i,m_j} \varphi^g(r, \Omega), j = 1, \dots, J_{\sigma t}; g = 1, \dots, G, \tag{73}$$

$$\psi_{1,j}^{(2),g}(r_d, \Omega) = 0, \Omega \cdot \mathbf{n} < 0; j = 1, \dots, J_{\sigma t}; g = 1, \dots, G, \tag{74}$$

$$A^{(1),g}(\alpha^0) \psi_{2,j}^{(2),g}(r, \Omega) = -\delta_{g,j} N_{i,m_j} \psi^{(1),g}(r, \Omega), j = 1, \dots, J_{\sigma t}; g = 1, \dots, G, \tag{75}$$

$$\psi_{2,j}^{(2),g}(r_d, \Omega) = 0, \Omega \cdot \mathbf{n} > 0; j = 1, \dots, J_{\sigma t}; g = 1, \dots, G. \tag{76}$$

Adding Equations (71) and (72) yields the following expression:

$$\begin{aligned} \left(\frac{\partial^2 L}{\partial t_j \partial s_{m_2}}\right)_{(t=\sigma_t, s=\sigma_{s,l}=0)} &= \left(\frac{\partial^2 L}{\partial t_j \partial s_{m_2}}\right)_{(t=\sigma_t, s=\sigma_{s,l}=0)}^{(1)} + \left(\frac{\partial^2 L}{\partial t_j \partial s_{m_2}}\right)_{(t=\sigma_t, s=\sigma_{s,l}=0)}^{(2)} \\ &= - \sum_{g=1}^G \int_V dV \int_{4\pi} d\Omega \psi^{(1),g}(r, \Omega) \varphi^g(r, \Omega) \frac{\partial^2 \Sigma_t^g(\mathbf{t})}{\partial t_j \partial s_{m_2}} \\ &\quad - \sum_{g=1}^G \int_V dV \int_{4\pi} d\Omega \left[\psi_{1,j}^{(2),g}(r, \Omega) \psi^{(1),g}(r, \Omega) + \psi_{2,j}^{(2),g}(r, \Omega) \varphi^g(r, \Omega) \right] \frac{\partial \Sigma_t^g(\mathbf{t})}{\partial s_{m_2}} \\ &\quad + \sum_{g=1}^G \int_V dV \int_{4\pi} d\Omega \psi_{1,j}^{(2),g}(r, \Omega) \sum_{g'=1}^G \int_{4\pi} d\Omega' \psi^{(1),g'}(r, \Omega') \frac{\partial \Sigma_s^{g \rightarrow g'}(\mathbf{s}; \Omega \rightarrow \Omega')}{\partial s_{m_2}} \\ &\quad + \sum_{g=1}^G \int_V dV \int_{4\pi} d\Omega \psi_{2,j}^{(2),g}(r, \Omega) \sum_{g'=1}^G \int_{4\pi} d\Omega' \varphi^{g'}(r, \Omega') \frac{\partial \Sigma_s^{g' \rightarrow g}(\mathbf{s}; \Omega' \rightarrow \Omega)}{\partial s_{m_2}}, \end{aligned} \tag{77}$$

for $j = 1, \dots, J_{\sigma t}; m_2 = 1, \dots, J_{\sigma s, l=0}$.

Noting that

$$\frac{\partial^2 \Sigma_t^g(\mathbf{t})}{\partial t_j \partial s_{m_2}} = \frac{\partial^2 \Sigma_t^g(\mathbf{t})}{\partial \sigma_{t, i_j}^{g_j} \partial \sigma_{s, l_{m_2}, i_{m_2}}^{g'_{m_2} j \rightarrow g_{m_2}}} = 0, \tag{78}$$

inserting the results obtained in Equations (78), (34), (39) and (40) into Equation (77), using the addition theorem for spherical harmonics in one-dimensional geometry, performing the respective angular integrations, and setting $l_{m_2} = 0$ in the resulting expression yields:

$$\begin{aligned} \left(\frac{\partial^2 L}{\partial t_j \partial s_{m_2}}\right)_{(t=\sigma_t, s=\sigma_{s,l}=0)} &= N_{i_{m_2}, m_{m_2}} \int_V dV \left[\xi_0^{(1), g_{m_2}}(r) \xi_{1, j; 0}^{(2), g'_{m_2}}(r) + \varphi_0^{g'_{m_2}}(r) \xi_{2, j; 0}^{(2), g_{m_2}}(r) \right] \\ &\quad - N_{i_{m_2}, m_{m_2}} \int_V dV \int_{4\pi} d\Omega \left[\psi_{1, j}^{(2), g'_{m_2}}(r, \Omega) \psi^{(1), g'_{m_2}}(r, \Omega) + \psi_{2, j}^{(2), g'_{m_2}}(r, \Omega) \varphi^{g'_{m_2}}(r, \Omega) \right], \end{aligned} \tag{79}$$

for $j = 1, \dots, J_{\sigma t}; m_2 = 1, \dots, J_{\sigma s, l=0}$.

3.2.2. Second-Order Sensitivities $\left(\frac{\partial^2 L}{\partial t_j \partial s_{m_2}}\right)_{(t=\sigma_t, s=\sigma_{s,l} \geq 1)}$, $j = 1, \dots, J_{\sigma t}; m_2 = 1, \dots, J_{\sigma s, l \geq 1}$

The contributions to $\left(\frac{\partial^2 L}{\partial t_j \partial s_{m_2}}\right)_{(t=\sigma_t, s=\sigma_{s,l} \geq 1)}$, $j = 1, \dots, J_{\sigma t}; m_2 = 1, \dots, J_{\sigma s, l \geq 1}$ stem only from the right side of the general expression shown in Equation (71), which takes on the following specific form in this case:

$$\begin{aligned} \left(\frac{\partial^2 L}{\partial t_j \partial s_{m_2}}\right)_{(t=\sigma_t, s=\sigma_{s,l} \geq 1)} &= \sum_{g=1}^G \int_V dV \int_{4\pi} d\Omega \psi_{1, j}^{(2), g}(r, \Omega) \sum_{g'=1}^G \int_{4\pi} d\Omega' \psi^{(1), g'}(r, \Omega') \frac{\partial \Sigma_s^{g \rightarrow g'}(\mathbf{s}; \Omega \rightarrow \Omega')}{\partial s_{m_2}} \\ &\quad + \sum_{g=1}^G \int_V dV \int_{4\pi} d\Omega \psi_{2, j}^{(2), g}(r, \Omega) \sum_{g'=1}^G \int_{4\pi} d\Omega' \varphi^{g'}(r, \Omega') \frac{\partial \Sigma_s^{g' \rightarrow g}(\mathbf{s}; \Omega' \rightarrow \Omega)}{\partial s_{m_2}}, \end{aligned} \tag{80}$$

$j = 1, \dots, J_{\sigma t}; m_2 = 1, \dots, J_{\sigma s, l \geq 1}$.

For this case, $t_j \equiv \sigma_{t, i_j}^{g_j}$ enumerates the parameters underlying the total cross sections, while $s_{m_2} \equiv \sigma_{s, l_{m_2}, i_{m_2}}^{g'_{m_2} \rightarrow g_{m_2}}$ enumerates the parameters underlying the l^{th} -order ($l \geq 1$) scattering cross sections. Using the result obtained in Equations (39) and (40) in Equation (80) transforms the latter into the following form:

$$\begin{aligned} \left(\frac{\partial^2 L}{\partial t_j \partial s_{m_2}}\right)_{(t=\sigma_t, s=\sigma_{s,l} \geq 1)} &= N_{i_{m_2}, m_{m_2}} (2l_{m_2} + 1) \int_V dV \left[\xi_{l_{m_2}}^{(1), g_{m_2}}(r) \xi_{1, j; l_{m_2}}^{(2), g'_{m_2}}(r) + \varphi_{l_{m_2}}^{g'_{m_2}}(r) \xi_{2, j; l_{m_2}}^{(2), g_{m_2}}(r) \right], \end{aligned} \tag{81}$$

for $j = 1, \dots, J_{\sigma t}; m_2 = 1, \dots, J_{\sigma s, l \geq 1}; l = 1, \dots, ISCT$.

3.3. Numerical Results for $\partial^2 L / \partial t_j \partial s_{m_2}$, $j = 1, \dots, J_{\sigma t}$; $m_2 = 1, \dots, J_{\sigma s}$

The second-order absolute sensitivities, $\partial^2 L / \partial t_j \partial s_{m_2}$, $j = 1, \dots, J_{\sigma t}$; $m_2 = 1, \dots, J_{\sigma s}$, of the leakage response with respect to the total cross sections and the scattering cross sections for all isotopes of the PERP benchmark have been computed using Equations (79) and (81), and have been independently verified by re-computing them using Equations (68) and (70), respectively. The dimensions of the matrix $\partial^2 L / \partial t_j \partial s_{m_2}$, $j = 1, \dots, J_{\sigma t}$; $m_2 = 1, \dots, J_{\sigma s}$ is $J_{\sigma t} \times J_{\sigma s}$ ($= 180 \times 21600$), where $J_{\sigma t} = G \times I = 30 \times 6 = 180$ and $J_{\sigma s} = G \times G \times (ISCT + 1) \times I = 30 \times 30 \times 4 \times 6 = 21600$. For convenient comparisons, the numerical results presented in this sub-section are displayed in unit-less values of the relative sensitivities corresponding to $\partial^2 L / \partial t_j \partial s_{m_2}$, which are denoted as $\mathbf{S}^{(2)}(\sigma_{t,i}^g, \sigma_{s,l,k}^{g' \rightarrow h})$ and are defined as follows:

$$\mathbf{S}^{(2)}(\sigma_{t,i}^g, \sigma_{s,l,k}^{g' \rightarrow h}) \triangleq \frac{\partial^2 L}{\partial \sigma_{t,i}^g \partial \sigma_{s,l,k}^{g' \rightarrow h}} \left(\frac{\sigma_{t,i}^g \sigma_{s,l,k}^{g' \rightarrow h}}{L} \right), \quad l = 0, \dots, 3; \quad i, k = 1, \dots, 6; \quad g, g', h = 1, \dots, 30. \quad (82)$$

To facilitate the presentation and interpretation of the numerical results, the $J_{\sigma t} \times J_{\sigma s}$ ($= 180 \times 21600$) matrix $\mathbf{S}^{(2)}(\sigma_{t,i}^g, \sigma_{s,l,k}^{g' \rightarrow h})$ was partitioned into $I \times I \times (ISCT + 1) = 6 \times 6 \times 4$ submatrices, each of dimensions $G \times (G \cdot G) = 30 \times 900$; the respective results are summarized in following four subsections, which present the results for scattering orders $l = 0$, $l = 1$, $l = 2$, and $l = 3$, respectively.

3.3.1. Results for the Relative Sensitivities $\mathbf{S}^{(2)}(\sigma_{t,i}^g, \sigma_{s,l=0,k}^{g' \rightarrow h})$

The results for second-order relative sensitivities of the leakage response with respect to the total cross sections and the zeroth-order scattering cross sections between all isotopes, $\mathbf{S}^{(2)}(\sigma_{t,i}^g, \sigma_{s,l=0,k}^{g' \rightarrow h}) \triangleq \left(\partial^2 L / \partial \sigma_{t,i}^g \partial \sigma_{s,l=0,k}^{g' \rightarrow h} \right) \left(\sigma_{t,i}^g \sigma_{s,l=0,k}^{g' \rightarrow h} / L \right)$, $l = 0$; $i, k = 1, \dots, 6$; $g, g', h = 1, \dots, 30$, are presented in Table 12. For every submatrix in Table 12 that comprises components having absolute values greater than 1.0, the total number of such elements are counted and shown in the table. Otherwise, if the absolute values of all elements in such a submatrix are less than 1.0, only the value of the largest element of the respective submatrix is shown in Table 12. It is noteworthy that most of the largest elements of $\mathbf{S}^{(2)}(\sigma_{t,i}^g, \sigma_{s,l=0,k}^{g' \rightarrow h}) \triangleq \left(\partial^2 L / \partial \sigma_{t,i}^g \partial \sigma_{s,l=0,k}^{g' \rightarrow h} \right) \left(\sigma_{t,i}^g \sigma_{s,l=0,k}^{g' \rightarrow h} / L \right)$ are negative, and the vast majority of them are very small. For example, of the 30×900 elements in the submatrix $\mathbf{S}^{(2)}(\sigma_{t,1}^g, \sigma_{s,l=0,1}^{g' \rightarrow h})$, 7658 elements are negative, 2482 elements are positive, and the rest are zero.

Table 12. Summary of second-order relative sensitivities of the leakage response with respect to the total cross sections and the zeroth-order ($l = 0$) scattering cross sections for all isotopes: $\mathbf{S}^{(2)}\left(\sigma_{t,i}^g, \sigma_{s,l=0,k}^{g'\rightarrow h}\right) \triangleq \left(\partial^2 L / \partial \sigma_{t,i}^g \partial \sigma_{s,l=0,k}^{g'\rightarrow h}\right) \left(\sigma_{t,i}^g, \sigma_{s,l=0,k}^{g'\rightarrow h} / L\right)$, $l = 0$; $i, k = 1, \dots, 6$; $g, g', h = 1, \dots, 30$.

	$k = 1$ (^{239}Pu)	$k = 2$ (^{240}Pu)	$k = 3$ (^{69}Ga)	$k = 4$ (^{71}Ga)	$k = 5$ (C)	$k = 6$ (^1H)
$i = 1$ (^{239}Pu)	$\mathbf{S}^{(2)}\left(\begin{matrix} \sigma_{t,1'}^g \\ \sigma_{s,l=0,1}^{g'\rightarrow h} \end{matrix}\right)$ Min. value = -6.44×10^{-1} at $g=12$, $g'=12, h=12$	$\mathbf{S}^{(2)}\left(\begin{matrix} \sigma_{t,1'}^g \\ \sigma_{s,l=0,2}^{g'\rightarrow h} \end{matrix}\right)$ Min. value = -4.26×10^{-2} at $g=12$, $g'=12, h=12$	$\mathbf{S}^{(2)}\left(\begin{matrix} \sigma_{t,1'}^g \\ \sigma_{s,l=0,3}^{g'\rightarrow h} \end{matrix}\right)$ Min. value = -2.46×10^{-3} at $g=12$, $g'=12, h=12$	$\mathbf{S}^{(2)}\left(\begin{matrix} \sigma_{t,1'}^g \\ \sigma_{s,l=0,4}^{g'\rightarrow h} \end{matrix}\right)$ Min. value = -1.58×10^{-3} at $g=12$, $g'=12, h=12$	$\mathbf{S}^{(2)}\left(\begin{matrix} \sigma_{t,1'}^g \\ \sigma_{s,l=0,5}^{g'\rightarrow h} \end{matrix}\right)$ Min. value = -2.65×10^{-1} at $g=12$, $g'=12, h=12$	$\mathbf{S}^{(2)}\left(\begin{matrix} \sigma_{t,1'}^g \\ \sigma_{s,l=0,6}^{g'\rightarrow h} \end{matrix}\right)$ Min. value = -3.48×10^{-1} at $g=12$, $g'=12, h=13$
$i = 2$ (^{240}Pu)	$\mathbf{S}^{(2)}\left(\begin{matrix} \sigma_{t,2'}^g \\ \sigma_{s,l=0,1}^{g'\rightarrow h} \end{matrix}\right)$ Min. value = -4.08×10^{-2} at $g=12$, $g'=12, h=12$	$\mathbf{S}^{(2)}\left(\begin{matrix} \sigma_{t,2'}^g \\ \sigma_{s,l=0,2}^{g'\rightarrow h} \end{matrix}\right)$ Min. value = -2.70×10^{-3} at $g=12$, $g'=12, h=12$	$\mathbf{S}^{(2)}\left(\begin{matrix} \sigma_{t,2'}^g \\ \sigma_{s,l=0,3}^{g'\rightarrow h} \end{matrix}\right)$ Min. value = -1.56×10^{-4} at $g=12$, $g'=12, h=12$	$\mathbf{S}^{(2)}\left(\begin{matrix} \sigma_{t,2'}^g \\ \sigma_{s,l=0,4}^{g'\rightarrow h} \end{matrix}\right)$ Min. value = -1.01×10^{-4} at $g=12$, $g'=12, h=12$	$\mathbf{S}^{(2)}\left(\begin{matrix} \sigma_{t,2'}^g \\ \sigma_{s,l=0,5}^{g'\rightarrow h} \end{matrix}\right)$ Min. value = -1.69×10^{-2} at $g=12$, $g'=12, h=12$	$\mathbf{S}^{(2)}\left(\begin{matrix} \sigma_{t,2'}^g \\ \sigma_{s,l=0,6}^{g'\rightarrow h} \end{matrix}\right)$ Min. value = -2.20×10^{-2} at $g=12$, $g'=12, h=13$
$i = 3$ (^{69}Ga)	$\mathbf{S}^{(2)}\left(\begin{matrix} \sigma_{t,3'}^g \\ \sigma_{s,l=0,1}^{g'\rightarrow h} \end{matrix}\right)$ Min. value = -1.83×10^{-3} at $g=12$, $g'=12, h=12$	$\mathbf{S}^{(2)}\left(\begin{matrix} \sigma_{t,3'}^g \\ \sigma_{s,l=0,2}^{g'\rightarrow h} \end{matrix}\right)$ Min. value = -1.27×10^{-4} at $g=13$, $g'=13, h=13$	$\mathbf{S}^{(2)}\left(\begin{matrix} \sigma_{t,3'}^g \\ \sigma_{s,l=0,3}^{g'\rightarrow h} \end{matrix}\right)$ Min. value = -7.01×10^{-6} at $g=12$, $g'=12, h=12$	$\mathbf{S}^{(2)}\left(\begin{matrix} \sigma_{t,3'}^g \\ \sigma_{s,l=0,4}^{g'\rightarrow h} \end{matrix}\right)$ Min. value = -4.54×10^{-6} at $g=13$, $g'=13, h=13$	$\mathbf{S}^{(2)}\left(\begin{matrix} \sigma_{t,3'}^g \\ \sigma_{s,l=0,5}^{g'\rightarrow h} \end{matrix}\right)$ Min. value = -7.57×10^{-4} at $g=12$, $g'=12, h=12$	$\mathbf{S}^{(2)}\left(\begin{matrix} \sigma_{t,3'}^g \\ \sigma_{s,l=0,6}^{g'\rightarrow h} \end{matrix}\right)$ Min. value = -1.03×10^{-3} at $g=16$, $g'=16, h=16$
$i = 4$ (^{71}Ga)	$\mathbf{S}^{(2)}\left(\begin{matrix} \sigma_{t,4'}^g \\ \sigma_{s,l=0,1}^{g'\rightarrow h} \end{matrix}\right)$ Min. value = -1.24×10^{-3} at $g=12$, $g'=12, h=12$	$\mathbf{S}^{(2)}\left(\begin{matrix} \sigma_{t,4'}^g \\ \sigma_{s,l=0,2}^{g'\rightarrow h} \end{matrix}\right)$ Min. value = -8.58×10^{-5} at $g=13$, $g'=13, h=13$	$\mathbf{S}^{(2)}\left(\begin{matrix} \sigma_{t,4'}^g \\ \sigma_{s,l=0,3}^{g'\rightarrow h} \end{matrix}\right)$ Min. value = -4.75×10^{-6} at $g=12$, $g'=12, h=12$	$\mathbf{S}^{(2)}\left(\begin{matrix} \sigma_{t,4'}^g \\ \sigma_{s,l=0,4}^{g'\rightarrow h} \end{matrix}\right)$ Min. value = 1.93×10^{-5} at $g=22$, $g'=22, h=22$	$\mathbf{S}^{(2)}\left(\begin{matrix} \sigma_{t,4'}^g \\ \sigma_{s,l=0,5}^{g'\rightarrow h} \end{matrix}\right)$ Min. value = -5.13×10^{-4} at $g=12$, $g'=12, h=12$	$\mathbf{S}^{(2)}\left(\begin{matrix} \sigma_{t,4'}^g \\ \sigma_{s,l=0,6}^{g'\rightarrow h} \end{matrix}\right)$ Min. value = 1.03×10^{-3} at $g=22$, $g'=22, h=23$
$i = 5$ (C)	$\mathbf{S}^{(2)}\left(\begin{matrix} \sigma_{t,5'}^g \\ \sigma_{s,l=0,1}^{g'\rightarrow h} \end{matrix}\right)$ Min. value = -1.71×10^{-1} at $g=30$, $g'=12, h=12$	$\mathbf{S}^{(2)}\left(\begin{matrix} \sigma_{t,5'}^g \\ \sigma_{s,l=0,2}^{g'\rightarrow h} \end{matrix}\right)$ Min. value = -1.13×10^{-2} at $g=30$, $g'=12, h=12$	$\mathbf{S}^{(2)}\left(\begin{matrix} \sigma_{t,5'}^g \\ \sigma_{s,l=0,3}^{g'\rightarrow h} \end{matrix}\right)$ Min. value = -6.54×10^{-4} at $g=30$, $g'=12, h=12$	$\mathbf{S}^{(2)}\left(\begin{matrix} \sigma_{t,5'}^g \\ \sigma_{s,l=0,4}^{g'\rightarrow h} \end{matrix}\right)$ Min. value = -4.20×10^{-4} at $g=30$, $g'=12, h=12$	$\mathbf{S}^{(2)}\left(\begin{matrix} \sigma_{t,5'}^g \\ \sigma_{s,l=0,5}^{g'\rightarrow h} \end{matrix}\right)$ Min. value = -1.13×10^{-1} at $g=30$, $g'=12, h=12$	$\mathbf{S}^{(2)}\left(\begin{matrix} \sigma_{t,5'}^g \\ \sigma_{s,l=0,6}^{g'\rightarrow h} \end{matrix}\right)$ Min. value = -9.03×10^{-1} at $g=30$, $g'=30, h=30$
$i = 6$ (^1H)	$\mathbf{S}^{(2)}\left(\begin{matrix} \sigma_{t,6'}^g \\ \sigma_{s,l=0,1}^{g'\rightarrow h} \end{matrix}\right)$ g8 elements with absolute values >1.0	$\mathbf{S}^{(2)}\left(\begin{matrix} \sigma_{t,6'}^g \\ \sigma_{s,l=0,2}^{g'\rightarrow h} \end{matrix}\right)$ Min. value = -1.35×10^{-1} at $g=30$, $g'=12, h=12$	$\mathbf{S}^{(2)}\left(\begin{matrix} \sigma_{t,6'}^g \\ \sigma_{s,l=0,3}^{g'\rightarrow h} \end{matrix}\right)$ Min. value = -7.80×10^{-3} at $g=30$, $g'=12, h=12$	$\mathbf{S}^{(2)}\left(\begin{matrix} \sigma_{t,6'}^g \\ \sigma_{s,l=0,4}^{g'\rightarrow h} \end{matrix}\right)$ Min. value = -5.01×10^{-3} at $g=30$, $g'=12, h=12$	$\mathbf{S}^{(2)}\left(\begin{matrix} \sigma_{t,6'}^g \\ \sigma_{s,l=0,5}^{g'\rightarrow h} \end{matrix}\right)$ 3 elements with absolute values >1.0	$\mathbf{S}^{(2)}\left(\begin{matrix} \sigma_{t,6'}^g \\ \sigma_{s,l=0,6}^{g'\rightarrow h} \end{matrix}\right)$ 26 elements with absolute values >1.0

As shown in Table 12, the largest absolute values of the mixed second-order sensitivities mostly involve the zeroth-order self-scattering cross sections in the 12th energy group of the isotopes, and either the total cross sections for the 12th energy group for isotopes $^{239}\text{Pu}, ^{240}\text{Pu}, ^{69}\text{Ga}$ and ^{71}Ga , or the total cross sections for the 30th energy group for isotopes C and ^1H .

Additional information regarding the three submatrices in Table 12 that have elements with absolute values greater than 1.0 is provided below:

- (1) The eight elements in the submatrix $\mathbf{S}^{(2)}\left(\sigma_{t,i=6'}^g, \sigma_{s,l=0,k=1}^{g'\rightarrow h}\right)$, $g, g', h = 1, \dots, 30$ (of second-order sensitivities of the leakage response with respect to the total cross sections of ^1H and to the zeroth-order scattering cross sections of ^{239}Pu) that have values greater than 1.0 are presented in Table 14. All of these relative sensitivities are with respect to the same total cross section parameter $\sigma_{t,6}^{g=30}$ and to the zeroth-order self-scattering cross sections. The relative sensitivities with respect to the 0th-order in-scattering and out-scattering cross sections are all smaller than 1.0.

- (2) The sensitivity matrix $\mathbf{S}^{(2)}\left(\sigma_{t,i=6}^g, \sigma_{s,l=0,k=5}^{g' \rightarrow h}\right)$, $g, g', h = 1, \dots, 30$, comprising the second-order mixed sensitivities of the leakage response with respect to the total cross sections of ^1H and to the zeroth-order scattering cross sections of C, includes 3 elements that have values greater than 1.0: $S^{(2)}\left(\sigma_{t,i=6}^{30}, \sigma_{s,l=0,k=5}^{12 \rightarrow 12}\right) = -1.346$, $S^{(2)}\left(\sigma_{t,i=6}^{30}, \sigma_{s,l=0,k=5}^{13 \rightarrow 13}\right) = -1.284$, and $S^{(2)}\left(\sigma_{t,i=6}^{30}, \sigma_{s,l=0,k=5}^{14 \rightarrow 14}\right) = -1.031$. These three sensitivities are with respect to the same total cross section parameter $\sigma_{t,6}^{g=30}$ and to the zeroth-order self-scattering cross sections, just as the sensitivities presented in Table 14.
- (3) The sensitivity matrix $\mathbf{S}^{(2)}\left(\sigma_{t,i=6}^g, \sigma_{s,l=0,k=6}^{g' \rightarrow h}\right)$, $g, g', h = 1, \dots, 30$, comprising the second-order sensitivities of the leakage response with respect to the total cross sections of ^1H and to the zeroth-order scattering cross sections of ^1H , includes 26 elements that have values greater than 1.0, as listed in Table 13. All these 26 relative sensitivities are with respect to the total cross section $\sigma_{t,6}^{g=30}$. The element having the largest absolute value is $S^{(2)}\left(\sigma_{t,i=6}^{30}, \sigma_{s,l=0,k=6}^{30 \rightarrow 30}\right) = -10.77$.

Table 13. Elements of $\mathbf{S}^{(2)}\left(\sigma_{t,i=6}^g, \sigma_{s,l=0,k=6}^{g' \rightarrow h}\right)$, $g, g', h = 1, \dots, 30$ with absolute values greater than 1.0.

	$g' \rightarrow h$ 11 → 12	$g' \rightarrow h$ 12 → 12	$g' \rightarrow h$ 12 → 13	$g' \rightarrow h$ 13 → 13	$g' \rightarrow h$ 12 → 14	$g' \rightarrow h$ 13 → 14	$g' \rightarrow h$ 14 → 14	$g' \rightarrow h$ 12 → 15	$g' \rightarrow h$ 13 → 15
g=30	-1.205	-1.332	-2.338	-1.329	-1.609	-2.252	-1.170	-1.076	-1.539
	$g' \rightarrow h$ 14 → 15	$g' \rightarrow h$ 12 → 16	$g' \rightarrow h$ 13 → 16	$g' \rightarrow h$ 14 → 16	$g' \rightarrow h$ 15 → 16	$g' \rightarrow h$ 16 → 16	$g' \rightarrow h$ 15 → 17	$g' \rightarrow h$ 16 → 17	$g' \rightarrow h$ 17 → 17
g=30	-1.967	-1.152	-1.677	-2.198	-2.618	-2.157	-1.099	-3.087	-1.485
	$g' \rightarrow h$ 16 → 18	$g' \rightarrow h$ 17 → 18	$g' \rightarrow h$ 18 → 18	$g' \rightarrow h$ 18 → 19	$g' \rightarrow h$ 19 → 20	$g' \rightarrow h$ 20 → 21	$g' \rightarrow h$ 29 → 30	$g' \rightarrow h$ 30 → 30	
g=30	-1.266	-2.023	-1.089	-1.496	-1.243	-1.039	-1.205	-10.77	

Table 14. Elements of $\mathbf{S}^{(2)}\left(\sigma_{t,i=6}^g, \sigma_{s,l=0,k=1}^{g' \rightarrow h}\right)$, $g, g', h = 1, \dots, 30$, with absolute values greater than 1.0.

	$g' \rightarrow h$ 7 → 7	$g' \rightarrow h$ 8 → 8	$g' \rightarrow h$ 9 → 9	$g' \rightarrow h$ 10 → 10	$g' \rightarrow h$ 11 → 11	$g' \rightarrow h$ 12 → 12	$g' \rightarrow h$ 13 → 13	$g' \rightarrow h$ 14 → 14
g=30	-1.598	-1.262	-1.313	-1.244	-1.118	-2.039	-1.739	-1.268

3.3.2. Results for the Relative Sensitivities $\mathbf{S}^{(2)}\left(\sigma_{t,i}^g, \sigma_{s,l=1,k}^{g' \rightarrow h}\right)$

The numerical results for $\mathbf{S}^{(2)}\left(\sigma_{t,i}^g, \sigma_{s,l=1,k}^{g' \rightarrow h}\right) \triangleq \left(\partial^2 L / \partial \sigma_{t,i}^g \partial \sigma_{s,l=1,k}^{g' \rightarrow h}\right) \left(\sigma_{t,i}^g, \sigma_{s,l=1,k}^{g' \rightarrow h} / L\right)$, $l = 1$; $i, k = 1, \dots, 6$, $g, g', h = 1, \dots, 30$, comprising the second-order relative sensitivities of the leakage response with respect to the total cross sections and the first-order scattering cross sections between all isotopes, are summarized in Table 15. Only 15 components of $\mathbf{S}^{(2)}\left(\sigma_{t,i}^g, \sigma_{s,l=1,k}^{g' \rightarrow h}\right)$ have relative sensitivities greater than 1.0.

Table 15. Summary of second-order relative sensitivities of the leakage response with respect to the total cross sections and the first-order ($l = 1$) scattering cross sections for all isotopes: $\mathbf{S}^{(2)}\left(\sigma_{t,i'}^g \sigma_{s,l=1,k}^{g' \rightarrow h}\right) \triangleq \left(\partial^2 L / \partial \sigma_{t,i}^g \partial \sigma_{s,l=1,k}^{g' \rightarrow h}\right) \left(\sigma_{t,i}^g \sigma_{s,l=1,k}^{g' \rightarrow h} / L\right)$, $l = 1$; $i, k = 1, \dots, 6$; $g, g', h = 1, \dots, 30$.

	$k = 1$ (^{239}Pu)	$k = 2$ (^{240}Pu)	$k = 3$ (^{69}Ga)	$k = 4$ (^{71}Ga)	$k = 5$ (C)	$k = 6$ (^1H)
$i = 1$ (^{239}Pu)	$\mathbf{S}^{(2)}\left(\begin{matrix} \sigma_{s,l=1,1}^g \\ \sigma_{s,l=1,1}^{g' \rightarrow h} \end{matrix}\right)$ Max. value = 3.34×10^{-1} at $g=7,$ $g'=7, h=7$	$\mathbf{S}^{(2)}\left(\begin{matrix} \sigma_{s,l=1,2}^g \\ \sigma_{s,l=1,2}^{g' \rightarrow h} \end{matrix}\right)$ Max. value = 2.07×10^{-2} at $g=12,$ $g'=12, h=12$	$\mathbf{S}^{(2)}\left(\begin{matrix} \sigma_{s,l=1,3}^g \\ \sigma_{s,l=1,3}^{g' \rightarrow h} \end{matrix}\right)$ Max. value = 6.84×10^{-4} at $g=12,$ $g'=12, h=12$	$\mathbf{S}^{(2)}\left(\begin{matrix} \sigma_{s,l=1,4}^g \\ \sigma_{s,l=1,4}^{g' \rightarrow h} \end{matrix}\right)$ Max. value = 4.10×10^{-4} at $g=7,$ $g'=7, h=7$	$\mathbf{S}^{(2)}\left(\begin{matrix} \sigma_{s,l=1,5}^g \\ \sigma_{s,l=1,5}^{g' \rightarrow h} \end{matrix}\right)$ Max. value = 1.10×10^{-1} at $g=12,$ $g'=12, h=12$	$\mathbf{S}^{(2)}\left(\begin{matrix} \sigma_{s,l=1,6}^g \\ \sigma_{s,l=1,6}^{g' \rightarrow h} \end{matrix}\right)$ Max. value = 3.46×10^{-1} at $g=12,$ $g'=12, h=12$
$i = 2$ (^{240}Pu)	$\mathbf{S}^{(2)}\left(\begin{matrix} \sigma_{s,l=1,1}^g \\ \sigma_{s,l=1,1}^{g' \rightarrow h} \end{matrix}\right)$ Max. value = 2.10×10^{-2} at $g=12,$ $g'=12, h=12$	$\mathbf{S}^{(2)}\left(\begin{matrix} \sigma_{s,l=1,2}^g \\ \sigma_{s,l=1,2}^{g' \rightarrow h} \end{matrix}\right)$ Max. value = 1.31×10^{-3} at $g=12,$ $g'=12, h=12$	$\mathbf{S}^{(2)}\left(\begin{matrix} \sigma_{s,l=1,3}^g \\ \sigma_{s,l=1,3}^{g' \rightarrow h} \end{matrix}\right)$ Max. value = 4.33×10^{-5} at $g=12,$ $g'=12, h=12$	$\mathbf{S}^{(2)}\left(\begin{matrix} \sigma_{s,l=1,4}^g \\ \sigma_{s,l=1,4}^{g' \rightarrow h} \end{matrix}\right)$ Max. value = 2.57×10^{-5} at $g=7,$ $g'=7, h=7$	$\mathbf{S}^{(2)}\left(\begin{matrix} \sigma_{s,l=1,5}^g \\ \sigma_{s,l=1,5}^{g' \rightarrow h} \end{matrix}\right)$ Max. value = 6.98×10^{-5} at $g=12,$ $g'=12, h=12$	$\mathbf{S}^{(2)}\left(\begin{matrix} \sigma_{s,l=1,6}^g \\ \sigma_{s,l=1,6}^{g' \rightarrow h} \end{matrix}\right)$ Max. value = 2.20×10^{-2} at $g=12,$ $g'=12, h=12$
$i = 3$ (^{69}Ga)	$\mathbf{S}^{(2)}\left(\begin{matrix} \sigma_{s,l=1,1}^g \\ \sigma_{s,l=1,1}^{g' \rightarrow h} \end{matrix}\right)$ Max. value = 9.42×10^{-4} at $g=12,$ $g'=12, h=12$	$\mathbf{S}^{(2)}\left(\begin{matrix} \sigma_{s,l=1,2}^g \\ \sigma_{s,l=1,2}^{g' \rightarrow h} \end{matrix}\right)$ Max. value = 5.90×10^{-5} at $g=12,$ $g'=12, h=12$	$\mathbf{S}^{(2)}\left(\begin{matrix} \sigma_{s,l=1,3}^g \\ \sigma_{s,l=1,3}^{g' \rightarrow h} \end{matrix}\right)$ Max. value = 1.95×10^{-6} at $g=12,$ $g'=12, h=12$	$\mathbf{S}^{(2)}\left(\begin{matrix} \sigma_{s,l=1,4}^g \\ \sigma_{s,l=1,4}^{g' \rightarrow h} \end{matrix}\right)$ Max. value = 1.09×10^{-6} at $g=7,$ $g'=7, h=7$	$\mathbf{S}^{(2)}\left(\begin{matrix} \sigma_{s,l=1,5}^g \\ \sigma_{s,l=1,5}^{g' \rightarrow h} \end{matrix}\right)$ Max. value = 3.14×10^{-4} at $g=12,$ $g'=12, h=12$	$\mathbf{S}^{(2)}\left(\begin{matrix} \sigma_{s,l=1,6}^g \\ \sigma_{s,l=1,6}^{g' \rightarrow h} \end{matrix}\right)$ Max. value = 1.02×10^{-3} at $g=16,$ $g'=16, h=16$
$i = 4$ (^{71}Ga)	$\mathbf{S}^{(2)}\left(\begin{matrix} \sigma_{s,l=1,1}^g \\ \sigma_{s,l=1,1}^{g' \rightarrow h} \end{matrix}\right)$ Max. value = 6.39×10^{-4} at $g=12,$ $g'=12, h=12$	$\mathbf{S}^{(2)}\left(\begin{matrix} \sigma_{s,l=1,2}^g \\ \sigma_{s,l=1,2}^{g' \rightarrow h} \end{matrix}\right)$ Max. value = 4.00×10^{-5} at $g=12,$ $g'=12, h=12$	$\mathbf{S}^{(2)}\left(\begin{matrix} \sigma_{s,l=1,3}^g \\ \sigma_{s,l=1,3}^{g' \rightarrow h} \end{matrix}\right)$ Max. value = 1.32×10^{-6} at $g=12,$ $g'=12, h=12$	$\mathbf{S}^{(2)}\left(\begin{matrix} \sigma_{s,l=1,4}^g \\ \sigma_{s,l=1,4}^{g' \rightarrow h} \end{matrix}\right)$ Max. value = 7.24×10^{-7} at $g=7,$ $g'=7, h=7$	$\mathbf{S}^{(2)}\left(\begin{matrix} \sigma_{s,l=1,5}^g \\ \sigma_{s,l=1,5}^{g' \rightarrow h} \end{matrix}\right)$ Max. value = 2.13×10^{-4} at $g=12,$ $g'=12, h=12$	$\mathbf{S}^{(2)}\left(\begin{matrix} \sigma_{s,l=1,6}^g \\ \sigma_{s,l=1,6}^{g' \rightarrow h} \end{matrix}\right)$ Max. value = 6.71×10^{-4} at $g=13,$ $g'=12, h=13$
$i = 5$ (C)	$\mathbf{S}^{(2)}\left(\begin{matrix} \sigma_{s,l=1,1}^g \\ \sigma_{s,l=1,1}^{g' \rightarrow h} \end{matrix}\right)$ Max. value = 1.12×10^{-1} at $g=30,$ $g'=7, h=7$	$\mathbf{S}^{(2)}\left(\begin{matrix} \sigma_{s,l=1,2}^g \\ \sigma_{s,l=1,2}^{g' \rightarrow h} \end{matrix}\right)$ Max. value = 6.74×10^{-3} at $g=30,$ $g'=7, h=7$	$\mathbf{S}^{(2)}\left(\begin{matrix} \sigma_{s,l=1,3}^g \\ \sigma_{s,l=1,3}^{g' \rightarrow h} \end{matrix}\right)$ Max. value = 2.26×10^{-4} at $g=30,$ $g'=7, h=7$	$\mathbf{S}^{(2)}\left(\begin{matrix} \sigma_{s,l=1,4}^g \\ \sigma_{s,l=1,4}^{g' \rightarrow h} \end{matrix}\right)$ Max. value = 1.37×10^{-4} at $g=30,$ $g'=7, h=7$	$\mathbf{S}^{(2)}\left(\begin{matrix} \sigma_{s,l=1,5}^g \\ \sigma_{s,l=1,5}^{g' \rightarrow h} \end{matrix}\right)$ Max. value = 4.34×10^{-2} at $g=30,$ $g'=12, h=12$	$\mathbf{S}^{(2)}\left(\begin{matrix} \sigma_{s,l=1,6}^g \\ \sigma_{s,l=1,6}^{g' \rightarrow h} \end{matrix}\right)$ Max. value = 5.86×10^{-1} at $g=30,$ $g'=30, h=30$
$i = 6$ (^1H)	$\mathbf{S}^{(2)}\left(\begin{matrix} \sigma_{s,l=1,1}^g \\ \sigma_{s,l=1,1}^{g' \rightarrow h} \end{matrix}\right)$ 2 elements with absolute values >1.0	$\mathbf{S}^{(2)}\left(\begin{matrix} \sigma_{s,l=1,2}^g \\ \sigma_{s,l=1,2}^{g' \rightarrow h} \end{matrix}\right)$ Max. value = 8.04×10^{-2} at $g=30,$ $g'=7, h=7$	$\mathbf{S}^{(2)}\left(\begin{matrix} \sigma_{s,l=1,3}^g \\ \sigma_{s,l=1,3}^{g' \rightarrow h} \end{matrix}\right)$ Max. value = 2.70×10^{-3} at $g=30,$ $g'=7, h=7$	$\mathbf{S}^{(2)}\left(\begin{matrix} \sigma_{s,l=1,4}^g \\ \sigma_{s,l=1,4}^{g' \rightarrow h} \end{matrix}\right)$ Max. value = 1.64×10^{-3} at $g=30,$ $g'=7, h=7$	$\mathbf{S}^{(2)}\left(\begin{matrix} \sigma_{s,l=1,5}^g \\ \sigma_{s,l=1,5}^{g' \rightarrow h} \end{matrix}\right)$ Max. value = 5.18×10^{-1} at $g=30,$ $g'=12, h=12$	$\mathbf{S}^{(2)}\left(\begin{matrix} \sigma_{s,l=1,6}^g \\ \sigma_{s,l=1,6}^{g' \rightarrow h} \end{matrix}\right)$ 13 elements with absolute values >1.0

As shown in Table 15, the largest absolute values of the mixed second-order sensitivities involve mostly the first-order self-scattering cross sections in the 7th, 12th, or 30th energy groups of the isotopes, along (mostly) with either the total cross sections for the 7th or 12th energy group for isotopes $^{239}\text{Pu}, ^{240}\text{Pu}, ^{69}\text{Ga}$ and ^{71}Ga , or (occasionally) the total cross sections for the 30th energy group for isotopes C and ^1H .

Additional details regarding the two submatrices in Table 15 that comprise several elements with absolute values greater than 1.0, are provided below:

- (1) The matrix $\mathbf{S}^{(2)}\left(\sigma_{t,i=6}^g, \sigma_{s,l=1,k=1}^{g'\rightarrow h}\right) \triangleq \left(\partial^2 L / \partial \sigma_{t,i=6}^g \partial \sigma_{s,l=1,k=1}^{g'\rightarrow h}\right) \left(\sigma_{t,i=6}^g \sigma_{s,l=1,k=1}^{g'\rightarrow h} / L\right)$, $g, g', h = 1, \dots, 30$, of second-order sensitivities of the leakage response with respect to the total cross sections of ^1H and to the first-order scattering cross sections of ^{239}Pu , comprises two elements that have values greater than 1.0, namely $S^{(2)}\left(\sigma_{t,i=6}^{30}, \sigma_{s,l=1,k=1}^{7\rightarrow 7}\right) = 1.337$ and $S^{(2)}\left(\sigma_{t,i=6}^{30}, \sigma_{s,l=1,k=1}^{12\rightarrow 12}\right) = 1.018$. Both are related to the total cross section parameter $\sigma_{t,i=6}^{g=30}$ and the first-order self-scattering cross sections.
- (2) The matrix $\mathbf{S}^{(2)}\left(\sigma_{t,i=6}^g, \sigma_{s,l=1,k=6}^{g'\rightarrow h}\right) = \left(\partial^2 L / \partial \sigma_{t,i=6}^g \partial \sigma_{s,l=1,k=6}^{g'\rightarrow h}\right) \left(\sigma_{t,i=6}^g \sigma_{s,l=1,k=6}^{g'\rightarrow h} / L\right)$, $g, g', h = 1, \dots, 30$, of second-order sensitivities of the leakage response with respect to the total cross sections of ^1H and the first-order scattering cross sections of ^1H , comprises 13 elements that have values greater than 1.0 which are listed in Table 16. All the 13 sensitivities presented in this table are with respect to the total cross section parameter $\sigma_{t,i=6}^{g=30}$. The largest sensitivity is $S^{(2)}\left(\sigma_{t,i=6}^{30}, \sigma_{s,l=1,k=6}^{30\rightarrow 30}\right) = 6.996$.

Table 16. Elements of $\mathbf{S}^{(2)}\left(\sigma_{t,i=6}^g, \sigma_{s,l=1,k=6}^{g'\rightarrow h}\right)$, $g, g', h = 1, \dots, 30$, having values greater than 1.0.

	$g' \rightarrow h$ 11 → 12	$g' \rightarrow h$ 12 → 12	$g' \rightarrow h$ 12 → 13	$g' \rightarrow h$ 13 → 13	$g' \rightarrow h$ 13 → 14	$g' \rightarrow h$ 14 → 14	$g' \rightarrow h$ 14 → 15
g=30	1.212	1.628	2.003	1.522	1.779	1.289	1.448
	$g' \rightarrow h$ 15 → 16	$g' \rightarrow h$ 16 → 16	$g' \rightarrow h$ 16 → 17	$g' \rightarrow h$ 17 → 17	$g' \rightarrow h$ 17 → 18	$g' \rightarrow h$ 30 → 30	
g=30	1.631	1.979	1.642	1.312	1.096	6.996	

3.3.3. Results for the Relative Sensitivities $\mathbf{S}^{(2)}\left(\sigma_{t,i}^g, \sigma_{s,l=2,k}^{g'\rightarrow h}\right)$

Table 17 summarizes the results obtained for the second-order relative sensitivities of the leakage response with respect to the total cross sections and the second-order scattering cross sections between all isotopes, $\mathbf{S}^{(2)}\left(\sigma_{t,i}^g, \sigma_{s,l=2,k}^{g'\rightarrow h}\right) = \left(\partial^2 L / \partial \sigma_{t,i}^g \partial \sigma_{s,l=2,k}^{g'\rightarrow h}\right) \left(\sigma_{t,i}^g \sigma_{s,l=2,k}^{g'\rightarrow h} / L\right)$, $l = 2; i, k = 1, \dots, 6; g', g, h = 1, \dots, 30$. All components of this matrix have absolute values smaller than 1.0. The largest negative value is $S^{(2)}\left(\sigma_{t,i=6}^{30}, \sigma_{s,l=2,k=6}^{12\rightarrow 12}\right) = -4.258 \times 10^{-1}$.

As shown in Table 17, the largest values of the mixed second-order sensitivities in each of the respective submatrix involve the second-order self-scattering cross sections in the 7th or 12th energy groups of the isotopes, and the total cross sections corresponding either to the 7th energy group for isotopes $^{239}\text{Pu}, ^{240}\text{Pu}, ^{69}\text{Ga}$ and ^{71}Ga , or to the 30th energy group for isotopes C and ^1H , respectively.

Table 17. Summary of second-order relative sensitivities of the leakage response with respect to the total cross sections and the second-order ($l = 2$) scattering cross sections for all isotopes: $\mathbf{S}^{(2)}\left(\sigma_{t,i'}^g, \sigma_{s,l=2,k}^{g'\rightarrow h}\right) = \left(\partial^2 L / \partial \sigma_{t,i}^g \partial \sigma_{s,l=2,k}^{g'\rightarrow h}\right) \left(\sigma_{t,i}^g, \sigma_{s,l=2,k}^{g'\rightarrow h} / L\right)$, $l = 2$; $i, k = 1, \dots, 6$; $g, g', h = 1, \dots, 30$.

	$k = 1$ (^{239}Pu)	$k = 2$ (^{240}Pu)	$k = 3$ (^{69}Ga)	$k = 4$ (^{71}Ga)	$k = 5$ (C)	$k = 6$ (^1H)
$i = 1$ (^{239}Pu)	$\mathbf{S}^{(2)}\left(\begin{matrix} \sigma_{t,1'}^g \\ \sigma_{s,l=2,1}^{g'\rightarrow h} \end{matrix}\right)$ Min. value = -2.51×10^{-2} at $g=7,$ $g'=7, h=7$	$\mathbf{S}^{(2)}\left(\begin{matrix} \sigma_{t,1'}^g \\ \sigma_{s,l=2,2}^{g'\rightarrow h} \end{matrix}\right)$ Min. value = -1.54×10^{-3} at $g=7,$ $g'=7, h=7$	$\mathbf{S}^{(2)}\left(\begin{matrix} \sigma_{t,1'}^g \\ \sigma_{s,l=2,3}^{g'\rightarrow h} \end{matrix}\right)$ Min. value = -4.61×10^{-5} at $g=7,$ $g'=7, h=7$	$\mathbf{S}^{(2)}\left(\begin{matrix} \sigma_{t,1'}^g \\ \sigma_{s,l=2,4}^{g'\rightarrow h} \end{matrix}\right)$ Min. value = -2.86×10^{-5} at $g=7,$ $g'=7, h=7$	$\mathbf{S}^{(2)}\left(\begin{matrix} \sigma_{t,1'}^g \\ \sigma_{s,l=2,5}^{g'\rightarrow h} \end{matrix}\right)$ Min. value = -2.63×10^{-2} at $g=7,$ $g'=7, h=7$	$\mathbf{S}^{(2)}\left(\begin{matrix} \sigma_{t,1'}^g \\ \sigma_{s,l=2,6}^{g'\rightarrow h} \end{matrix}\right)$ Min. value = -1.23×10^{-1} at $g=12,$ $g'=12, h=12$
$i = 2$ (^{240}Pu)	$\mathbf{S}^{(2)}\left(\begin{matrix} \sigma_{t,2'}^g \\ \sigma_{s,l=2,1}^{g'\rightarrow h} \end{matrix}\right)$ Min. value = -1.58×10^{-3} at $g=7,$ $g'=7, h=7$	$\mathbf{S}^{(2)}\left(\begin{matrix} \sigma_{t,2'}^g \\ \sigma_{s,l=2,2}^{g'\rightarrow h} \end{matrix}\right)$ Min. value = -9.66×10^{-5} at $g=7,$ $g'=7, h=7$	$\mathbf{S}^{(2)}\left(\begin{matrix} \sigma_{t,2'}^g \\ \sigma_{s,l=2,3}^{g'\rightarrow h} \end{matrix}\right)$ Min. value = -2.90×10^{-6} at $g=7,$ $g'=7, h=7$	$\mathbf{S}^{(2)}\left(\begin{matrix} \sigma_{t,2'}^g \\ \sigma_{s,l=2,4}^{g'\rightarrow h} \end{matrix}\right)$ Min. value = -1.79×10^{-6} at $g=7,$ $g'=7, h=7$	$\mathbf{S}^{(2)}\left(\begin{matrix} \sigma_{t,2'}^g \\ \sigma_{s,l=2,5}^{g'\rightarrow h} \end{matrix}\right)$ Min. value = -1.65×10^{-3} at $g=7,$ $g'=7, h=7$	$\mathbf{S}^{(2)}\left(\begin{matrix} \sigma_{t,2'}^g \\ \sigma_{s,l=2,6}^{g'\rightarrow h} \end{matrix}\right)$ Min. value = -7.77×10^{-3} at $g=12,$ $g'=12, h=12$
$i = 3$ (^{69}Ga)	$\mathbf{S}^{(2)}\left(\begin{matrix} \sigma_{t,3'}^g \\ \sigma_{s,l=2,1}^{g'\rightarrow h} \end{matrix}\right)$ Min. value = -6.71×10^{-5} at $g=7,$ $g'=7, h=7$	$\mathbf{S}^{(2)}\left(\begin{matrix} \sigma_{t,3'}^g \\ \sigma_{s,l=2,2}^{g'\rightarrow h} \end{matrix}\right)$ Min. value = -4.10×10^{-6} at $g=7,$ $g'=7, h=7$	$\mathbf{S}^{(2)}\left(\begin{matrix} \sigma_{t,3'}^g \\ \sigma_{s,l=2,3}^{g'\rightarrow h} \end{matrix}\right)$ Min. value = -1.23×10^{-7} at $g=7,$ $g'=7, h=7$	$\mathbf{S}^{(2)}\left(\begin{matrix} \sigma_{t,3'}^g \\ \sigma_{s,l=2,4}^{g'\rightarrow h} \end{matrix}\right)$ Min. value = -7.64×10^{-8} at $g=7,$ $g'=7, h=7$	$\mathbf{S}^{(2)}\left(\begin{matrix} \sigma_{t,3'}^g \\ \sigma_{s,l=2,5}^{g'\rightarrow h} \end{matrix}\right)$ Min. value = -7.01×10^{-5} at $g=7,$ $g'=7, h=7$	$\mathbf{S}^{(2)}\left(\begin{matrix} \sigma_{t,3'}^g \\ \sigma_{s,l=2,6}^{g'\rightarrow h} \end{matrix}\right)$ Min. value = -3.49×10^{-4} at $g=12,$ $g'=12, h=12$
$i = 4$ (^{71}Ga)	$\mathbf{S}^{(2)}\left(\begin{matrix} \sigma_{t,4'}^g \\ \sigma_{s,l=2,1}^{g'\rightarrow h} \end{matrix}\right)$ Min. value = -4.45×10^{-5} at $g=7,$ $g'=7, h=7$	$\mathbf{S}^{(2)}\left(\begin{matrix} \sigma_{t,4'}^g \\ \sigma_{s,l=2,2}^{g'\rightarrow h} \end{matrix}\right)$ Min. value = -2.72×10^{-6} at $g=7,$ $g'=7, h=7$	$\mathbf{S}^{(2)}\left(\begin{matrix} \sigma_{t,4'}^g \\ \sigma_{s,l=2,3}^{g'\rightarrow h} \end{matrix}\right)$ Min. value = -8.16×10^{-8} at $g=7,$ $g'=7, h=7$	$\mathbf{S}^{(2)}\left(\begin{matrix} \sigma_{t,4'}^g \\ \sigma_{s,l=2,4}^{g'\rightarrow h} \end{matrix}\right)$ Min. value = -5.06×10^{-8} at $g=7,$ $g'=7, h=7$	$\mathbf{S}^{(2)}\left(\begin{matrix} \sigma_{t,4'}^g \\ \sigma_{s,l=2,5}^{g'\rightarrow h} \end{matrix}\right)$ Min. value = -4.65×10^{-5} at $g=7,$ $g'=7, h=7$	$\mathbf{S}^{(2)}\left(\begin{matrix} \sigma_{t,4'}^g \\ \sigma_{s,l=2,6}^{g'\rightarrow h} \end{matrix}\right)$ Min. value = -2.37×10^{-4} at $g=12,$ $g'=12, h=12$
$i = 5$ (C)	$\mathbf{S}^{(2)}\left(\begin{matrix} \sigma_{t,5'}^g \\ \sigma_{s,l=2,1}^{g'\rightarrow h} \end{matrix}\right)$ Min. value = -4.86×10^{-3} at $g=30,$ $g'=7, h=7$	$\mathbf{S}^{(2)}\left(\begin{matrix} \sigma_{t,5'}^g \\ \sigma_{s,l=2,2}^{g'\rightarrow h} \end{matrix}\right)$ Min. value = -2.97×10^{-4} at $g=30,$ $g'=7, h=7$	$\mathbf{S}^{(2)}\left(\begin{matrix} \sigma_{t,5'}^g \\ \sigma_{s,l=2,3}^{g'\rightarrow h} \end{matrix}\right)$ Min. value = -8.91×10^{-6} at $g=30,$ $g'=7, h=7$	$\mathbf{S}^{(2)}\left(\begin{matrix} \sigma_{t,5'}^g \\ \sigma_{s,l=2,4}^{g'\rightarrow h} \end{matrix}\right)$ Min. value = -5.53×10^{-6} at $g=30,$ $g'=7, h=7$	$\mathbf{S}^{(2)}\left(\begin{matrix} \sigma_{t,5'}^g \\ \sigma_{s,l=2,5}^{g'\rightarrow h} \end{matrix}\right)$ Min. value = -1.02×10^{-2} at $g=30,$ $g'=7, h=7$	$\mathbf{S}^{(2)}\left(\begin{matrix} \sigma_{t,5'}^g \\ \sigma_{s,l=2,6}^{g'\rightarrow h} \end{matrix}\right)$ Min. value = -3.57×10^{-2} at $g=30,$ $g'=12, h=12$
$i = 6$ (^1H)	$\mathbf{S}^{(2)}\left(\begin{matrix} \sigma_{t,6'}^g \\ \sigma_{s,l=2,1}^{g'\rightarrow h} \end{matrix}\right)$ Min. value = -5.79×10^{-2} at $g=30,$ $g'=7, h=7$	$\mathbf{S}^{(2)}\left(\begin{matrix} \sigma_{t,6'}^g \\ \sigma_{s,l=2,2}^{g'\rightarrow h} \end{matrix}\right)$ Min. value = -3.55×10^{-3} at $g=30,$ $g'=7, h=7$	$\mathbf{S}^{(2)}\left(\begin{matrix} \sigma_{t,6'}^g \\ \sigma_{s,l=2,3}^{g'\rightarrow h} \end{matrix}\right)$ Min. value = -1.06×10^{-4} at $g=30,$ $g'=7, h=7$	$\mathbf{S}^{(2)}\left(\begin{matrix} \sigma_{t,6'}^g \\ \sigma_{s,l=2,4}^{g'\rightarrow h} \end{matrix}\right)$ Min. value = -6.60×10^{-5} at $g=30,$ $g'=7, h=7$	$\mathbf{S}^{(2)}\left(\begin{matrix} \sigma_{t,6'}^g \\ \sigma_{s,l=2,5}^{g'\rightarrow h} \end{matrix}\right)$ Min. value = -1.22×10^{-1} at $g=30,$ $g'=7, h=7$	$\mathbf{S}^{(2)}\left(\begin{matrix} \sigma_{t,6'}^g \\ \sigma_{s,l=2,6}^{g'\rightarrow h} \end{matrix}\right)$ Min. value = -4.26×10^{-1} at $g=30,$ $g'=12, h=12$

3.3.4. Results for the Relative Sensitivities $\mathbf{S}^{(2)}\left(\sigma_{t,i'}^g, \sigma_{s,l=3,k}^{g'\rightarrow h}\right)$

Table 18 summarizes the results for the matrix $\mathbf{S}^{(2)}\left(\sigma_{t,i'}^g, \sigma_{s,l=3,k}^{g'\rightarrow h}\right) = \left(\partial^2 L / \partial \sigma_{t,i}^g \partial \sigma_{s,l=3,k}^{g'\rightarrow h}\right) \left(\sigma_{t,i}^g, \sigma_{s,l=3,k}^{g'\rightarrow h} / L\right)$, $l = 3$; $i, k = 1, \dots, 6$; $g', g, h = 1, \dots, 30$, comprising the second-order relative sensitivities of the leakage response with respect to the total cross sections and the third-order scattering cross sections for all isotopes. The largest absolute values of these mixed second-order sensitivities involve the third-order self-scattering cross sections in the 6th or 7th or 12th energy group, and either the total cross sections for the 7th or 12th energy group for isotopes $^{239}\text{Pu}, ^{240}\text{Pu}, ^{69}\text{Ga}$ and ^{71}Ga , or the total cross sections for the 30th energy group for isotopes C and ^1H , respectively. All of these relative sensitivities have values much smaller than 1.0; the largest value is $\mathbf{S}^{(2)}\left(\sigma_{t,i=6}^{30}, \sigma_{s,l=3,k=6}^{12\rightarrow 12}\right) = 7.13 \times 10^{-2}$.

Table 18. Summary of the second-order relative sensitivities of the leakage response with respect to the total cross sections and the third-order ($l = 3$) scattering cross sections between all isotopes:

$$\mathbf{S}^{(2)}\left(\sigma_{t,i'}^g, \sigma_{s,l=3,k}^{g' \rightarrow h}\right) = \left(\partial^2 L / \partial \sigma_{t,i'}^g \partial \sigma_{s,l=3,k}^{g' \rightarrow h}\right) \left(\sigma_{t,i'}^g, \sigma_{s,l=3,k}^{g' \rightarrow h} / L\right), i, k = 1, \dots, 6; g', g, h = 1, \dots, 30.$$

	$k = 1$ (²³⁹ Pu)	$k = 2$ (²⁴⁰ Pu)	$k = 3$ (⁶⁹ Ga)	$k = 4$ (⁷¹ Ga)	$k = 5$ (C)	$k = 6$ (¹ H)
$i = 1$ (²³⁹ Pu)	$\mathbf{S}^{(2)}\left(\begin{matrix} \sigma_{t,1'}^g \\ \sigma_{s,l=3,1}^{g' \rightarrow h} \end{matrix}\right)$ Max. value = 9.12×10^{-5} at $g=7,$ $g'=7, h=7$	$\mathbf{S}^{(2)}\left(\begin{matrix} \sigma_{t,1'}^g \\ \sigma_{s,l=3,2}^{g' \rightarrow h} \end{matrix}\right)$ Max. value = 5.61×10^{-6} at $g=7,$ $g'=7, h=7$	$\mathbf{S}^{(2)}\left(\begin{matrix} \sigma_{t,1'}^g \\ \sigma_{s,l=3,3}^{g' \rightarrow h} \end{matrix}\right)$ Max. value = 1.59×10^{-7} at $g=7,$ $g'=7, h=7$	$\mathbf{S}^{(2)}\left(\begin{matrix} \sigma_{t,1'}^g \\ \sigma_{s,l=3,4}^{g' \rightarrow h} \end{matrix}\right)$ Max. value = 1.00×10^{-7} at $g=7,$ $g'=7, h=7$	$\mathbf{S}^{(2)}\left(\begin{matrix} \sigma_{t,1'}^g \\ \sigma_{s,l=3,5}^{g' \rightarrow h} \end{matrix}\right)$ Max. value = 7.12×10^{-3} at $g=7,$ $g'=7, h=7$	$\mathbf{S}^{(2)}\left(\begin{matrix} \sigma_{t,1'}^g \\ \sigma_{s,l=3,6}^{g' \rightarrow h} \end{matrix}\right)$ Max. value = 2.76×10^{-2} at $g=12,$ $g'=12, h=12$
$i = 2$ (²⁴⁰ Pu)	$\mathbf{S}^{(2)}\left(\begin{matrix} \sigma_{t,2'}^g \\ \sigma_{s,l=3,1}^{g' \rightarrow h} \end{matrix}\right)$ Max. value = 5.73×10^{-6} at $g=7,$ $g'=7, h=7$	$\mathbf{S}^{(2)}\left(\begin{matrix} \sigma_{t,2'}^g \\ \sigma_{s,l=3,2}^{g' \rightarrow h} \end{matrix}\right)$ Max. value = 3.52×10^{-7} at $g=7,$ $g'=7, h=7$	$\mathbf{S}^{(2)}\left(\begin{matrix} \sigma_{t,2'}^g \\ \sigma_{s,l=3,3}^{g' \rightarrow h} \end{matrix}\right)$ Max. value = 1.00×10^{-8} at $g=7,$ $g'=7, h=7$	$\mathbf{S}^{(2)}\left(\begin{matrix} \sigma_{t,2'}^g \\ \sigma_{s,l=3,4}^{g' \rightarrow h} \end{matrix}\right)$ Max. value = 6.28×10^{-9} at $g=7,$ $g'=7, h=7$	$\mathbf{S}^{(2)}\left(\begin{matrix} \sigma_{t,2'}^g \\ \sigma_{s,l=3,5}^{g' \rightarrow h} \end{matrix}\right)$ Max. value = 4.47×10^{-4} at $g=7,$ $g'=7, h=7$	$\mathbf{S}^{(2)}\left(\begin{matrix} \sigma_{t,2'}^g \\ \sigma_{s,l=3,6}^{g' \rightarrow h} \end{matrix}\right)$ Max. value = 1.75×10^{-3} at $g=12,$ $g'=12, h=12$
$i = 3$ (⁶⁹ Ga)	$\mathbf{S}^{(2)}\left(\begin{matrix} \sigma_{t,3'}^g \\ \sigma_{s,l=3,1}^{g' \rightarrow h} \end{matrix}\right)$ Max. value = 2.43×10^{-7} at $g=7,$ $g'=7, h=7$	$\mathbf{S}^{(2)}\left(\begin{matrix} \sigma_{t,3'}^g \\ \sigma_{s,l=3,2}^{g' \rightarrow h} \end{matrix}\right)$ Max. value = 1.50×10^{-8} at $g=7,$ $g'=7, h=7$	$\mathbf{S}^{(2)}\left(\begin{matrix} \sigma_{t,3'}^g \\ \sigma_{s,l=3,3}^{g' \rightarrow h} \end{matrix}\right)$ Max. value = 4.25×10^{-10} at $g=7,$ $g'=7, h=7$	$\mathbf{S}^{(2)}\left(\begin{matrix} \sigma_{t,3'}^g \\ \sigma_{s,l=3,4}^{g' \rightarrow h} \end{matrix}\right)$ Max. value = 2.67×10^{-10} at $g=7,$ $g'=7, h=7$	$\mathbf{S}^{(2)}\left(\begin{matrix} \sigma_{t,3'}^g \\ \sigma_{s,l=3,5}^{g' \rightarrow h} \end{matrix}\right)$ Max. value = 1.90×10^{-5} at $g=7,$ $g'=7, h=7$	$\mathbf{S}^{(2)}\left(\begin{matrix} \sigma_{t,3'}^g \\ \sigma_{s,l=3,6}^{g' \rightarrow h} \end{matrix}\right)$ Max. value = 7.85×10^{-5} at $g=12,$ $g'=12, h=12$
$i = 4$ (⁷¹ Ga)	$\mathbf{S}^{(2)}\left(\begin{matrix} \sigma_{t,4'}^g \\ \sigma_{s,l=3,1}^{g' \rightarrow h} \end{matrix}\right)$ Max. value = 1.61×10^{-7} at $g=7,$ $g'=7, h=7$	$\mathbf{S}^{(2)}\left(\begin{matrix} \sigma_{t,4'}^g \\ \sigma_{s,l=3,2}^{g' \rightarrow h} \end{matrix}\right)$ Max. value = 9.93×10^{-9} at $g=7,$ $g'=7, h=7$	$\mathbf{S}^{(2)}\left(\begin{matrix} \sigma_{t,4'}^g \\ \sigma_{s,l=3,3}^{g' \rightarrow h} \end{matrix}\right)$ Max. value = 2.82×10^{-10} at $g=7,$ $g'=7, h=7$	$\mathbf{S}^{(2)}\left(\begin{matrix} \sigma_{t,4'}^g \\ \sigma_{s,l=3,4}^{g' \rightarrow h} \end{matrix}\right)$ Max. value = 1.77×10^{-10} at $g=7,$ $g'=7, h=7$	$\mathbf{S}^{(2)}\left(\begin{matrix} \sigma_{t,4'}^g \\ \sigma_{s,l=3,5}^{g' \rightarrow h} \end{matrix}\right)$ Max. value = 1.26×10^{-5} at $g=7,$ $g'=7, h=7$	$\mathbf{S}^{(2)}\left(\begin{matrix} \sigma_{t,4'}^g \\ \sigma_{s,l=3,6}^{g' \rightarrow h} \end{matrix}\right)$ Max. value = 5.32×10^{-5} at $g=12,$ $g'=12, h=12$
$i = 5$ (C)	$\mathbf{S}^{(2)}\left(\begin{matrix} \sigma_{t,5'}^g \\ \sigma_{s,l=3,1}^{g' \rightarrow h} \end{matrix}\right)$ Max. value = -3.67×10^{-6} at $g=30,$ $g'=12, h=12$	$\mathbf{S}^{(2)}\left(\begin{matrix} \sigma_{t,5'}^g \\ \sigma_{s,l=3,2}^{g' \rightarrow h} \end{matrix}\right)$ Max. value = -2.34×10^{-7} at $g=30,$ $g'=12, h=12$	$\mathbf{S}^{(2)}\left(\begin{matrix} \sigma_{t,5'}^g \\ \sigma_{s,l=3,3}^{g' \rightarrow h} \end{matrix}\right)$ Max. value = -3.63×10^{-9} at $g=30,$ $g'=10, h=10$	$\mathbf{S}^{(2)}\left(\begin{matrix} \sigma_{t,5'}^g \\ \sigma_{s,l=3,4}^{g' \rightarrow h} \end{matrix}\right)$ Max. value = 2.14×10^{-9} at $g=30,$ $g'=6, h=6$	$\mathbf{S}^{(2)}\left(\begin{matrix} \sigma_{t,5'}^g \\ \sigma_{s,l=3,5}^{g' \rightarrow h} \end{matrix}\right)$ Max. value = 2.39×10^{-3} at $g=30,$ $g'=7, h=7$	$\mathbf{S}^{(2)}\left(\begin{matrix} \sigma_{t,5'}^g \\ \sigma_{s,l=3,6}^{g' \rightarrow h} \end{matrix}\right)$ Max. value = 5.98×10^{-3} at $g=30,$ $g'=12, h=12$
$i = 6$ (¹ H)	$\mathbf{S}^{(2)}\left(\begin{matrix} \sigma_{t,6'}^g \\ \sigma_{s,l=3,1}^{g' \rightarrow h} \end{matrix}\right)$ Max. value = -4.38×10^{-5} at $g=30,$ $g'=12, h=12$	$\mathbf{S}^{(2)}\left(\begin{matrix} \sigma_{t,6'}^g \\ \sigma_{s,l=3,2}^{g' \rightarrow h} \end{matrix}\right)$ Max. value = -2.79×10^{-6} at $g=30,$ $g'=12, h=12$	$\mathbf{S}^{(2)}\left(\begin{matrix} \sigma_{t,6'}^g \\ \sigma_{s,l=3,3}^{g' \rightarrow h} \end{matrix}\right)$ Max. value = -4.33×10^{-8} at $g=30,$ $g'=10, h=10$	$\mathbf{S}^{(2)}\left(\begin{matrix} \sigma_{t,6'}^g \\ \sigma_{s,l=3,4}^{g' \rightarrow h} \end{matrix}\right)$ Max. value = 2.56×10^{-8} at $g=30,$ $g'=6, h=6$	$\mathbf{S}^{(2)}\left(\begin{matrix} \sigma_{t,6'}^g \\ \sigma_{s,l=3,5}^{g' \rightarrow h} \end{matrix}\right)$ Max. value = 2.85×10^{-2} at $g=30,$ $g'=7, h=7$	$\mathbf{S}^{(2)}\left(\begin{matrix} \sigma_{t,6'}^g \\ \sigma_{s,l=3,6}^{g' \rightarrow h} \end{matrix}\right)$ Max. value = 7.13×10^{-2} at $g=30,$ $g'=12, h=12$

Comparing the results for the matrices $\mathbf{S}^{(2)}\left(\sigma_{t,i'}^g, \sigma_{s,l,k}^{g' \rightarrow h}\right)$, for scattering orders $l = 0, l = 1, l = 2$, and $l = 3$, as summarized in Tables 12, 15, 17 and 18, respectively, indicates that for a submatrix that is located in the same position in these tables, the higher the scattering order, the smaller the absolute value of the second-order mixed sensitivities. For example, for the submatrix $\mathbf{S}^{(2)}\left(\sigma_{t,i=6'}^g, \sigma_{s,l,k=6}^{g' \rightarrow h}\right)$ located at the lower right corner in each table, the largest absolute values decrease as the scattering order increases, i.e., $S^{(2)}\left(\sigma_{t,i=6'}^{30}, \sigma_{s,l=0,k=6}^{30 \rightarrow 30}\right) = -10.77$, $S^{(2)}\left(\sigma_{t,i=6'}^{30}, \sigma_{s,l=1,k=6}^{30 \rightarrow 30}\right) = 6.996$, $S^{(2)}\left(\sigma_{t,i=6'}^{30}, \sigma_{s,l=2,k=6}^{12 \rightarrow 12}\right) = -4.258 \times 10^{-1}$, and $S^{(2)}\left(\sigma_{t,i=6'}^{30}, \sigma_{s,l=3,k=6}^{12 \rightarrow 12}\right) = 7.13 \times 10^{-2}$, respectively.

4. Uncertainties in the PERP Leakage Response Induced by Uncertainties in Scattering Cross Sections

Since correlations among the group cross sections are not available for the PERP benchmark, the maximum entropy principle (see, e.g., [8]) indicates that neglecting them minimizes the inadvertent introduction of spurious information into the computations of the various response moments. As has

been discussed in Part I [1], up to second-order response sensitivities, the expected value of the PERP benchmark's leakage response has the following expression:

$$[E(L)]_s = L(\boldsymbol{\alpha}^0) + [E(L)]_s^{(2,U)}, \quad (83)$$

where the subscript "s" indicates contributions solely from the group-averaged uncorrelated scattering microscopic cross sections, and where the second-order contributions, $[E(L)]_s^{(2,U)}$, to the expected value, $[E(L)]_s$, of the leakage response $L(\boldsymbol{\alpha})$, is given by the following expression:

$$[E(L)]_s^{(2,U)} = \frac{1}{2} \sum_{g=1}^G \sum_{g'=1}^G \sum_{i=1}^I \sum_{l=0}^{ISCT} \frac{\partial^2 L(\boldsymbol{\alpha})}{\partial \sigma_{s,l,i}^{g' \rightarrow g} \partial \sigma_{s,l,i}^{g' \rightarrow g}} \left(s_{s,l,i}^{g' \rightarrow g} \right)^2, \quad G = 30, I = 6, ISCT = 3. \quad (84)$$

In Equation (84), the quantity $s_{s,l,i}^{g' \rightarrow g}$ denotes the standard deviation associated with the imprecisely known model parameter $\sigma_{s,l,i}^{g' \rightarrow g}$.

Taking into account contributions solely from the group-averaged uncorrelated and normally-distributed scattering microscopic cross sections (which will be indicated by using the superscript "(U,N)" in the following equations), the expression for computing the variance, denoted as $[\text{var}(L)]_s^{(U,N)}$, of the leakage response of the PERP benchmark takes on the following form:

$$[\text{var}(L)]_s^{(U,N)} = [\text{var}(L)]_s^{(1,U,N)} + [\text{var}(L)]_s^{(2,U,N)}, \quad (85)$$

where the first-order contribution term, $[\text{var}(L)]_s^{(1,U,N)}$, to the variance $[\text{var}(L)]_s^{(U,N)}$ is defined as

$$[\text{var}(L)]_s^{(1,U,N)} \triangleq \sum_{g=1}^G \sum_{g'=1}^G \sum_{i=1}^I \sum_{l=0}^{ISCT} \left[\frac{\partial L(\boldsymbol{\alpha})}{\partial \sigma_{s,l,i}^{g' \rightarrow g}} \right]^2 \left(s_{s,l,i}^{g' \rightarrow g} \right)^2, \quad G = 30, I = 6, ISCT = 3, \quad (86)$$

while the second-order contribution term, $[\text{var}(L)]_s^{(2,U,N)}$, to the variance $[\text{var}(L)]_s^{(U,N)}$ is defined as

$$[\text{var}(L)]_s^{(2,U,N)} \triangleq \frac{1}{2} \sum_{g=1}^G \sum_{g'=1}^G \sum_{i=1}^I \sum_{l=0}^{ISCT} \left[\frac{\partial^2 L(\boldsymbol{\alpha})}{\partial \sigma_{s,l,i}^{g' \rightarrow g} \partial \sigma_{s,l,i}^{g' \rightarrow g}} \left(s_{s,l,i}^{g' \rightarrow g} \right)^2 \right]^2, \quad G = 30, I = 6, ISCT = 3. \quad (87)$$

Again, taking into account contributions solely from the group-averaged uncorrelated scattering microscopic cross sections, the third-order moment, $[\mu_3(L)]_s^{(U,N)}$, of the leakage response for the PERP benchmark takes on the following form:

$$[\mu_3(L)]_s^{(U,N)} = 3 \sum_{g=1}^G \sum_{g'=1}^G \sum_{i=1}^I \sum_{l=0}^{ISCT} \left[\frac{\partial L(\boldsymbol{\alpha})}{\partial \sigma_{s,l,i}^{g' \rightarrow g}} \right]^2 \frac{\partial^2 L(\boldsymbol{\alpha})}{\partial \sigma_{s,l,i}^{g' \rightarrow g} \partial \sigma_{s,l,i}^{g' \rightarrow g}} \left(s_{s,l,i}^{g' \rightarrow g} \right)^4, \quad G = 30, I = 6, ISCT = 3. \quad (88)$$

As Equation (88) indicates, if the second-order sensitivities were unavailable, the third moment $[\mu_3(L)]_s^{(U,N)}$ would vanish and the response distribution would by default be assumed to be Gaussian. The skewness, $[\gamma_1(L)]_s^{(U,N)}$, induced by the variances of microscopic scattering cross sections in the leakage response, L , is defined as follows:

$$[\gamma_1(L)]_s^{(U,N)} = [\mu_3(L)]_s^{(U,N)} / \left\{ [\text{var}(L)]_s^{(U,N)} \right\}^{3/2}. \quad (89)$$

The effects of the first- and, respectively, second-order sensitivities on the response's expected value, variance and skewness can be quantified by considering typical values for the standard deviations for the uncorrelated group-averaged isotopic scattering cross sections, using these values together with

the respective sensitivities computed in Section 2 in Equations (84)–(89). The results thus obtained are presented in Table 19, considering uniform parameter standard deviations of 1%, 5%, and 10%, respectively. These results indicate that the effects of both the first- and second-order sensitivities on the expected response value, its standard deviation and skewness are negligible, which is not surprising in view of the values for the first- and second-order sensitivities already presented in Tables 6–11.

Table 19. Comparison of Response Moments for Different Relative Standard Deviations of the Uncorrelated Scattering Cross Section Parameters.

Relative Standard Deviation	10%	5%	1%
$L(\alpha^0)$	1.7648×10^6	1.7648×10^6	1.7648×10^6
$[E(L)]_s^{(2,U)}$	-1.3473×10^4	-3.3682×10^3	-1.3473×10^2
$[E(L)]_s = L(\alpha^0) + [E(L)]_s^{(2,U)}$	1.7513×10^6	1.7614×10^6	1.7647×10^6
$[\text{var}(L)]_s^{(1,U,N)}$	1.2379×10^8	3.0947×10^9	102379×10^8
$[\text{var}(L)]_s^{(2,U,N)}$	4.3207×10^7	2.7004×10^6	4.3207×10^3
$[\text{var}(L)]_s^{(U,N)} = [\text{var}(L)]_s^{(1,U,N)} + [\text{var}(L)]_s^{(2,U,N)}$	1.2422×10^{10}	3.0974×10^9	1.2379×10^8
$[\mu_3(L)]_s^{(U,N)}$	-4.9281×10^{12}	-3.0800×10^{11}	-4.9281×10^8
$[\gamma_1(L)]_s^{(U,N)} = [\mu_3(L)]_s^{(U,N)} / \{[\text{var}(L)]_s^{(U,N)}\}^{3/2}$	-3.5595×10^{-3}	-1.7868×10^{-3}	-3.5780×10^{-4}

The contributions to the leakage response moments stemming from the group-averaged uncorrelated microscopic scattering cross sections are much smaller than the corresponding contributions stemming from the group-averaged uncorrelated microscopic total cross sections. This fact can be readily illustrated by considering standard deviations of 10% for all of the group-averaged uncorrelated microscopic scattering and total cross sections, and by comparing the corresponding results in Table 19 and Table 25 of Part I [1], which reveals that:

$$\begin{aligned}
 [E(L)]_s^{(2,U)} &= -1.3473 \times 10^4 \ll [E(L)]_t^{(2,U)} = 4.5980 \times 10^6, \\
 [\text{var}(L)]_s^{(1,U,N)} &= 1.2379 \times 10^{10} \ll [\text{var}(L)]_t^{(1,U,N)} = 3.4196 \times 10^{12}, \\
 [\text{var}(L)]_s^{(2,U,N)} &= 4.3207 \times 10^7 \ll [\text{var}(L)]_t^{(2,U,N)} = 2.8789 \times 10^{13}, \\
 |[\gamma_1(L)]_s^{(U,N)}| &= 3.5595 \times 10^{-3} \ll [\gamma_1(L)]_t^{(U,N)} = 0.3407.
 \end{aligned}$$

It is noteworthy that several mixed second-order sensitivities of the leakage response with respect to the total and scattering cross sections, as shown in Section 3, have values that are significantly larger (by several orders of magnitude) than the values of the unmixed sensitivities. Recall that the following sensitivities have absolute values larger than 1.0:

- (a) 8 elements of the matrix $\mathbf{S}^{(2)} \left(\sigma_{t,i=6}^g, \sigma_{s,l=0,k=1}^{g' \rightarrow h} \right)$, $g, g', h = 1, \dots, 30$, presented in Table 14;
- (b) 3 elements of the matrix $\mathbf{S}^{(2)} \left(\sigma_{t,i=6'}^g, \sigma_{s,l=0,k=5}^{g' \rightarrow h} \right)$, $g, g', h = 1, \dots, 30$, as listed in Table 12;
- (c) 26 elements of the matrix $\mathbf{S}^{(2)} \left(\sigma_{t,i=6'}^g, \sigma_{s,l=0,k=6}^{g' \rightarrow h} \right)$, $g, g', h = 1, \dots, 30$, as listed in Table 13;
- (d) 2 elements of the matrix $\mathbf{S}^{(2)} \left(\sigma_{t,i=6'}^g, \sigma_{s,l=1,k=1}^{g' \rightarrow h} \right)$, $g, g', h = 1, \dots, 30$, as listed in Table 15;
- (e) 13 elements of the matrix $\mathbf{S}^{(2)} \left(\sigma_{t,i=6'}^g, \sigma_{s,l=1,k=6}^{g' \rightarrow h} \right)$, $g, g', h = 1, \dots, 30$, as listed in Table 16.

The above results indicate that it would be very important to obtain correlations among the various model parameter, since these correlations could contribute, in conjunction with the mixed second-order sensitivities, to the ultimate values of the response moments. Since the mixed second-order sensitivities of the leakage response to the group-averaged total and scattering microscopic cross sections are significantly larger than the unmixed second-order sensitivities of the leakage response to

the group-averaged scattering microscopic cross sections, it is likely that the *correlations* among the respective total and scattering cross sections could provide significantly larger contributions to the response moments than just the standard deviations of the scattering cross sections.

5. Conclusions

This work has presented results for the first- and second-order sensitivities of the PERP total leakage response with respect to the benchmark's group-averaged microscopic scattering and total cross sections.

1. The first-order sensitivities of the leakage response with respect to the zeroth-order self-scattering cross sections can be compared directly to the corresponding unmixed second-order sensitivities. For all six of the isotopes contained in the PERP benchmark, both the first- and the second-order unmixed relative sensitivities of the leakage response with respect to the zeroth-order self-scattering cross sections are small, and the second-order relative sensitivities are much smaller, by at least an order of magnitude, than the corresponding first-order relative sensitivities.
2. For the second-order mixed sensitivities $\partial^2 L / \partial s_j \partial s_{m_2}$, $j = 1, \dots, J_{\sigma s}$; $m_2 = 1, \dots, J_{\sigma s}$, the numerical values of the corresponding relative sensitivities are very small, the largest of them being of the order of 10^{-2} . The largest second-order relative sensitivity is $S^{(2)}(\sigma_{s,l=0,i=1}^{12 \rightarrow 12}, \sigma_{s,l=0,k=1}^{13 \rightarrow 13}) = 3.579 \times 10^{-2}$. The largest relative sensitivities in each of the respective submatrix $\mathbf{S}^{(2)}(\sigma_{s,l,i}^{g' \rightarrow g}, \sigma_{s,l',k}^{h' \rightarrow h})$, $l, l' = 0, \dots, 3$; $i, k = 1, \dots, 6$; $g, g', h, h' = 1, \dots, 30$ are mostly with respect to the self-scattering cross sections, rather than to the in-scattering or out-scattering cross sections.
3. For the second-order mixed sensitivities $\partial^2 L / \partial t_j \partial s_{m_2}$, $j = 1, \dots, J_{\sigma t}$; $m_2 = 1, \dots, J_{\sigma s}$, the corresponding relative sensitivities are generally very small, with a few exceptions. Among all the $J_{\sigma t} \times J_{\sigma s} = 180 \times 21600$ elements, only 52 of them have absolute values of the relative sensitivities greater than 1.0; most of these elements belong to the submatrices $\mathbf{S}^{(2)}(\sigma_{t,6'}^g, \sigma_{s,l=0,1}^{g' \rightarrow h})$, $\mathbf{S}^{(2)}(\sigma_{t,6'}^g, \sigma_{s,l=0,6}^{g' \rightarrow h})$, $\mathbf{S}^{(2)}(\sigma_{t,6'}^g, \sigma_{s,l=1,1}^{g' \rightarrow h})$ and $\mathbf{S}^{(2)}(\sigma_{t,6'}^g, \sigma_{s,l=1,6}^{g' \rightarrow h})$, where $g, g', h = 1, \dots, 30$. All of these large values are related to the total cross section parameter $\sigma_{t,6}^{30}$ of isotope 6 (^1H). Also, the largest absolute values in each of those submatrices are mostly related to the self-scattering cross sections in the 12th or 30th energy groups of isotope 1 (^{239}Pu) and isotope 6 (^1H), respectively. The overall largest mixed relative sensitivity is $S^{(2)}(\sigma_{t,6'}^{30}, \sigma_{s,l=0,6}^{30 \rightarrow 30}) = -10.77$.
4. In each submatrix of $\mathbf{S}^{(2)}(\sigma_{t,i'}^g, \sigma_{s,l,k}^{g' \rightarrow h})$, $l = 0, \dots, 3$; $i, k = 1, \dots, 6$; $g, g', h = 1, \dots, 30$, most of the largest absolute value of the 2nd-order relative sensitivities are negative when involving odd-order ($l = 1, 3$) scattering cross sections; in contradistinction, most of these large sensitivities are positive when involving even-order ($l = 0, 2$) scattering cross sections. Furthermore, the larger the Legendre expansion order ($l = 0, \dots, 3$), the smaller the absolute values of the corresponding second-order mixed relative sensitivities.
5. This work has not taken into consideration the effects of the mixed second-order sensitivities of the leakage response with respect to the scattering and total microscopic cross section parameters since no correlations among these parameters are available. However, several mixed second-order sensitivities of the leakage response to the group-averaged microscopic total and scattering cross sections are significantly larger than the unmixed second-order sensitivities of the leakage response with respect to the group-averaged microscopic scattering cross sections. Therefore, it would be very important to obtain correlations among the respective total and scattering cross sections, since these correlations could provide, through the mixed second-order sensitivities, significantly larger contributions to the response moments than just the contributions from the standard deviations of the scattering cross sections.

Subsequent works will report the values and effects of the first- and second-order sensitivities of the PERP's leakage response with respect to the group-averaged isotopic fission cross sections and average number of neutrons per fission [9], source parameters [10], isotopic number densities and fission spectrum [11]. The overall conclusions and implications of this pioneering and uniquely comprehensive second-order sensitivity and uncertainty analysis of a paradigm reactor physics benchmark will also be presented in [11].

Author Contributions: D.G.C. conceived and directed the research reported herein, developed the general theory of the second-order comprehensive adjoint sensitivity analysis methodology to compute 1st- and 2nd-order sensitivities of flux functionals in a multiplying system with source, and the uncertainty equations for response moments. R.F. derived the expressions of the various derivatives with respect to the model parameters to the PERP benchmark and performed all the numerical calculations.

Acknowledgments: This work was partially funded by the United States National Nuclear Security Administration's Office of Defense Nuclear Nonproliferation Research & Development, grant number 155040-FD50.

Conflicts of Interest: The authors declare no conflict of interest. The funding sponsors had no role in the design of the study; in the collection, analyses, or interpretation of data; in the writing of the manuscript, and in the decision to publish the results.

References

1. Cacuci, D.G.; Fang, R.; Favorite, J.A. Comprehensive Second-Order Adjoint Sensitivity Analysis Methodology (2nd-ASAM) Applied to a Subcritical Experimental Reactor Physics Benchmark: I. Effects of Imprecisely Known Microscopic Total Cross Sections. *Energies* **2019**. under review. [[CrossRef](#)]
2. Valentine, T.E. Polyethylene-Reflected Plutonium Metal Sphere Subcritical Noise Measurements, SUB-PU-METMIXED-001. In *International Handbook of Evaluated Criticality Safety Benchmark Experiments*; NEA/NSC/DOC(95)03/I-IX; Organization for Economic Co-operation and Development, Nuclear Energy Agency: Paris, France, 2006.
3. Cacuci, D.G. Application of the Second-Order Comprehensive Adjoint Sensitivity Analysis Methodology to Compute 1st-and 2nd-Order Sensitivities of Flux Functionals in a Multiplying System with Source. *Nucl. Sci. Eng.* **2019**, *193*, 555–600. [[CrossRef](#)]
4. Alcouffe, R.E.; Baker, R.S.; Dahl, J.A.; Turner, S.A.; Ward, R. *PARTISN: A Time-Dependent, Parallel Neutral Particle Transport Code System*; LA-UR-08-07258; Los Alamos National Laboratory: Los Alamos, NM, USA, 2008.
5. Wilson, W.B.; Perry, R.T.; Shores, E.F.; Charlton, W.S.; Parish, T.A.; Estes, G.P.; Brown, T.H.; Arthur, E.D.; Bozoian, M.; England, T.R.; et al. SOURCES4C: A Code for Calculating (α,n), Spontaneous Fission, and Delayed Neutron Sources and Spectra. In Proceedings of the 12th Biennial Topical Meeting, Santa Fe, NM, USA, 14–18 April 2002. LA-UR-02-1839.
6. Conlin, J.L.; Parsons, D.K.; Gardiner, S.J.; Gray, M.G.; Lee, M.B.; White, M.C. *MENDF71X: Multigroup Neutron Cross-Section Data Tables Based upon ENDF/B-VII.1*; Los Alamos National Laboratory report LA-UR-15-29571 (7 October 2013); Los Alamos National Lab.(LANL): Los Alamos, NM, USA, 2015.
7. Chadwick, M.B.; Herman, M.; Obložinský, P.; Dunn, M.E.; Danon, Y.; Kahler, A.C.; Smith, D.L.; Pritychenko, B.; Arbanas, G.; Arcilla, R.; et al. ENDF/B-VII.1: Nuclear Data for Science and Technology: Cross Sections, Covariances, Fission Product Yields and Decay Data. *Nucl. Data Sheets* **2011**, *112*, 2887–2996. [[CrossRef](#)]
8. Cacuci, D.G. *BERRU Predictive Modeling: Best Estimate Results with Reduced Uncertainties*; Springer: Heidelberg, Germany; New York, NY, USA, 2018.
9. Cacuci, D.G.; Fang, R.; Favorite, J.A.; Badea, M.C.; Di Rocco, F. Comprehensive Second-Order Adjoint Sensitivity Analysis Methodology (2nd-ASAM) Applied to a Subcritical Experimental Reactor Physics Benchmark: III. Effects of Imprecisely Known Microscopic Fission Cross Sections and Average Number of Neutrons per Fission. *Energies* **2019**. accepted for publication. [[CrossRef](#)]

10. Fang, R.; Cacuci, D.G. Comprehensive Second-Order Adjoint Sensitivity Analysis Methodology (2nd-ASAM) Applied to a Subcritical Experimental Reactor Physics Benchmark: IV. Effects of Imprecisely Known Source Parameters. *Energies* **2019**. to be submitted. [[CrossRef](#)]
11. Cacuci, D.G.; Fang, R.; Favorite, J.A. Comprehensive Second-Order Adjoint Sensitivity Analysis Methodology (2nd-ASAM) Applied to a Subcritical Experimental Reactor Physics Benchmark: V. Effects of Imprecisely Known Isotopic Number Densities, Fission Spectrum and Overall Conclusions. *Energies* **2019**. to be submitted. [[CrossRef](#)]



© 2019 by the authors. Licensee MDPI, Basel, Switzerland. This article is an open access article distributed under the terms and conditions of the Creative Commons Attribution (CC BY) license (<http://creativecommons.org/licenses/by/4.0/>).